TA01 3/28/97

LA-UR-96-320

Title: **ANALYSIS OF LIQUID PHASE TRANSPORT IN THE UNSATURATED ZONE AT A MESA TOP DISPOSAL FACILITY**

Author(s): **Erik L. Vold**

Submitted to: U.S. Department of Energy, as support documentation for the Los Alamos Area G Performance Assessment

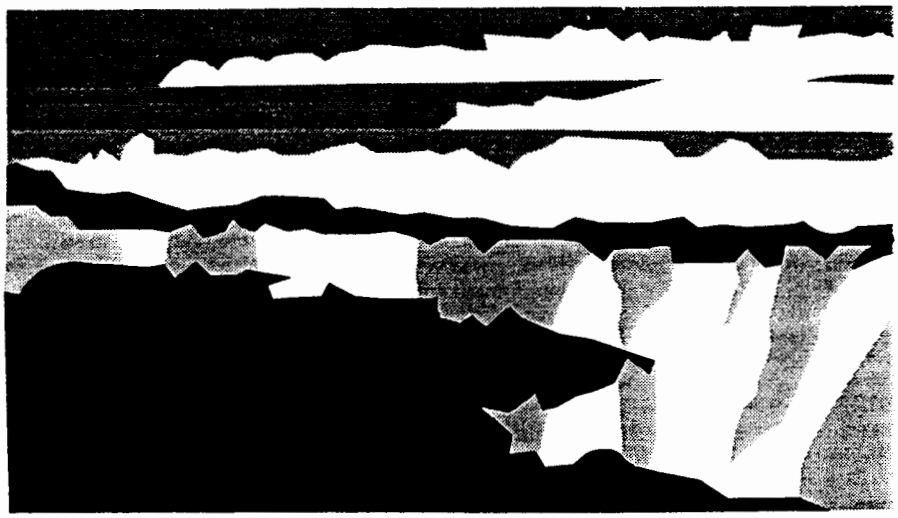

Los Alamos
NATIONAL LABORATORY

Los Alamos National Laboratory, an affirmative action/equal opportunity employer, is operated by the University of California for the U.S. Department of Energy under contract W-7405-ENG-36. By acceptance of this article, the publisher recognizes that the U.S. Government retains a nonexclusive, royalty-free license to publish or reproduce the published form of this contribution, or to allow others to do so, for U.S. Government purposes. The Los Alamos National Laboratory requests that the publisher identify this article as work performed under the auspices of the U.S. Department of Energy.

3243

Appendix 2c

ANALYSIS OF LIQUID PHASE TRANSPORT IN THE UNSATURATED ZONE AT A MESA TOP DISPOSAL FACILITY

TABLE OF CONTENTS

ABSTRACT 1
INTRODUCTION 2
ANALYSIS 3
- Methods 3
- Application to Area G 6

RESULTS 8
- Matric Head and Unsaturated Conductivity Results 8
- Field Borehole Results 9
- Bounding Case Results 14

UNCERTAINTY 15
- Accuracy 15
- Error Analysis 16
- Minimum Detectable Flux 19

DISCUSSION 23
- Three Subsurface Transport Regions 23
- Source Term at Vapor Phase Notch 24
- Uncertainty Implications 25
- Flux Implications 26
- Disposal Operations 27
- Numerical Modeling Implications 27

CONCLUSIONS 28
ACKNOWLEDGMENTS 29
REFERENCES 29

Tables I - II 36

Figure 1-31 38

Appendix 2c

ANALYSIS OF LIQUID PHASE TRANSPORT IN THE UNSATURATED ZONE AT A MESA TOP DISPOSAL FACILITY

ABSTRACT

Analysis of liquid phase transport in the unsaturated zone beneath a mesa-top disposal facility is described. The analysis infers vertical moisture flux and a source term derived from the gradient of vertical flux, based on moisture profiles with empirical analytic forms for the moisture flux as a function of moisture content. The source term, expressed as a characteristic time scale for change in moisture content, varies from about one year in high flux regions to over one thousand years in low flux regions. Results show the moisture flux and source terms within the mesa fall into three regions. A 'near surface region' (<10m depth) is found to have an average net downward liquid phase flux of about 1 cm/yr and exhibits a significant evaporative loss, presumably from surface-connected fractures. This region has a large variation in flux characteristics and is influenced by disposal operations. Relatively large moisture content and inferred flux in this region at one location illustrates the potential for disposal operations to significantly alter the natural hydrology at least of the near surface on the mesa.

Beneath this is a 'low flux region' which extends downward at least to a horizon near the base of the mesa. In this region the average inferred vertical flux is 0.0017 cm/yr upward with a maximum downward flux at any location observed to be 0.006 cm/yr, suggesting there is negligible liquid phase movement through this region.

A third region near the base of the mesa is characterized by a peak in the vertical profile of moisture and is associated with a 'vapor phase notch', at the interface of the vitrified and the devitrified volcanic tuff. The analysis indicates a small average downward flux of 0.07 cm/yr in this region and suggests a local moisture source. This may indicate lateral flow, connectivity to alluvium of greater saturation in the adjacent canyon, or may signify the elevation of the bottom a network of surface-connected fractures. However, the apparent moisture source may be negligible if the local matric properties differ from the stratigraphic unit averaged values.

The flux magnitude indicated at most locations, including the apparent source at the vapor phase notch, is comparable to the uncertainty derived in an error analysis. Therefore, the results indicate trends in the flux profiles, while fluxes at specific points are best quantified as values below the derived detection limits. Results are ambiguous in the vapor phase notch region due to limited matric properties and indicate a need to determine the properties in this region, and thus to better understand the moisture flux to deeper horizons beneath the mesa.

ANALYSIS OF LIQUID PHASE TRANSPORT IN THE UNSATURATED ZONE AT A MESA TOP DISPOSAL FACILITY

INTRODUCTION

The Los Alamos National Laboratory (LANL) Low-Level Radioactive Waste (LLRW) Disposal Facility at Area G is being evaluated for subsurface transport of contaminants from the disposal site, as part of the Performance Assessment[1] required by the U.S. Department of Energy (US DOE) Order 5820.2A for US DOE facilities that dispose of radioactive waste. Environmental transport at the Area G disposal facility is complicated by the complex terrain consisting of finger-like mesas, typically 100' (30m) above the adjacent canyon floors. Figure 1 shows the site facilities imposed on a terrain map. The terrain is shaded to reflect the magnitude of the local slope so that the edges of the mesas are visible. Area G is located on top of a mesa, Mesita del Buey, with Pajarito Canyon to the south and Canada del Buey to the north. The mesa top, the canyon floors, and the water table (about 300m below the mesa top) are all sloping gently at about 3 percent grade downward towards the Rio Grande to the east.

Subsurface transport is complicated by the layered stratigraphy (Fig. 2) which has resulted from the deposition of multiple layers of volcanic flows and ash[2]. Site-specific hydrologic transport properties, defined in terms of van Genuchten parameters[3], porosity, and saturated hydraulic conductivity are available[2]. These are based on analyses by Rogers[4] and Rogers and Gallaher[5], for the upper layers of the Bandelier Tuff, Tshirege Member units 2b, 2a, 1b, 1a, (redesignated, respectively as 2, 1vu, 1vc, 1g) and Otowi Member, but there are no site-specific hydraulic or transport properties available for the deeper units. The upper layers of the Tshirege are fractured with an average fracture spacing of about 1m and aperture of about 3 mm reported at Area G[6].

This semi-arid region receives about 35 cm/yr of precipitation, mostly in brief intense summer thunderstorms and in winter snow fall. It has been hypothesized that transient infiltration events and long term evaporation from the surface-connected fractures play a dominant role in controlling the hydrologic transport, at least in the upper layers[7]. Modeling studies of the steady state moisture flux through the matrix (tuff) show that a single value for the vertical flux cannot match the field observations of moisture profiles at all depths simultaneously[8]. This suggests there are significant sources (or sinks) as a function of elevation in the upper layers of the Bandelier Tuff.

An early assessment of hydrology in the area[9] based on field studies[10,11] specified only a range for the magnitude of the vertical flux at Area G. A maximum downward flux was indicated to be near 0.4 ft/yr, or about 12 cm/yr. The uncertainty in field data allowed a range in the vertical flux estimate such that the net vertical flux may be a small upward quantity. The assessment of flux was based on intrinsic permeability, matric potential determinations on samples, and in-situ matric potential from thermocouple psychrometers placed in boreholes in and near to Area G. The methods did not fully resolve conditions in the range of the in-situ moisture content, so the flux estimates were maximum values estimated using higher moisture contents than observed in-situ. It was concluded[9] the actual flux is probably at least an order of magnitude less than their measured maximum value, or thus less than about 1.2 cm/yr downward. Neutron probe measurements of moisture content indicated that moisture profiles did not change appreciably in time below a depth of 1-2m.

Using typical values for the van Genuchten parameters for Bandelier Tuff and for in-situ moisture content observed in subsurface profiles, an unsaturated hydraulic conductivity for the disposal site was estimated to be less than or equal to 0.1 cm/yr[12]. In that study, it is noted that this conductivity equals the downward vertical flux under assumptions of unit gradient conditions. The vertical flux in a borehole at Area G (borehole G5 - to be discussed in the present study) was estimated as a function of depth[13] from in-situ moisture content data, with recovered core sample analyses for the matric characteristic curves and with measured values for the unsaturated conductivity. Their results showed a maximum magnitude for downward flux of about 1 cm/yr at 32', decreasing with greater depth to less than 0.2 cm/yr below 50', which was about the limit of resolution of those measurements and analyses.

From the previous studies, hydrologic transport in the Area G unsaturated zone is still not well quantified nor even understood conclusively where or when the vertical flux is upward or downward. The present study examines field data from Area G in an analysis designed to address some of the present uncertainties in the unsaturated transport in the upper stratigraphic layers below this disposal site. Specifically, the vertical flux and its gradient (an effective source term) implied by field data from several monitoring bore holes throughout Area G (as seen in Fig. 1) are examined to help quantify our understanding of flux in the vadose zone.

ANALYSIS

Methods

In the complex stratigraphy within and beneath the mesa, an important step in understanding the subsurface transport, is to know if there are local sources or sinks to the liquid phase moisture flux or recharge rate in the tuff matrix. This would imply interactions with vapor phase or with a second permeable media, possibly a connected network of fractures. Without knowledge of specific subsurface sources, numerical models applied to subsurface transport in this region can only justify one source, a net infiltration at the surface. However, this source alone was seen to be inadequate to match all horizons within the mesa simultaneously[8]. The present analysis derives a vertically localized liquid-phase moisture flux (the vertical component of the Darcy flux) and a source term for the moisture content from field data to improve our understanding of the recharge rate and its variations within the mesa region. This is turn improves our understanding of the moisture movement within the mesa interior and its potential for contaminant transport.

A governing transport equation for moisture content in the unsaturated zone is discretized along the vertical axis. An inverse 'finite-difference' procedure is applied to field measurements of the moisture content to evaluate the vertical flux and its gradient. The empirical relationships defining the unsaturated hydrologic properties in terms of moisture content and its gradients are used in the finite discretized equations.

The vertical gradient of the moisture content is related to the vertical component of the divergence of flux. As such, it is an effective source term for vertical flux or recharge rate which includes effects of horizontal flux or time dependent change in the local moisture content. This source term is discussed in the following sections in terms of the possible physical mechanisms that may influence the vertical flux within the mesa subsurface.

A schematic summarizing the analysis is shown in Figure 3 for a cylindrical control volume. In brief, the divergence of flux includes a contribution from the differences in vertical flux, Γ_z, across the top and bottom faces, and from differences in horizontal flux, Γ_x, across the side areas. This

flux divergence equals the volumetric source term, $S_\theta(i)$, plus the change in local moisture content, $\frac{\partial \theta}{\partial t}(i)$, where i is the index of the discrete elevation at which the quantity is evaluated. The field data provide an estimate of the vertical component of the divergence of the flux. This estimate is a measure of an 'effective source term to the vertical flux' which may include contributions from horizontal flux, vapor or matrix volumetric exchange, or time dependent variations in the moisture storage. Terms are defined more rigorously and elaborated in the following analysis.

A continuity equation for moisture content, θ [volume fraction], can be written

$$\frac{\partial \theta}{\partial t} + \nabla \cdot \Gamma = S_\theta \qquad (1)$$

where Γ is the flux and S_θ is a source $(S_\theta>0)$ or sink $(S_\theta<0)$ term representing a volumetric addition to or loss from the matrix liquid phase. In the unsaturated zone, considering liquid phase transport only, the flux can be written

$$\Gamma = -K[\theta]\{\nabla h_m[\theta] + z\} \qquad (2)$$

where $[\theta]$ denotes a functional dependence upon the moisture content. Here, h_m is a matric head[14] representing the capillary suction forces. It is equal to the matric potential, Ψ_m expressed as a head, $h_m = \Psi_m/\rho g$. The matric head is a negative quantity since the matric potential, Ψ_m, is by convention a negative quantity. The unit vector in the vertical axis, z, is directed upward, so the vertical component of flux can be written

$$\Gamma_z = -K[\theta]\{(\partial h_m[\theta]/\partial z) + 1.\}. \qquad (3)$$

Applying Eqn.(1) to flow in the matrix, the source term, S_θ, represents volumetric source or sink terms relative to the matrix liquid phase. The source can include moisture exchange with the vapor phase. In a matrix volume which is near surface-connected fractures open to the atmosphere, the moisture content can be significantly reduced from the conditions expected in the mesa interior. Therefore, this source term includes moisture exchanged with fractures or other surface-connected zones of high permeability distributed throughout the matrix. This term, S_θ, includes evaporative loss to the vapor phase when the source term is negative (a sink term), and could, for example, imply a net evaporative loss to a surface-connected feature within the local volume.

Combining terms above and accounting for one horizontal flux component, Γ_x, along an arbitrary horizontal axis, x, the continuity equation can be rewritten,

$$\frac{\partial \Gamma_z}{\partial z} = S_{zeff} = S_\theta - \frac{\partial \Gamma_x}{\partial x} - \frac{\partial \theta}{\partial t} \qquad (4)$$

where the left hand side is the vertical component of the divergence of flux, equal to an effective source term for the vertical flux, S_{zeff}. This source term equals the right hand side terms, respectively representing local exchange with another media (e.g., fractures) or with another phase (e.g., vapor), horizontal movement of liquid phase in the matrix, and transients which reflect the change in local storage of moisture content. The horizontal flux, Γ_x, could be evaluated using Eqn. 2 with the unit vertical vector equal to zero.

The term representing the volumetric source, S_θ, and the term for the horizontal gradient of flux in Eqn.(4) are expected to be physically related when the moisture at a specific location is influenced by horizontal movement towards or away from a fracture. In this case of a fractured medium, these two terms can be related to the same physical mechanism and need to be evaluated together to represent a moisture source or an evaporative loss.

In steady state, the last term in Eqn.(4) is negligible. In areas where recent disposal operations have disturbed the area, this last term is likely to be significant due to the increased moisture content associated with disturbances due to operations. The time scale where transients are likely to be important is evaluated in the results.

The left hand side of Eqn.(4) can be expressed in terms of a discretized approximation at a vertical point with index, i:

$$\frac{\partial \Gamma_z}{\partial z} = \frac{\{\, \Gamma_z(i+1/2) \;-\; \Gamma_z(i-1/2) \,\}}{\{\, z(i+1/2) \;-\; z(i-1/2) \,\}} \tag{5}$$

where the discretized vertical flux from Eqn. 2 evaluated at node, i+1/2, is

$$\Gamma_z(i+1/2) = -K[\theta]_{i+1/2}\left(\frac{(h_m[\theta]_{i+1} \;-\; h_m[\theta]_i)}{(z(i+1) \;-\; z(i))} \;+\; 1. \right) \tag{6}$$

and a similar expression with the indices decremented by one holds for the flux at i-$1/2$. The notation $h_m[\theta]_i$ means the matric head is evaluated at the moisture content at elevation, i, and $K[\theta]_{i+1/2}$ implies hydraulic conductivity is evaluated as an average between the two elevations at i and $i+1$. Empirical relations required to define $K[\theta]$ and $h_m[\theta]$ are discussed in the following section. Using field data and these empirical relations, Eqns. 6 and 5 can be evaluated for the vertical flux and its gradient, respectively.

It is convenient to express this gradient or effective source term to vertical flux in a number of ways. Multiplying Eqn. 5 through by $\Delta z = \{z(i+1/2) \;-\; z(i-1/2)\}$ gives the effective source term, $S1$ (as in Fig. 3), as

$$S1 = S_{zeff}\ \Delta z = \{\, \Gamma_z(i+1/2) \;-\; \Gamma_z(i-1/2) \,\} \tag{7}$$

expressed as an equivalent flux, in cm/yr for instance, which can be compared more directly to the local flux, to a net infiltration rate, or to the precipitation rate for comparison. This source term is not normalized per unit depth and so represents the total source (or sink) over the depth interval between the adjacent field data points at $z(i+1/2)$ and at $z(i-1/2)$.

The vertical gradient in flux, $\frac{\partial \Gamma_z}{\partial z}$, can also be considered as an effective source term, S_{zeff}, (in Eqns. 4 and 7) to the vertical flux or to the recharge rate. In this form, this effective source has units of inverse time and represents the change in vertical Darcy flux per unit vertical distance, with units for example as [yr^{-1} = (m^3_w/m^3) m/yr /m], where (m^3_w/m^3) represents the dimensionless volumetric water fraction, θ. In this form, we interpret the source term loosely to represent an inverse of the time scale over which the *vertical moisture flux* is changing. The

inverse of this S_{zeff} in Eqn. 4., the characteristic time scale for *moisture flux*, is denoted $S_{t\text{-}inv}$ in the Results figures.

The time scale for which the *moisture content* is changing is this effective source term for vertical flux times the moisture content. This effective vertical source for moisture content (denoted *Sinv* in Fig. 3, and denoted, $S_{t\text{-}inv}$*vol%, in the Result figures) is written in several equivalent forms

$$Sinv = \frac{\theta\,\Delta z}{S1} = \frac{\theta\,\Delta z}{\{\,\Gamma_z(i+1/2) - \Gamma_z(i\text{-}1/2)\,\}}$$

$$= S_{t\text{-}inv}*vol\% = S_{t\text{-}inv}\,\theta = (S_{zeff})^{-1}\,\theta. \qquad (8)$$

One can interpret this as a characteristic time scale for vertical movement, v_z, to change the moisture content, or, if the local source term is completely attributed to the time dependent change in moisture content (Eqn. 4) then this is the minimum time scale over which that moisture content is changing at the present flux rates.

The finite difference equations, 5 and 6, form the basis for the flux analysis with the alternate source term formulations in Eqns. 7 and 8. Each term in these equations has an associated error based on the field measurement and analysis uncertainty which contributes to the net uncertainty for the expression. This is an important consideration in interpretation of the results and will be discussed in a later section.

To summarize, the gradient of vertical flux implies a source term to the local recharge rate which can be expressed as a flux, *S1* (in Eqn. 7), or as a characteristic time scale, *Sinv* (Eqn.(8)). The flux source, *S1*, is interpreted as the moisture flux needed to account for the observed magnitude of the vertical flux gradient if steady state conditions prevail. The source term, expressed as a characteristic time scale, *Sinv*, is the minimum time over which the moisture content is changing if all of the vertical flux gradient is attributed to a time dependent change in moisture content at that location. In the field situation some combination of these two limiting cases is likely to apply. This combination will vary with location as discussed in the Results section for each of the field boreholes.

Application to Area G

The approach is to combine moisture content data with empirical fits for the functions, $K[\theta]$ and $h_m[\theta]$, to evaluate the vertical flux and its divergence. Moisture content data are examined from several monitor holes as indicated on Fig. 1. Data from most holes are from neutron probe measurements because these show good precision and, if properly calibrated, reasonable accuracy. Thus, moisture content gradients are determined relatively well, as discussed more quantitatively in the Uncertainty Section.

Moisture content profiles for each of the holes labeled *NPH#* (Neutron Probe Hole) in Fig. 1 were made during the summer to fall seasons of 1994. These were reported in Loaiza and Vold[15], as determined with a neutron moisture probe which measures directly in moisture content volume percent $(100\times\theta)$. Calibrations for each type of hole casing and hole diameter are documented[15]. Measurements in a monitor hole (NPH-1) into an active disposal unit confirmed earlier findings that moisture content does not change appreciably in time below 1-2m depth. The moisture content

in the two holes labeled LGM-85-# were taken from plots of results in a previous report[10] where the measurements were also made by neutron probe.

Borehole 54-1002 (in the LANL Environmental Restoration Program) is located on the mesa top about 1/2 km to the west of Area G, and is included because it is the deepest of the holes reported here. The moisture data are from gravimetric measurements of core samples from the borehole. Analytic determinations of the bulk density were averaged in each stratigraphic layer as summarized elsewhere[2] and used here to convert this moisture content to a volumetric basis. The values used for bulk density averaged for each stratigraphic unit are shown in Table I. Because of these extra steps in the analytic procedures, the gravimetric profiles contain more uncertainty than the neutron probe-determined profiles especially in the deeper layers where relatively few samples (2 in the Tsankawi-Cerro Toledo layers) were used to characterize the bulk density and unit-averaged hydrologic parameters.

Empirical relations required to define unsaturated moisture flux as functions of moisture content, $K[\theta]$ and $h_m[\theta]$, have been compiled by stratigraphic units at Area G[2] based on van Genuchten-Maulem analyses[3,16] as reported previously[4,5]. Stratigraphic unit mean values are used in the present study as summarized with their standard deviations in Table I. Although residual moisture content, θ-residual, is determined from curve fits, it is not applicable to the present analysis when field moisture data are less than the residual, $\theta(i) < \theta\text{-residual}$, therefore *θ-residual* was set equal to zero in this analysis. The stratigraphic unit interfaces in each borehole were determined from the borehole logs where borehole logs were available. Otherwise, a simple interpolation estimate was used by comparing depths of moisture profile peaks and inflection points, with those in logged holes.

Only one of the holes (54-1002) which was used to determine the mean stratigraphic unit transport parameters in Table I is the same as the holes examined in this present study. However, the moisture profiles in both sets are similar and so the transport properties used here are expected to be representative of the unit mean values. Recent data from borehole G5 [Ref.17] at Area G were not included in calculating the means used in this study, however, as seen in Table I, in the last column, by including the G5 data for Unit 2b, the van Genuchten-Maulem fits are not changed greatly.

Fitting parameters for the transport properties for the crushed tuff were taken from a separate reference[18] and are the same as the values used in the preliminary PA modeling and analyses[1]. (Note that these values have been revised for subsequent PA analyses, however, they provide a basis for comparisons here and for an understanding of the sensitivity of the flux results to the assumed matric properties.) The origin of the crushed tuff samples is Unit 3[4], not the same as the stratigraphic unit of interest here, Unit 2b. Unit 2b is the nearest surface stratum at Area G and therefore comprises most or all of the crushed tuff used in the disposal operations as fill for the waste disposal pits and shafts. The difference in the source of the crushed tuff samples led to comparison tests discussed in the Results Section.

Trends in the property variations within each unit have not yet been examined in detail and so possible systematic effects (e.g., a consistent vertical gradient of the fit parameters within a unit) are ignored in the field analyses, but considered to a limited extent in the uncertainty analyses. Matrix properties at a particular elevation, which deviate consistently from the mean value for the unit in which that elevation is included, can produce an error in the present analysis.

Unsaturated hydraulic conductivity was measured directly on several samples from hole G5[19] using the UFA centrifuge technique[20]. As discussed elsewhere[13,21] these measurements are in good agreement (factors of 2-3 difference near in-situ range of moisture content) with predictions from the van Genuchten-Maulem fits in some cases and in poor agreement (an order of magnitude or greater difference) in other cases. In several of the cases with poor agreement, the centrifuge measurements suggested that liquid phase flow does not occur at the in-situ moisture content.[19]

RESULTS

Results are presented in three similar plots for each monitor hole, which show (A) the moisture profile, (B) the vertical flux (Eqn. 6) with the effective source expressed as a flux (Eqn. 7), and (C) the inverse source term expressed as a characteristic time for the moisture flux (Eqn. 5) and for the moisture content (Eqn. 8). In the vertical flux plots, the flux is downward if negative and upward if positive, and the source term is into the matrix volume if positive and out from the matrix (e.g., evaporation) if negative. In the source term plots, the source term is a magnitude only on a log scale and does not indicate a direction in or out from the matrix. In several cases, the flux and effective sources are dominated by large values in limited ranges of depth and so these terms are then replotted over selected depth ranges to focus on the trends in the 'low flux' depth range.

Matric Head and Unsaturated Conductivity Results

Intermediate results used in this analysis are useful to understand the limitations in interpreting the results in the following figures. Moisture content, matric head and the unsaturated conductivity are shown in Fig. 4 for a particularly dry moisture profile, in hole NPH-9, ER-1111, as located in Fig. 1.

Fig. 4A identifies the interface locations between the stratigraphic units and shows the matric head with the moisture content for reference. The calculated values of matric head, h_m, over the two ranges of depth, 0-10m and below 26m, are most consistent with the in-situ psychrometer data previously reported[9] in the range, $h_m \sim 10\text{-}100m$. The higher matric potential values seen at the intermediate depth range are associated with a very low moisture content region, and there the matric potential fit curves may exaggerate the actual matric potential.

In Fig. 4B, the vertical flux is compared to the unsaturated hydraulic conductivity. Both values appear to be negligible throughout most of the depth range. The more significant peaks in vertical flux are not associated with peaks in conductivity, but are associated with maxima in the local head gradient.

The absolute magnitudes of conductivity and vertical flux are plotted together in Fig. 5A, to allow a log-scale presentation. Here one sees that the magnitude of the flux is generally 1-2 orders of magnitude larger than that of the hydraulic conductivity suggesting that a 'unit gradient assumption' holds at few if any of these specific points in this dry borehole. This is clear in Fig. 5B, which shows the absolute value of the vertical flux function, $(\partial h_m/\partial z + 1)$. At most points, this function is much greater than one, showing the differences in matric potential are critical in determining the magnitude of the moisture flux.

This becomes very important in the very low moisture region, where very small changes in moisture content are associated with large changes in matric potential through the unit-averaged

analytic fits. In actuality, small local changes in matric properties may smooth the matric potential profile. However, using the stratigraphic unit averaged properties, then small variations in moisture content increase the magnitude of the vertical flux above the unsaturated conductivity. For this reason, the results may be 'noisy', with spikes attributed to the limitations of the unit-averaged analyses. This effect is pronounced in these figures because this is a particularly dry borehole at Area G. An important implication is that it is necessary to look for trends common to many borehole profiles to 'smooth over' the noise of the analysis artifacts and to derive meaningful results.

Field Borehole Results

The field monitor holes are located as in Fig. 1 (with one hole not shown, 54-1002 located on the mesa top about 1/2 km to the west of Area G). The drainage divide along the mesa top runs NNW to SSE near the north mesa edge approximately through holes NPH-2, NPH-3, and LGM-85-11. These holes should be near the locations of maximum surface run-off and are expected to be among the drier boreholes.

The results from monitoring holes are presented roughly in order from drier to moister, looking first at a group of five shallower holes (<20m) which do not reach the depth of the adjacent canyon floors, and then at the deeper holes (>30m) which extend slightly below the depth of the Unit 1b-1a interface. This interface is nearly coincident with the elevation of the adjacent canyon floor (Pajarito Canyon). This layer is identified as the vapor phase notch, just at or above the 1b-1a unit interface, the transition region from vitrified tuff (1b) to devitrified tuff (2a). This notch has been identified at outcroppings as a layer of preferential weathering[22]. It may have unique hydrologic transport properties but these have not yet been determined.

Results for borehole NPH-2 (a background hole in relatively undisturbed tuff near pit 37) are shown in Fig. 6. This moisture curve in Fig. 6A is assumed to be a nominal 'undisturbed' case, with moisture decreasing somewhat linearly with depth from 6-7% near the surface and leveling out at about 1% below 6m. The inferred moisture flux in Fig. 6B is negligible below about 3m depth. In the upper most 3m interval, the vertical flux is predominantly downward, at 1-3 cm/yr. The associated moisture source is predominantly negative and of comparable magnitude to the flux suggesting a loss of the downward flux, possibly to evaporation in surface-connected fractures. The corresponding inverse sources in Fig. 6C suggest moisture content profiles are not changing within a 50 year time scale below 3m, and not changing within 500 years below 7m. In the top 2-3 m, the time scale for change is about 0.5 yr, consistent with a source term frequency of 2/yr, suggesting a seasonal source, possibly the summer rains and the winter snow melts.

Similar results are seen in Fig. 7 for hole NPH-3 another 'background hole' in a relatively undisturbed area also near the mesa top drainage divide. The moisture gradient and the flux become negligible at 4m depth. The flux is less than 1 cm/yr in the near-surface region (0.45 cm/yr average to depth of 4m). The time scales are slightly longer than in the previous case, with no changes seen here on a time scale shorter than 2 years even at 1m from the surface.

Fig. 8 expands the scale for flux and the flux source term over the depth range where the flux appears to be negligible in Fig. 7B. The flux and its source appear to be fluctuating with depth, with a maximum local magnitude of less than 0.4 mm/yr and an average flux of less than 10^{-3} cm/yr directed downward over this range in depth from 4m to 20m. The fluctuations may be artifacts of the analysis due to the large changes in matric potential implied by small changes in moisture at the dry end of the moisture range. The magnitude of implied moisture movement appears to be small compared to the error in the analysis as discussed later in the Uncertainty

Section. On the other hand, the apparent fluctuations may have a real physical basis, suggesting small localized 'pockets' of moisture flux moving at slow rates in different directions.

Results in hole NPH-7c are seen in Fig. 9. This hole is in the tritium disposal shaft area and adjacent to a series of old burial trenches. This is considered a 'disturbed area', and shows the increased moisture content relative to the previous two cases. The near surface moisture profile behaves similarly to the previous cases, but now decreases from about 12% near the surface and levels out at a depth of about 8m to 2% or less. The vertical flux in the top 6m is 2.4 cm/yr downward. The source in this region is negative on average (-0.7 cm/yr) indicating net loss from the matrix. A distinct positive spike in the source is seen in Fig. 9B at a depth of 3m, the location of a local maximum in moisture. This suggests a net influx of moisture either transported from a nearby moist region, a fracture or a disturbed trench excavation, or a time dependent residual related to previous surface wetting and more recent surface drying. The minimum time scale for moisture change is about once per two years as seen in Fig. 9C, suggesting that if the profile is attributed to recent drying, the previous wetting cycle was at least two years ago, perhaps during a 'wetter than average' year.

Results for hole NPH-6 in the southeast corner of Area G are shown in Fig. 10. Moisture is about 8% maximum and decreases from 3m to about 10m, similar to the previous case. The local maximum at 3m depth is again possibly related to horizontal migration from nearby disturbances or to a time dependent response of a previously greater rate of surface infiltration followed by more recent drying. The positive (upward) Darcy flux in the top 3m suggests that the moisture profile is relaxing by upward moisture flux driven by surface or near surface evaporation. The positive source term in this depth range shows moisture is now (or recently) moving towards this region. The minimum time scale for moisture change is about once per two years as seen in Fig. 10C.

A unique set of results are seen in Fig. 11 for hole NPH-4. This moisture content of 30% near the surface and the very slow decrease with depth were not observed at any other location. This hole is in an engineered drainage area where surface run-off is diverted towards this hole and so the infiltration is expected to be considerably higher than at any undisturbed location. Note that the monitor hole itself is cased and is not expected to be conducting water to the subsurface region. The average downward Darcy flux inferred in the upper depths is in the range of 100-200 cm/yr depending on the exact interval, corresponding to 3 to 6 times the annual average precipitation rate.

The average source term over the same depth is negative indicating a net evaporation or loss in the mesa top. The drying is not sufficient to reduce the moisture in the top 16m to the typical observed background levels below 2%. The time scales for moisture content change are seen in Fig. 11c to be well below one year at most depths, with a minimum value (at depth = 14m) of about 0.05 year or a frequency of about one per two weeks, and with several near surface points at 0.1 year or a frequency of about once per month. Thus, changes at this location (NPH-4) are rapid relative to any other monitor hole.

The monitor holes discussed up to this point did not extend deep enough to reach the elevation of the adjacent canyon floors. The remaining monitor holes are deeper than the adjacent canyon floors and show a characteristic moisture peak associated with the vapor phase notch near the unit 1b-1a interface. Fig. 12 shows the results in hole LGM-85-06, using the moisture profile previously reported[10]. Moisture content increases with depth beginning at about 20m, and shows a moisture peak at 30m. The borehole logging data shows this peak is in the 1b unit, with the 1b-1a interface at 32m. The profile in Fig. 12A is typical for a relatively undisturbed area near the surface.

The Darcy flux and associated source term flux (Fig. 12B) decrease rapidly near the surface and appear to be significant again near the moisture spike at 30m. In this region the Darcy vertical flux

and the source term flux show a trend which is seen in nearly all of the holes which penetrate this depth. The apparent source term exhibits a large positive value at the depth of the moisture peak suggesting net infiltration, in this case equivalent to about 5 cm/yr. To either side of this source spike, the source is negative suggesting net evaporative losses over a depth range of 1-3 m. The corresponding Darcy flux is positive above the source spike suggesting upward movement away from the spike and negative below the spike suggesting downward flux from the source.

This pattern suggests a source with movement away to either side and as the moisture moves away it evaporates as indicated by the negative sources to either side of the spike. Another interpretation of the data is possible, if there is a horizon near the moisture spike which has significantly different matric properties than the average values used for unit 1b (or 1a), then the moisture spike could still represent a static equilibrium, and correspond to negligible flux through the region.

In this hole, LGM-85-06, the average vertical flux from 25m to 35m depth is -0.43 cm/yr, and the average source in that range is 0.016 cm/yr, indicating a significant downward movement but a negligibly small net source. The minimum time scale for moisture content movement is about one year and occurs at the depth of the moisture peak as seen in Fig. 12C. There is a region from about 15m to almost 25m depth where the minimum time scale is almost 1000 years indicating negligibly slow changes in this 'low flux region'.

Hole LGM-85-11 (Fig. 13) shows higher moisture content compared to the previous case but similar trends with depth, decreasing from 15% near surface to 2% at 5m, and increasing slowly to 20-25m and then building to a local maximum or moisture spike at 28m, apparently the depth of the vapor phase notch at this location. The increased moisture content corresponds to much larger fluxes than the previous case, about 30 cm/yr near the surface and 10-20 cm/yr at the moisture spike at 28m. Except for one point at 5 m, the time scale for moisture content change (Fig. 13c) is one year or greater with the minimum values occurring near 28m. From 7 to 23m (a low flux region in this borehole) the source term time scale is greater than 100 years.

Each of the two previous cases showed negligible flux throughout the intermediate ranges of depth. In Fig. 14, the Darcy fluxes in the limited range are replotted to resolve this 'low flux' region for both holes. The vertical flux and source term in each case oscillate about zero with a maximum local magnitude of about 0.1-0.15 cm/yr. The average flux over this region is -0.0017 cm/yr and the average source is -0.013 cm/yr for hole LGM-85-06, and for hole LGM-85-11, these respective values are 0.01 and -0.07 cm/yr.

Results in Fig. 15 for hole NPH-8, near the tritium shaft field, show a modestly high near-surface moisture content consistent with profiles from other 'disturbed locations', falling to below 2% at depth 11m, more consistent with an 'undisturbed location' at depth. The maximum in moisture content at depth of 5m, with positive vertical flux and sources at shallower depths, is also consistent with a disturbed location as discussed for holes NPH-7c and NPH-6 in Figs. 9 and 10. The moisture peak at 27m is similar to that discussed for the previous two holes which penetrate the 1b-1a interface. The minimum time scale in Fig. 15C is about one year, with most points in the range of 20-1000 years. Fig. 16 shows the Darcy fluxes in this hole on an expanded scale over the 'low flux' region from 12 to 25 m depth. The maximum downward flux in this region is -0.033 cm/yr, the average flux over this range is -0.0038 cm/yr and the average sink over this range is -0.0024 cm/yr.

Fig. 17 shows results for hole NPH-9 (ER#1111) located near the high activity tritium shafts. The low moisture content throughout the profile suggests this area at least locally is relatively undisturbed by the nearby disposal operations, or it is dry due to its proximity to the mesa edge. The moisture spike at the 1b-1a interface is at about 25m depth at this location and small in magnitude, producing a minor perturbation in the vertical flux or flux source term. A moisture buildup at 10m depth does show the same trends as previously observed at the 1b-1a interface

moisture spike, a positive source dissipating with movement in the upward and downward directions and with adjacent negative sources possibly attributed to evaporation. Except for two points, the time scale in this hole is ten years or greater as seen in Fig. 17C.

Results are seen in Fig. 18 for hole NPH-5 (also identified as G-5[13,21]), located in a central portion of Area G between a shaft field and older disposal units. This hole was previously selected for detailed hydrologic transport assessments including complete matric characteristic curves[17] and UFA centrifuge measurements of the unsaturated hydraulic conductivity curves[19] on core samples removed at 10' intervals. These data have been discussed previously[13,21], and will be considered further in the Discussion Section.

The results in Fig. 18 reflect an atypical moisture profile, decreasing from about 10% to 7-8% in the top 15m, and then dropping precipitously to less than 2% at 16m. The interface of units 2b-2a occurs at this abrupt change in moisture content. Throughout the top 15m, the vertical flux is consistently downward with an average value over this interval of -1.1 cm/yr, and this average increases to -1.7 cm/yr in the top 17m, due to the large downward flux apparent at the abrupt drop in moisture. The net source term over these ranges are respectively, +0.36 cm/yr and +0.01 cm/yr. This condition may imply a significant connectivity between this hole and adjacent disturbed areas of increased moisture or adjacent surface-connected fractures which contribute to wetting the hole at certain depths and to drying the hole at other depths.

There is an apparent sink at 17m of -6.5 cm/yr (Fig. 16c) which seems to be removing the downward vertical flux above that depth. Surge beds at this depth have been proposed as a surface connected feature which may preferentially dry this horizon[23,13]. The source and flux values at this horizon are equal to that seen at 4m depth where the moisture profile undergoes a minor drying trend as evidenced by the local minimum in moisture content. In comparison to the profiles at other holes in this study, it appears that this is not a typical characteristic but is unique to this hole. [Note however, in a recently drilled borehole (Environmental Restoration Program, 54-1107) located near to G5, the moisture and matric potential profiles[24] are similar to that seen at G5 suggesting an area near the middle of Area G with similar characteristics, and similarly influenced by disposal operations and or by surface-connected fractures down through Unit 2b.]

The hole ER-1002 is located on the mesa top about 1/2 km to the west of Area G. It is included because it is deeper than any hole within Area G, penetrating into the Cerro-Toledo member at 78m depth. The hole was drilled at 22° from the vertical but all depths reported here are corrected to vertical. The moisture data is from gravimetric analyses on recovered bore hole samples corrected to a volumetric basis with stratigraphic unit averaged bulk densities (Table I) and is thus considered to have a larger uncertainty than the neutron probe measurements.

Results for hole 54-1002 in Fig. 19 show the trend expected for a relatively undisturbed area, 6-7% near surface moisture falling to 2% or less by 5m depth, with the moisture spike at the 1b-1a interface or vapor phase notch, at a depth of 40m at this location. Below this the moisture increases slightly until depths of 80-90 m where the moisture content increases and fluctuates significantly with depth. Using the limited data for the unit average properties at this depth, an apparent vertical flux and source term flux is seen (Fig. 19B) in the range 80-100 cm/yr at about 80m depth and several values near 10-20 cm/yr occur at points below 80 m.

If these data are valid, they suggest a moisture source at a very localized horizon at 80m which is primarily moving upward and evaporating or otherwise lost above 80m. This apparent flux may not be real however, it may be attributed to poor data in moisture content or to stratigraphic property variations at this depth which have not been resolved. The associated time scale in Fig.

19c is less than one year for several points in this range. The magnitude of the apparent source at first seems unlikely to represent a real physical source at this depth. However, similar apparent sources have been seen in recent analyses on moisture profiles underneath nearby canyon locations, suggesting the possibility of lateral mixing at this horizon.

Figure 20 (top) shows the rescaled Darcy fluxes down to 78m to avoid the erratic behavior near 80m and deeper. This now agrees well with data from previous holes, showing negligible flux or sources except near the surface and at the vapor phase notch (~40m here). Fig. 20 (bottom) shows the limited range of depth from 8 to 29m. Over this range, the average vertical flux is -0.0005 cm/yr and the derived sink is -0.0006 cm/yr. Deeper intervals have similarly negligible flux values until one includes the data below 76m. The vertical flux in this region is positive indicating an upward movement of 6.6 cm/yr which suggests the data and or analysis in this region are of questionable reliability. The average flux values over several intervals are included in the following table.

Average flux values for hole, 54-1002

depth interval	average vertical flux (cm/yr)	average source term (cm/yr)
0 - 7 m	- 0.51	- 0.16
8 - 29 m	- 0.0005	- 0.0006
30 - 44 m	- 0.005	+ 0.0005
45 - 75 m	- 0.004	+ 0.0003
76 - 90 m	+ 6.6	+ 0.15

Results for hole NPH-1 are shown in Fig. 21. This is a cased hole going through a portion of an active and nearly filled disposal unit, pit #37. The zero depth in the figure is the current pit surface which is about 10m below grade, while the pit bottom is about 30m below grade or about 10m below the accessible 10m portion of this monitoring hole. The moisture profile is strongly inverted with a maximum at 6m depth consistent with on-going fill and disposal operations in the open pit.

The matric properties used in generating the fluxes and source terms in Fig. 21 B and C are for 'crushed tuff' as reported in [18,8]. Fig. 21B shows that in spite of a moisture gradient driving upward flux the net flux is gravity driven, downward throughout the profile. The source term expressed as a flux in Fig. 21B is small and only positive near the 5-6m depth, probably indicating moisture sources from recent disposal operations. Fig. 21c shows that the minimum characteristic time scale for moisture content movement is about 20 years, suggesting that seasonal or other short term fluctuations are dampened out in the crushed tuff matrix.

The crushed tuff used as fill at Area G is mostly from the unit 2b. However, the stratigraphic unit which served as the source of the 'crushed tuff' data is not from Unit 2b [p.17, Ref.5]. There have been some indications that crushed tuff and in-situ tuff do not behave too differently in unsaturated hydraulic conductivity[19], nor in matric properties[5]. Some differences in matric properties, expressed as different exponents in power law fits of matric potential as a function of moisture content, have been noted[25].

As a check on the sensitivity of these results to the actual matric properties used, the vertical flux and source terms were recalculated using the matric properties for in-situ unit 2b. These results, labeled (2b-i), are plotted with the previous results for the 'crushed tuff' properties, (2b-c), for comparison in Fig. 22. Using the in-situ matric properties it is seen that the upward slope of the moisture profile is now sufficient to drive a small upward flux (~1 cm/yr) between 4 and 5.5m depth, and a small upward spike at depth of 9m. For these properties, limited upward movement occurs. The extent could be examined in greater detail to determine if contaminant transport is

significant. Using the in-situ properties, the characteristic source term time scales in Fig. 22B are reduced from the previous 'crushed tuff' properties, and are now in the range of 1-2 years.

The van Genuchten values for crushed tuff used in the Results in Fig. 21 were used in the preliminary draft Area G Performance Assessment[1]. These parameter values have since been revised for subsequent PA work to a 'corrected' set of numbers for crushed tuff which are similar to those for the uncrushed Unit 2b average values used in this study. The results in Fig. 21 serve as a measure of the sensitivity of the vertical flux to the assumed matric properties, while results in Fig. 22 labeled *2b-i* represent expected field conditions.

Bounding Case Results

Results for two assumed profiles of moisture content are illustrated in Fig. 23, which bound the range in moisture content seen in the holes at Area G. The curves are useful to understand the limits of the basic analyses used here and to appreciate the nonlinear dependence of flux on the moisture content. Linear moisture profiles are assumed, one, from 6% near the surface decreasing to 1% at a depth of 15' (~5m), and two, 12% near the surface decreasing linearly to 2% at a depth of 30' (~10m), so that each has the same slope but in a different moisture range. These two profiles bracket the near surface profiles at Area G in all holes with one exception (NPH-4).

The slope in both profiles is $0.01 m^{-1}$, which was chosen as a 'typical value', close to an average of the observed vertical gradients in near-surface moisture. Many of the holes are seen to exhibit a near surface moisture gradient of about this magnitude independent of the near surface moisture content. Properties of Unit 2b are assumed in computing $K[\theta]$ and $h_m[\theta]$ in this example.

The associated Darcy flux in Fig. 23B shows the vertical flux as a curve and as a line segment for each of the two moisture curves. The drier moisture content corresponds to the smaller flux in Fig. 23B, which is less than 1 cm/yr, and the larger moisture profile corresponds to flux in the range of <1 - 7 cm/yr depending on the evaluation point. A curve and line segment for each moisture profile represent fluxes evaluated respectively, along the moisture profile curve (evaluated at each moisture point shown in Fig. 23A) and as an 'average' over the moisture profile curve (discretizing each moisture profile as a whole segment by evaluating Eqns.(4 - 6) using only the moisture profile endpoints and midpoint). The difference in flux in the continuous profiles and in these average segments is seen to be large. This indicates the sensitivity to the discretization in forming the non-linear difference expressions for the flux and for the source expressed as a flux. A reason for the sensitivity is that these flux expressions are 'integral measures between data points' and are not normalized per unit depth. This shows that the moisture profiles must be adequately resolved for meaningful results in these terms.

Similar considerations apply to the source term flux curves in Fig. 23B. The 'average' over each moisture range is now just a single point, using two values of vertical flux or three values of moisture content to evaluate the source term per Eqn. 5. The inverse of the source terms (Eqn. 7-8) are plotted as characteristic times in Fig. 23C. This source term is normalized per unit depth and so the difference between the source term calculated along the moisture profile and the source term calculated as an average over the moisture profile is in good agreement. The assumed linear moisture profiles lead to characteristic times for change in moisture content (indicated as *(St-inv)*vol%* in Fig. 3C) of 15 or more years at the lower moisture profile levels and about 5 years at the higher moisture content. The time scale for change in moisture flux in Fig. 23C is larger than that for the moisture content by the factor, θ^{-1}.

UNCERTAINTY

Accuracy

Accuracy of the results in this analysis depend on the accuracy of four main factors: the moisture profiles, the matric potential functions over the observed in-situ moisture range, the unsaturated conductivity function of moisture, and the application of stratigraphic unit average functions to all the data points within each unit. The application of unit averaged functions was discussed in relation to the vapor phase notch, with the implication that additional field data are required to resolve the hydraulic properties throughout that region. In other regions, the average stratigraphic unit properties seem to better represent the whole unit based on the results in the previous section.

The moisture profile accuracy is directly related to that of the neutron probe measurements for most of the data in this report. Neutron probe accuracy is estimated to be within 50% when properly calibrated, but the precision is expected to be better than 10%. In recent unpublished field data[26], it is seen in the dry regime in boreholes at Area G that the precision or reproducibility error, $\Delta\theta$, tends to about $\Delta\theta \sim 0.001$ or 0.1% (in moisture content volume percent), independent of moisture content. Thus at 1% moisture content, the relative error is $\Delta\theta/\theta \sim 0.001/0.01$ or 10% of the mean, and it is less at greater moisture content. It is the relative error or the difference between adjacent points as used in the moisture gradient determination which is important in this analysis and thus, 10% is a reasonable estimate for the error.

The accuracy of the van Genuchten fits for unsaturated conductivity has been discussed in several studies examining data from the G5 hole discussed in this report [13,19,21]. In that hole, unsaturated conductivity curves as a function of moisture content were measured by the UFA centrifuge method[19] and compared to van Genuchten fits using matric potential data[17] with the saturated conductivities. These curves were compared for 10 core samples, located approximately one every ten feet in the G-5 hole.

Of the 10 curve comparisons, two were based on unreliable data, one was ambiguous (at 9.5'), three were in relatively good agreement throughout the range of the curves and four were in poor agreement. This suggests almost half or 3 out of 7 of the reliable measurements are accurate based on comparable results from two different determinations for the unsaturated conductivity used in this study. Of the cases in poor agreement the tendency was for the experimental conductivity data (UFA determination) to asymptote at greater moisture content than expected[13,19]. In these cases, the actual conductivity at the in-situ moisture content was beyond the range of the experiment and therefore could not be determined. The discrepancy may have been attributed to experimental limitations, or to a real lack of liquid phase movement at the in-situ moisture content. The latter implies that the in-situ content could only be achieved by evaporation and vapor phase movement, a possibility considered further in a separate study[27].

Generally, the matric potentials (matric heads) found in this study are consistent with the range in the in-field psychrometer results reported previously[9-11]. A possible exception is at the driest moisture contents where the matric potential predicted from the van Genuchten fits in this study are of greater magnitude than previously observed. Matric potential results between van Genuchten fits and chilled mirror psychrometry (CMP) on recovered core samples from hole G5 were found in good agreement[13]. Matric potential from chilled mirror psychrometer measurements on recovered core samples compared well to van Genuchten fits with moisture data in horizontal

boreholes at Area G, at least at the dry range of moisture content[28]. Recent unpublished results on CMP matric potential from core recovered in Area G boreholes as part of the Environmental Restoration Program[24], agrees with results from moisture content combined with the unit-averaged van Genuchten functions within a factor of about two at most data points[27]. We find good agreement generally in matric potential observed in different studies and methods, however, it is difficult to quantify the overall accuracy of the matric potential determinations in these different studies without knowing which provides the 'right answer'.

Error Analysis

Assuming the overall validity of the analysis described in this report, an error analysis is used to understand the important contributions to error and the magnitude of the overall error associated with the analysis. The error or uncertainty associated with each variable is denoted as σ, subscripted with the appropriate variable name.

For a general function,

$$x = f(u,v,w,....),$$

the propagation of errors is based on the standard form[29],

$$\sigma_x^2 = \left(\frac{\partial f}{\partial u}\right)^2 \sigma_u^2 + \left(\frac{\partial f}{\partial v}\right)^2 \sigma_v^2 + \left(\frac{\partial f}{\partial w}\right)^2 \sigma_w^2 + ..., \qquad (9)$$

which applies when there is no correlation between the independent variables. This is assumed in the present analysis.

We are interested in determining the error associated with the flux given by Eqn. 6. In this section, simple analytic forms are assumed for the transport properties (rather than the van Genuchten fits) which make it more convenient to analytically evaluate the uncertainty. Power law fits[30] for unsaturated transport properties over the low moisture content range [2%-20%] have proven to have high correlation coefficients [>98%] in Bandelier Tuff[25]. The unsaturated transport properties, expressed here as matric head, $h_m[\theta]$, and unsaturated conductivity, $K[\theta]$, are estimated in this uncertainty analysis as

$$h_m[\theta=2\text{-}20\%] = a_h\,\theta^{b_h} \quad and \quad K[\theta=2\text{-}20\%] = a_k\,\theta^{b_k} \qquad (10)$$

where a_h, b_h, a_k, and b_k are fitting parameters.

Equation 6, for the flux, is approximated by evaluating all functions at a moisture content, θ, at location, i, (index along the z axis), and the moisture gradient is estimated here as $d\theta/dz = (\theta - \theta_-)/\Delta z$, where θ_- is the adjacent moisture measurement. Hydraulic properties are assumed to be only a function of moisture so that, $\nabla h_m = (dh_m/d\theta)\nabla\theta$. This does not apply to the interface region between two dissimilar units, which must be considered separately, i.e., this applies only within a unit with average hydrologic properties. The vertical flux, Γ_z, can then be expressed in several equivalent forms for this analysis based on

$$\Gamma_z = - D_z - K, \tag{11}$$

where D_z is a 'diffusive part' of the flux, and K is the convective part. These can be written out as,

$$\begin{aligned}
\Gamma_z &= - K[\theta] \{ (\partial h_m[\theta]/\partial z) + 1. \}, \\
&= - K[\theta] \left(\frac{\partial h_m[\theta](\theta - \theta_-)}{\partial \theta \quad \Delta z} + 1. \right), \\
&= - \frac{a_k a_h b_h}{\Delta z} \theta^{b_k + b_h} + \frac{a_k a_h b_h \theta_-}{\Delta z} \theta^{b_k + b_h - 1} - a_k \theta^{b_k}, \\
&\equiv - A + B - K. \qquad (12)
\end{aligned}$$

Based on these simplified analytic forms, the derivatives, $\partial\Gamma/\partial a_k$, $\partial\Gamma/\partial\theta$, etc., needed in Eqn.(9) for the propagation of errors can be evaluated and combined to obtain an estimate for the error in the flux, expressed as σ_Γ/Γ. This is found to be given by

$$\begin{aligned}
\left(\frac{\sigma_\Gamma}{\Gamma}\right)^2 = & \left(\frac{\sigma_{a_k}}{a_k}\right)^2 + \left(\frac{D}{\Gamma}\frac{\sigma_{a_h}}{a_h}\right)^2 + \left(\frac{D}{\Gamma}\frac{\sigma_{\Delta z}}{\Delta z}\right)^2 + \left(\frac{B}{\Gamma}\frac{\sigma_{\theta_-}}{\theta_-}\right)^2 \\
& + \left(ln\theta\, \sigma_{b_k}\right)^2 + \left(\frac{D}{\Gamma}\frac{\sigma_{b_h}}{b_h}\right)^2 + \left(ln\theta\, \frac{D}{\Gamma}\sigma_{b_h}\right)^2 \\
& + \left(\left(- \frac{A}{\Gamma}(b_h + b_k) + \frac{B}{\Gamma}(b_h + b_k - 1) - \frac{K}{\Gamma}(b_k) \right) \left(\frac{\sigma_\theta}{\theta}\right) \right)^2 .
\end{aligned}$$

(13)

Most of the terms have small uncertainties, probably about 10% (normalized) or better, considering a 'precision' error. Therefore the terms of the form $(\sigma_u/u)^2$, where u is any one of the independent variables, are each much less than unity. Similar terms including factors of D/Γ or B/Γ are also small since these factors are also less than one.

To simplify the term on the last line of Eqn. 13, we assume realistic values and evaluate these terms. Note that $|A/\Gamma|$, $|B/\Gamma|$, and $|K/\Gamma|$ are all less than or equal to one. Typical parameter values are $b_h = -1.3 \pm 0.3$ and $b_k \sim 7 \pm 0.5$ [Ref.25], and it is always true that $(b_h + b_k) < b_k$ since $b_h < 0$. This implies that the third line is less than $\left(b_k \left(\frac{\sigma_\theta}{\theta}\right)\right)^2$, which is approximately equal to 0.5 using $b_k = 7$, and $\sigma_\theta/\theta = 0.1$. The 'precision' error for neutron probe moisture measurements is better than 10% if the moisture volume content exceeds 1%, so this is a maximum magnitude for this term at most locations.

For $\theta = 0.02 - 0.2$, then $ln\theta \sim 2 - 4$, where 4 applies at the low moisture content end of the range. The two terms containing $ln\theta$ then both exceed unity and dominate the error propagation. Retaining these two terms, the total error is then approximately,

$$\left(\frac{\sigma_\Gamma}{\Gamma}\right)^2 \sim \left(ln\theta\, \sigma_{b_k}\right)^2 + \left(ln\theta\, \frac{D}{\Gamma}\sigma_{b_h}\right)^2, \tag{14}$$

which, in the low moisture content region, is estimated as

$$\left(\frac{\sigma_\Gamma}{\Gamma}\right)^2 \sim (4 \times 0.5)^2 + (4 \times 0.5 \times 0.3)^2 = 4 + 0.4 = 4.4,$$

or

$$\sigma_\Gamma^2 \sim 4.4\, \Gamma^2. \tag{15}$$

About 10% of the error comes from the uncertainty in the exponential parameter for the matric potential curve fit and the rest comes from the uncertainty in the exponential parameter describing the unsaturated hydraulic conductivity. While these exponents could be independently determined from experimental data, in the van Genuchten-Maulem model,[3,16] the exponents are not independent.

This uncertainty analysis shows that the error associated with each point is larger than the mean value. This is characteristic of a log-normal distribution, which in this analysis has $\sigma_g = \sqrt{4.4} \sim 2.1$ and is limited by the exponent of the moisture content used to characterize the unsaturated hydraulic conductivity. The implication, that the error for each point is larger than the mean, is that we need to interpret the results in terms of overall trends supported by each of the holes and by flux averages computed over large segments of the holes. In these average trends, the associated error is reduced in proportion to the number of observations included in the trend observation.

In this analysis, the error is dominated by a single term related to the uncertainty in the exponent for hydraulic conductivity. A direct analog in the van Genuchten-Maulem model does not exist, but in that case, the error must be related to the van Genuchten exponent, N, as confirmed in a numerical error analysis of the van Genuchten parameters[27], as summarized in the following section. Since N is typically 1.5 - 2 and $b_k \sim 7$, it is reasonable to conclude that the error in the van Genuchten scheme is proportional to about four times the error in the exponent, N. The magnitude of the error does not depend upon the fitting scheme used to define the unsaturated transport functions, so the result that $\sigma_g \sim 2.1$ applies, independently of the fitting model used. Note that this value depends upon the assumption that $\sigma_{b_k} = 0.5$, which was an estimate, and was not quantitatively determined from site data.

As a final note, a moisture source term examined in this study was given by Eqns. 7 or 8. This source is the difference between flux at two adjacent points. The propagation of errors applied to the difference of two terms will double the magnitude of the error for the source term relative to that derived above for the flux at each point, giving an error for the source terms in this analysis expressed as a geometric deviation of $\sigma_g = 2x2.1 = 4.2$.

Minimum Detectable Flux

A minimum detectable flux of the liquid phase can be derived from the uncertainty or error analysis. In this section, we numerically evaluate the uncertainty in the flux derived from unit-averaged van Genuchten relations. This is described in detail for the vapor phase flux elsewhere[27]. The minimum detectable flux can be considered as that flux which is statistically discernible from a zero flux estimate, and as such, is related to the standard deviation or width of the uncertainty of the flux estimate. We consider a marginally detectable liquid phase flux, Γ_{min}, (to be denoted *LLDflux* in the subsequent result figures, where *LLD* refers to a lower limit of detection) and define it to be equal to the error expressed as one standard deviation of the flux estimate, σ_Γ. Thus,

$$\Gamma_{min} = \sigma_\Gamma . \tag{16}$$

To evaluate the uncertainty in our flux estimates, Eqn. 3 is rewritten for the magnitude of the liquid flux in the form,

$$\Gamma[cm/yr] = -K[\theta]\{\nabla h_m + 1\} = \frac{K[cm/yr]}{\Delta z}(h_{m1} - h_{m2} + \Delta z), \tag{17}$$

where h_{m1} and h_{m2} are matric potentials (heads) evaluated at adjacent points separated in space by vertical distance, Δz, each evaluated in the same units of length. The uncertainty in the flux, σ_Γ, is evaluated in terms of uncertainties in h_{m1}, h_{m2} and K, represented respectively by σ_{h1}, σ_{h2} and σ_K. Assuming these uncertainties are not correlated and that uncertainties in the distance, Δz, are negligible, this gives

$$\sigma_\Gamma^2 = \left(\frac{\partial\Gamma}{\partial K}\right)^2 \sigma_K^2 + \left(\frac{\partial\Gamma}{\partial h_1}\right)^2 \sigma_{h1}^2 + \left(\frac{\partial\Gamma}{\partial h_2}\right)^2 \sigma_{h2}^2 . \tag{18}$$

Evaluating the derivatives in Eqn. 18 from the flux given by Eqn. 17, and further simplifying with the reasonable assumption that matric potential uncertainties at adjacent points are comparable, or $\sigma_{h1} = \sigma_{h2} = \sigma_{hm}$, then the flux uncertainty becomes

$$\sigma_\Gamma^2 = \left(\frac{h_{m1} - h_{m2}}{\Delta z} + 1\right)^2 \sigma_K^2 + 2.\left(\frac{K}{\Delta z}\right)^2 \sigma_{hm}^2 . \tag{19}$$

The minimum detectable difference in matric potentials, $|h_{m1} - h_{m2}|_{min}$, is related to the uncertainties in matric potential, and again using a 'marginally detectable' criteria related to one standard deviation then

$$|h_{m1} - h_{m2}|_{min} = 2\,\sigma_{hm} , \tag{20}$$

and so the flux uncertainty becomes

$$\sigma_\Gamma^2 = \left(\frac{2\,\sigma_{hm}}{\Delta z} + 1\right)^2 \sigma_K^2 + 2.\left(\frac{K}{\Delta z}\right)^2 \sigma_{hm}^2 . \tag{21}$$

In deriving h_m with the unit-averaged van Genuchten parameters from the moisture content, then the uncertainty in h_m is assumed to depend primarily on the uncertainties associated with the parameters, N_{vg}, α_{vg}, and moisture content, θ. Uncertainty in the porosity and residual moisture contents are neglected. This is reasonable for porosity when in the dry regime far from saturation. It is a necessary simplification for the residual content, since the analyses proceeded under the simplification that residual content equals zero in order to assure that all field data values for moisture content are associated with a real matric potential in the van Genuchten fits. In this simplification, the matric potential uncertainty from the van Genuchten method, σ_{hm}, is written,

$$\sigma_{hm}^{\ 2} = \left(\frac{\partial h_{vg}}{\partial \theta}\right)^2 \sigma_\theta^{\ 2} + \left(\frac{\partial h_{vg}}{\partial N_{vg}}\right)^2 \sigma_{nvg}^{\ 2} + \left(\frac{\partial h_{vg}}{\partial \alpha_{vg}}\right)^2 \sigma_{\alpha vg}^{\ 2} . \qquad (22)$$

The hydraulic conductivity is assumed to depend primarily upon the saturated hydraulic conductivity, K_{sat}, the moisture content, and the van Genuchten parameter, N_{vg}. The uncertainty in the unsaturated conductivity derived from the moisture profile and the van Genuchten relations is then,

$$\sigma_K^{\ 2} = \left(\frac{\partial K_{vg}}{\partial \theta}\right)^2 \sigma_\theta^{\ 2} + \left(\frac{\partial K_{vg}}{\partial N_{vg}}\right)^2 \sigma_{nvg}^{\ 2} + \left(\frac{\partial K_{vg}}{\partial K_{sat}}\right)^2 \sigma_{Ksat}^{\ 2} . \qquad (23)$$

The derivatives in these Eqns, 22 and 23, are evaluated numerically from the van Genuchten relations in a spreadsheet analysis. The best estimates for the uncertainties in the dependent terms as applied to this study are, $\sigma_\theta = 0.001$ [volume fraction], $\sigma_{nvg} = 0.06$ and, expressed as fractions of the mean values, $\sigma_{\alpha vg} = 0.2\ \alpha_{vg}$ and $\sigma_{Ksat} = 0.2\ K_{sat}$. The values for σ_θ and for $\sigma_{\alpha vg}$ are discussed in [27], and σ_{nvg} and σ_{Ksat} values are discussed in the following.

The variation in saturated hydraulic conductivity, K_{sat}, within a given stratigraphic unit is typically 100% or more [2,4,5]. However, the uncertainty we wish to characterize here is not an overall result accuracy but the uncertainty in assuming K_{sat} is constant between two adjacent measured points. Thus, we need a measure of the variability of K_{sat} between adjacent profile measurement points as used in the flux analysis. This is estimated by considering the values measured at Area G [17] in borehole NPH-5 (G-5) as seen in Fig. 24. The uncertainty at a given point is estimated to be equal to a normalized difference in K_{sat} at adjacent spatial locations, $\delta K_{sat}/K_{sat}$, evaluated as the in-field observed gradient in K_{sat} times the distance, δz_m, between two points where the moisture profile measurements are typically made. These assumptions are written as

$$\frac{\sigma_{Ksat}}{K_{sat}} \sim \frac{\delta K_{sat}}{K_{sat}} \sim \frac{\frac{\partial K_{sat}}{\partial z}\delta z_m}{K_{sat}} \sim \frac{(K_{sat1} - K_{sat2})\ 2\ \delta z_m}{(z_1 - z_2)\ (K_{sat1} + K_{sat2})} . \qquad (24)$$

This estimate of the error in the saturated hydraulic conductivity is labeled *dKsat/Ksat*dzm/dz* in Fig. 24 and shown for the in-situ data, assuming $\delta z_m = 3' \sim 1m$. The value is less than or equal to about 0.2 at most points. At most locations then, it is expected that $\frac{\sigma_{Ksat}}{K_{sat}} < 0.2$.

The uncertainty in the van Genuchten exponent, σ_{nvg}, is seen in numerical evaluations[27] to dominate the errors especially at low moisture content, consistent with the analytic results in the previous section. Typically, the Bandelier Tuff stratigraphic unit average statistics show a standard deviation for the van Genuchten exponent of about $\sigma_{nvg} = 0.2$ [Ref.2] or about 10% of N_{vg} across each stratigraphic unit. The variation between two adjacent points is likely to be much smaller. This is seen in Fig. 25 where the van Genuchten exponent, N_{vg}, derived from core samples recovered from 10 ft depth intervals[13] is plotted verses depth in borehole NPH-5 (G-5).

A normalized gradient is used to estimate the variance expected in N_{vg} between two adjacent measurement points (separated by 1m) as discussed above for the K_{sat} error estimate. This is shown in Fig. 25, labeled, $dN/N*dzm/dz$. Most values are seen to less than 0.03 and since N is typically close to 2, then the magnitude of the error in N_{vg} is about, $\sigma_{nvg} = 0.03 \times 2 = 0.06$ at most field locations. This method is a simple means of estimating a spatial correlation scale length for the parameter.

A simpler but less conservative estimate of the variance between two measurement points is to take the variance associated with the stratigraphic unit[2] and simply assume the variance between two adjacent measurement points will be the total unit variance times the distance between two measurement points divided by the total unit thickness. For a 'typical unit thickness' in Area G of about 10m, and $dzm = 1m$, then for $\sigma_{nvg} = 0.2$ associated with the unit, we expect $\sigma_{nvg} \sim 0.02$ associated with the variation between two measurement points at 1m separation.

Using these estimates of uncertainty or error between adjacent measurements in the field then the error terms in Eqns. 22 and 23 are determined, the derivatives are evaluated numerically using the van Genuchten relations, and the equations are solved for σ_{hm} and σ_K. These values are combined in Eqn. 21 which is a measure of the flux detection limit per Eqn. 16. This flux detection limit is shown as a function of moisture content in Fig. 26 for the three values discussed above of uncertainty in the van Genuchten exponent, σ_{nvg} (and labeled dN in the Figures). The value $\sigma_{nvg} = 0.06$ is assumed to apply to the present study. The detection limited flux as a fraction of unsaturated flux is actually decreasing with moisture content, but not as fast as the unsaturated flux increases, thus the detection limit increases significantly with moisture content.

Results in Fig. 26 apply to the averaged van Genuchten parameters for the stratigraphic Unit 2b. These results are compared to the flux detection limit using van Genuchten parameters for Unit 1b in Fig. 27. In Unit 1b, a lower liquid phase flux is detectable at any given moisture content. Results for Unit 2a are similar to that for 2b. Results for the other Bandelier Units are expected to be approximately bracketed between results for Units 2b and 1b, by comparison to their hydraulic conductivity curves[27].

The detection limits derived from this uncertainty analysis can be compared to flux results predicted in the field boreholes. The region around the vapor phase notch was seen to exhibit an apparent moisture source and large moisture flux. In Fig. 28 the maximum magnitude of liquid phase flux observed near the vapor phase notch, for each of the six boreholes in this study which penetrated that region, is plotted against the peak value of moisture content in that region from that borehole. This is compared to the detection limit curve for Unit 1b (in which the vapor phase notch lies), and it is seen that the magnitudes of observed flux in each hole is consistent with the expected uncertainty in that Unit at that moisture content. This supports the notion that the apparent source at the vapor phase notch may not be a source of real moisture but may be an unresolved variation in

matric properties which consistently occurs near the notch region. This possibility is consistent with unique properties of the notch observed at other locations outside of Area G [22].

On the other hand, the points in Fig. 28 are plotted at the maximum moisture content associated with the borehole profile. In some cases, this maximum is a narrow peak and not aligned exactly with the position where the maximum moisture flux is indicated. If one assumes that the actual moisture content is slightly less at the borehole position where the maximum flux occurs, then the borehole points in Fig. 28 move slightly to the left. Most points would then indicate flux levels which are above the detection limit, and correspond to a real source. Thus, the 'source' indicated at the notch region remains ambiguous.

In Fig. 29, the magnitude of the moisture flux resulting from the analysis at all depths in two of the boreholes is shown verses the moisture content at that borehole location. These two boreholes were chosen because they bracket the field results where LGM-85-11 is an 'extreme moist case' and NPH-9 (ER1111) is an 'extreme dry case'. The field results are compared to the minimum detectable liquid phase flux in Unit 2b and in Unit 1b, using the best estimate of the uncertainty in the van Genuchten exponent, σ_{nvg} (labeled *dN* in Fig.) = 0.06. It is seen that most of the flux levels determined are below the flux detection limits, and therefore cannot be considered as accurate values, but rather are 'below detection limit' results. As above, those points which lie very near to the detection limit curves are ambiguous and may or may not be significantly determined flux levels. About 10% of the moisture flux determinations appear to the left of the detection limit curves and are likely to indicate real flux values.

Figure 30 compares the minimum detectable liquid phase flux in Unit 2b to the uncertainty in unsaturated hydraulic conductivity, σ_K, (labeled *sigmaK* in the Fig.), for the best estimate of the uncertainty in the van Genuchten exponent, σ_{nvg} (labeled *dN* in Fig.) = 0.06. The *(sigmaK)* value is an estimate of the recharge or vertical flux uncertainty under unit gradient conditions where the recharge rate is simply the unsaturated hydraulic conductivity evaluated at the in-situ moisture content. The comparison shows that the flux uncertainty is dominated by that of the unsaturated hydraulic conductivity at higher moisture contents where the two curves are comparable. The minimum detectable gradient in matric potential contributes significantly to the overall flux uncertainty in the dry range, where the two curves diverge.

In regions where it can be shown that the unit gradient assumption applies (e.g., where moisture content and matric properties are on the average constant with depth), then the detection limit for the vertical flux or recharge rate will be just (*sigmaK*). There is a substantial improvement in detection limit and therefore in estimating small recharge rates in the dry moisture range, when the unit gradient assumption can be justified.

The flux detection limits under unit gradient conditions, expressed as *(sigmaK)* derived from the van Genuchten averaged properties in three stratigraphic units are shown in Fig. 31. It is seen, for example, that in a region within the Otowi member where the unit gradient assumption applies, if the moisture content is 10-20%, then the respective flux uncertainties are about 0.4 - 10 cm/yr. Conditions similar to this example are observed in moisture profiles under some canyon locations at Los Alamos[5]. The flux uncertainties at these locations are large and may limit meaningful predictions of flux levels.

The minimum detectable flux described here relates to each flux determination in the profile as an independent measurement. Each flux estimate which can be grouped within a similar region (e.g., the low flux region) contributes to a mean flux estimate over that region (as summarized in Table II) which has its own associated uncertainty. Propagation of errors analysis shows that the error associated with the mean of *n* determinations, each with an error, σ, is equal to $\sigma/\sqrt{n}$. A typical

borehole profile with 15 flux estimates throughout the 'low flux region' would then have an error in the average flux throughout that region of almost four times less than that associated with each flux determination.

The sum of all flux estimates over all boreholes (the summary mean values in Table II) involves about 100 points and therefore about a factor of ten reduction in the error associated with the mean estimated over that whole region. Referring to Fig. 29, one sees that a reduction by a factor of ten in detection limit puts us into the regime of most of the individual point flux estimates, e.g., the detection limit for a trend in flux averaged over 100 points in Unit 2b at 1.5% moisture content is about $1.x10^{-3}$ cm/yr. This suggests the region-averaged flux values are reasonable estimates of the region mean flux in spite of the high detection limits on each point. However, it is not clear if the variance throughout each region is associated with a real variation in flux or with variation in matric properties throughout the region.

DISCUSSION

Three Subsurface Transport Regions

The data and analyses reveal several trends. The Area G subsurface can generally be characterized by three regions. A 'near surface region' has a variable depth with hole location from about 5m to more than 10m and is characterized with a decreasing moisture content typically from 6-12% near the surface to < 2% at depth. Below this is a 'low flux region' characterized by low moisture content, and small vertical fluxes and source terms in this analysis which are typically less than 0.1 cm/yr locally (at any depth), less than 0.03 cm/yr in any hole, and less than 0.002 cm/yr averaged over the 'low flux' region and over all the holes. The third region is a moisture peak near the vapor phase notch or 1b-1a interface. This is apparently associated with a moisture source term and local flux although the average vertical flux over the range of this third region is small in most cases. Limited data below this third region makes it more uncertain, however, it appears in this analysis that below this 'notch region' the flux returns to a 'low flux regime'.

These trends are quantified in Table II which summarizes for each region, the depth intervals, the interval-averaged fluxes and source terms. The large variability associated with the 'near surface region' led to a geometric mean as the best characterization of the values in that region. The other regions were characterized with arithmetic means, required to meaningfully average the flux values of changing sign. Results at hole NPH-4, which was observed to be near an engineered drainage area and quite different from any other hole, were eliminated before taking the geometric mean because its inclusion skewed the results excessively.

The near surface region has a geometric mean depth of 7.8m (~25') with a geometric standard deviation of 1.6, suggesting that 'plus or minus one sigma' of the holes fall between 7.8/1.6 = 4.9m and 7.8*1.6 = 12.5m. The mean flux in this region is -0.94 cm/yr, about 1 cm/yr downward, with a geometric standard deviation of 3.9, characterizing a large variability in the results. The source term mean is -0.11 cm/yr, about 1 mm/yr net evaporative loss. The variability is huge ($\sigma_g = 20.6$) presumably skewed by two holes which have very small source terms (NPH5 and NPH9). Eliminating these holes from the statistical sum gives a reasonable source mean of -0.37 cm/yr, or about 40% of the vertical flux, and a more reasonable geometric deviation, $\sigma_g = 4.2$.

The depth, flux terms, and moisture content in this near surface region appear to be determined by the extent that the local site has been disturbed by adjacent engineered operations associated with

waste disposal. The natural distribution of surface-connected fractures in the immediate area of the monitor hole may also play a role in some holes, notably NPH-5 (G5), and in the nearby, recently drilled test hole, ER-1107 [ref.24].

A low flux region is characterized below the near surface region. In the Table II, this low flux region is characterized with a depth down to the 'vapor phase notch' region, however, the data are also consistent with a low flux region extending down to greater depths than examined in this study, with the vapor phase notch region imposed as a local perturbation on top of a low flux region continuing to greater depths. The depth of the vapor phase notch region has an arithmetic mean of 21 ± 5.4m. Over the low flux region, the maximum downward net flux in any hole is 0.007 cm/yr and the average flux over all the holes is 0.0017 cm/yr upward. The source term average is -0.013 cm/yr implying net evaporation, consistent with a net upward movement. The magnitude of these terms are all considered negligibly small, consistent with the large characteristic time scales for the source terms.

The vapor phase notch region, or units 1b-1a interface is somewhat arbitrarily identified in Table II as the range of depth for the moisture spike and the significant flux sources associated with this region, as seen in the earlier figures. This gives a mean range for the region from 21.3m to 34m. Though the local flux and source terms were seen to be significant in most cases, the integral flux and source terms over the region as shown in Table II, are small. The maximum region downward flux is 0.43 cm/yr calculated in two holes, while the average downward flux over all the holes over this region is 0.073 cm/yr or less than 1 mm/yr. The derived source magnitude is 0.032 cm/yr, for a small net influx. The standard deviations show a relatively large variability imposed on the small mean values, but the deviations are still small in terms of absolute values of flux, i.e., ±0.3 cm/yr for the vertical flux.

Source Term at Vapor Phase Notch

The vapor phase notch region shows interesting local characteristics in this analysis as seen in the previous figures. A positive source term, possibly influx from a localized horizon, is flanked by two horizons in which the moisture is moving away vertically (up above the source and down below the source) and simultaneously being lost to horizontal movement or evaporation in the two horizons adjacent to the source. The source average over the adjacent regions (in Table II) becomes a small net value for all of the boreholes examined. Alternatively, the results may reflect variable hydrologic properties in the region which are not well characterized.

One possible physical interpretation is that this source horizon is connected to a more saturated canyon region (Pajarito Canyon is the likely candidate at Area G) and the adjacent horizons are also surface-connected but to a less saturated region which thus acts as a sink. Another possible interpretation of the results is that this horizon is bringing in moisture from 'upstream' locations to the west (along the axis of the canyons), and the source represents a significant lateral moisture movement.

A third possibility to explain this apparent source as a real physical mechanism, is that there is a significant fracture network which is connected to the surface of the mesa and extends downward ending somewhat abruptly at the horizon of the vapor phase notch, or at the Units 1b-1a interface. This could allow infiltration through open fractures during heavy summer thunderstorms, which then moves rapidly downward to the bottom of the fracture network. The water sits there and is wicked horizontally into the Bandelier Tuff matrix at this horizon, producing the large local moisture peak. Simultaneously, the water spreads from the source horizon into the matrix and migrates back towards the fracture, driven by evaporation from the fracture. Eventually most of the water evaporates, leaving a small net source term when averaged over the region.

This possible source mechanism is consistent with the magnitude of the source term expressed as a characteristic time scale which was seen to be as small as one per year near this horizon in several borehole results. This supports the hypothesis of an annual influx. This mechanism would be consistent with stratigraphic unit properties which are approximately constant with elevation through the vapor phase notch region. This source mechanism seems a likely candidate to explain the field data and analyses, and will be tested against detailed field data to be collected in the near future. However, the moisture spike at the vapor phase notch is observed at other locations (e.g., TA-49) where the depth from the surface to the notch is much greater (~400'), making it less likely to be surface-connected by a fracture network, and more likely to be a region of significant lateral movement.

Another possibility is that the present analysis is giving erroneous results, and there is no significant source at this horizon. The analysis is based on the assumption that matric potential properties throughout a stratigraphic unit are approximated by the average value for the unit, although it is known there are large variations within a unit. If the variations are consistent in some way, e.g., the van Genuchten exponent, N, increases linearly with depth throughout unit 1b, then the present analysis can give erroneous results. If there exists a horizon near the vapor phase notch, where the matric properties are significantly different than the average values assumed (i.e., different from either unit 1b or 1a properties), then it would be possible to match the field observed moisture profiles while maintaining insignificant vertical flux and source term in these horizons. The flux detection limit analysis showed (Fig. 29) that the flux and source terms implied in the field near the notch region are within the range of uncertainty of the analysis, supporting the possibility that the apparent sources are not real but due to consistent matric property variations in the region.

The issue, whether or not a moisture source exists at the vapor phase notch, is important for understanding the unsaturated transport beneath the mesa. This will influence our understanding of the net vertical flux in and beneath the mesa top and therefore it is a critical issue for completing the Performance Assessment. The issue can be resolved by collecting core samples through the vapor phase notch region and doing a complete matric potential characteristic curve for each sample throughout this region. Care must be given in collecting the core to consider the possibility that the important controlling horizon may be very thin.

Below the vapor phase notch, there are limited data. In the present study, several holes (LGM-85-06, LGM-85-11, NPH-9, 54-1002) suggest a negligible vertical flux in the region below the vapor phase notch. The most data in this region included in the present study is from hole, 54-1002, (Fig. 19-20), which showed vertical flux << 0.1 cm/yr at all points (Fig. 20) and the average over the interval below the vapor phase notch (45-75m) of -0.004 cm/yr. The small average flux in that hole and the small average flux values over the vapor phase notch region as summarized in Table II each point to the possibility that the 'low flux region' actually extends deeper beyond the 'notch region' and that the 'notch region' is not more than a perturbation imposed on top of a continuous low flux region. The data in this hole, ER-1002, shows anomolously large flux magnitudes in the lowest interval, in the Cerro-Toledo unit. This needs further study to see if lateral flow or other effects are significant at that horizon.

Uncertainty Implications

The uncertainty analysis shows that the magnitudes of flux predicted at most borehole locations are within the range in the uncertainty in flux due to the variance in model parameters and field data. To some extent this variance is attributable to spatial variations in matric properties which could be resolved more carefully in field investigations. The potential moisture source term observed near the vapor phase notch region is significant enough to warrant such further investigation. At some

point where the variance due to real spatial variations is minimized, the flux detection limits derived from this analysis method will be limited by the experimental reproducibility in the determinations of the matric properties.

Most of the flux values implied at points throughout the borehole profiles in this analysis are not quantitatively accurate but are indications of flux below the 'detection limits', derived and quantified in this study. Thus it can be said that the flux at most points is less than the detection limits for a given moisture content as shown in Fig. 27. It is expected that the trends in moisture flux observed across the boreholes are qualitatively correct and that the average flux value determined for each of the different regions is a good 'representative value' of the 'expected flux' in each of those regions, as discussed at the end of the section on the Flux Detection Limits. This could be quantified more thoroughly in future work by evaluating in greater detail the reduction in error when estimating a mean quantity from a large number of independent estimates of that quantity.

Flux Implications

The results section presented the vertical flux source as a characteristic time scale for change in the moisture content. This value was seen to vary widely, with a minimum of about one year or more in the moist regions in most holes. A seasonal variation was evident in the near-surface of one hole (NPH-2). In an engineered drainage area, hole NPH-4 showed a time scale of less than one year. The magnitude of the source term in the low flux region of most holes increased to more than 1000 years reflecting the low turnover rate of moisture there by liquid phase movement.

Throughout the vertical profiles, and especially in the low moisture content region, the unit gradient assumption is not valid for estimating flux in this region. Small variations in moisture content correspond to large variations in matric potential which significantly change the vertical flux from that predicted as the unsaturated hydraulic conductivity. These small changes in moisture content often predict a small fluctuating moisture flux which may reflect real transport between local pockets or may reflect the error and uncertainty in this analysis.

Vapor phase loss by evaporation to surface connected features has been posited as a dominant mechanism in shaping the near-surface moisture profiles. Vapor phase transport, including effects of fractures in the matrix material, has not been analyzed in this report but will be the subject of a second report[27]. Anticipating those results, the vapor phase movement in the matrix is expected to play a role in the drier regions of the mesa top.

The present analysis showed that NPH-5 (G-5) did not exhibit the typical profile observed at many other locations, having a high moisture content which did not decrease appreciably with depth until below 17m. The observations may be consistent with a highly fractured region. The 17m horizon is coincident with the interface of units 2b and 2a (where 2b is more fractured) and also with the approximate depth of the adjacent disposal shafts and pits which could contribute to the flux and source terms seen at this hole. Moisture, including some infiltration from adjacent disturbed areas or from fractures, moves downward until the fractures end at the unit interface, and the remaining moisture at this depth evaporates to the fractures. This analysis shows that G-5 is not a good 'representative hole' for Area G profiles in general, however, it is similar to a recent profile in a nearby hole, ER-1107 {Ref.24], and may characterize a region in the central portion of Area G.

In previous analysis for hole G-5 [13], it was suggested that a unique horizon existed at the 2b-2a interface where vapor phase losses occur. The present analysis suggests that the horizon is not especially unique, but rather the increased moisture content and flux throughout the upper 2b layer is unique. This supports the notion of an effect from adjacent disposal operations or surface-

connected fractures. The impact of either could be reasonably expected to be limited to the Unit 2b layer. Vapor phase movement at this horizon will be discussed in a separate report[27], where it will be shown that vapor phase flux is significant under the moisture conditions observed in hole G5, only below the depth of 17m at the 2b-2a interface.

It is not clear that it would be worth applying the present analysis to moisture data in other deep holes due to the limited matric property data and therefore the large uncertainty in the results at the greater depths. On the other hand, it is important to pursue this type of analysis at greater depths for modeling calibrations and site characterization. It is expected that the flux at depths below possible canyon source terms is more characteristic of that through the bulk of the unsaturated zone, and therefore this is important to know for site performance. This can be examined in a future study.

Disposal Operations

Disposal operations appear to contribute to the moisture profiles in the near-surface layer and act to increase its variability above that expected in undisturbed locations. This was evidenced by increased moisture content and flux at locations adjacent to disposal units and trenches as discussed in the Results Section. At one location (NPH-4) the engineered drainage has increased the typical moisture content by 4-5 times corresponding to an increased vertical flux of 100-200 times that in the relatively 'undisturbed' locations. The borehole is not deep enough to determine if the increased infiltration has penetrated through the 'low flux region' at this location. The results show that the hydrology can be disturbed relatively easily by unchecked disposal operations, although long term effects are uncertain.

In relatively undisturbed areas, the mesa provides an excellent natural barrier to transport, however, in the disturbed locations the integrity of the natural transport barrier is compromised. A desirable goal in disposal operations is to minimize the potential for contaminant migration. This requires minimizing operations that add water to the mesa top and avoiding surface engineering which enhances local infiltration of natural precipitation or which reduces the large natural evapotranspiration. All surface paving, culverts, drainages, etc., should be designed to direct water away from covered and from open (actively used) disposal units. Adequate vegetative covers similar to the natural systems must be maintained to assure significant evapotranspiration. New and continuing operations should be reviewed regularly with respect to meeting specific requirements derived from these general considerations.

The depth of the low flux region or the top of the vapor phase notch region is comparable to the depth of the deeper disposal units in the area. As such, the low flux region may not provide a thick barrier to contaminants moving from the bottom of a disposal unit. This emphasizes the importance of determining if the 'low flux region' continues to greater depths with the vapor phase notch region as a small local perturbation.

Numerical Modeling Implications

These results have important implications for numerical modeling of the contaminant transport from the disposal unit and can be used to help calibrate numerical models to obtain realistic moisture flow fields which account for localized variations in recharge rate. Specifically, the source terms derived in this analysis can used to provide input to numerical models. This should provide better agreement between numerical models and the field data, than that obtained with the more restrictive source term assumptions of a net infiltration only at the mesa top surface. These results, in conjunction with other analyses on vapor transport[27], may be applied towards

completing a conceptual model of the complex flow in the mesa stratigraphy, and towards quantifying the contributions from liquid and vapor flux.

CONCLUSIONS

The flux analysis shows that unsaturated vertical transport in the mesa under the disposal site, Area G, can be characterized in three regions. A near surface region is influenced by infiltration and disposal operations and is spatially variable. It extends to 7.8m ± 1.6, has a downward vertical flux of 0.94 cm/yr ± 3.9, and a characteristic vertical flux source term of -0.37 cm/yr ± 4.2 (geometric means and standard deviations). The source term is about 40% of the vertical flux, with the difference assumed to be vapor transport, to be examined in a separate study. Below this variable near-surface region, a low moisture flux region exists to at least 21.3 ± 5.4 m with average vertical flux (upward) of +0.0017 ± 0.011 cm/yr (arithmetic values). These flux values are negligible and comparable to the analysis errors. At greater depths, the vapor phase notch region is characterized with a moisture peak and derived downward average flux of -0.073 ± 0.311 cm/yr. This large variability suggests the net flux from this region to greater depths depends strongly on location.

The data at the vapor phase notch suggest a moisture source which is dissipated by vertical motion and evaporation from the source horizon located at the peak in the moisture profile. A number of physical mechanisms were discussed which could contribute to this apparent source. One candidate mechanism, based on assessment to date, assumes a fracture network which is surface connected and ends abruptly near the Unit 1b-1a interface. Major storm events could potentially send water to the bottom of the fracture network where it will soak horizontally into the Bandelier Tuff matrix. This could produce the apparent source seen in the present analyses, and would represent a real and important source term possibly driving moisture flux at greater depths.

The apparent source may also be a non-physical artifact resulting from the analysis assumption of constant stratigraphic unit-averaged hydrologic properties. If this region has matric properties which are significantly different from the adjacent horizons, then the observed moisture profiles could be consistent with a flux which is everywhere negligible throughout the region. On the other hand, a horizon with distinct properties is likely to be associated with a real lateral moisture flux since the vertical variation in properties may act to interrupt vertical moisture flux. It is critical to distinguish these possibilities and determine if the apparent source term is physical or not, because this region may or may not provide a moisture source driving flux at greater depths throughout the unsaturated zone beneath the mesa. This controls the overall unsaturated transit time to the ground water and thus the impact on the site Performance Assessment depends critically upon resolving the hydrologic flows in this region. The source term derived in this analysis can be used in numerical studies to improve the accuracy in the Area G PA effort.

The large variability of moisture and flux in the near surface region indicates that operations may have a significant impact on the near surface unsaturated transport. Under extreme conditions as seen at the hole, NPH-4, near the drainage basin, operations could impact transport in deeper regions, and compromise the natural isolation provided by the low flux region. Any disposal operation which increases local moisture content or decreases evapotranspiration will degrade the natural integrity of the disposal site and degrade the site performance to some extent, and therefore, these operations should be reviewed regularly for impact.

The uncertainty analysis indicates that many of the flux result values are less than the estimate of the flux uncertainty, and therefore must be regarded as 'below the detection limits' of liquid flux

for this analysis method. While specific flux values are less than detectable, the flux trends indicated by the composite of values and by the averages over regions are good estimates of the average flux. The flux detection limits could be improved with additional field data, because the variance in the input parameters used in the present analysis reflects a real spatial variance in material properties which could be resolved in limited regions (e.g., in one or more selected boreholes). Ultimately, the flux detection limits in this type of analysis will be limited by the experimental uncertainty associated with the reproducibility in measuring the matrix properties needed to define the moisture characteristic curves and the saturated hydraulic conductivity.

ACKNOWLEDGMENTS

This work was sponsored by the U.S. Department of Energy, Waste Management Programs, as part of the Area G site Performance Assessment required per US DOE Order 5820.2A. The author wishes to thank Everett Springer and David Rogers for thorough and critical reviews of the draft manuscript, and David Broxton for helpful discussion on possible lateral flow at the vapor phase notch.

REFERENCES

[1] - D. Hollis, E. Vold, K. Birdsell, J. Turin, P. Longmire, E. Springer, W. Hansen, D. Krier, R. Shuman, "Performance Assessment of LANL TA-54, Area G, LLRW Disposal Facility - Preliminary Draft", Los Alamos National Laboratory, Los Alamos, NM, August, 1995.

[2] - D. Krier, P. Longmire, R. Gilkeson, H.J. Turin, "Geologic, Geohydrologic, and Geochemical Data Summary of MDA G, TA-54, LANL", Los Alamos National Laboratory Report LA-UR-95-2696, Los Alamos, NM, 1995.

[3] - van Genuchten, M. Th., "A closed-form equation for predicting the hydraulic conductivity of unsaturated soils", Soil Science Society of America Journal, 44, 892-898, 1980.

[4] - D. Rogers, "Unsaturated Hydraulic Characteristics of Bandelier Tuff at TA-54", Los Alamos National Laboratory Report LA-UR-95-1777, Los Alamos, NM, 1995.

[5] - Rogers, D. B., and B. M. Gallaher, "The Unsaturated Hydraulic Characteristics of the Bandelier Tuff"", 132 pp., Los Alamos National Laboratory Draft Report LA-12968-MS, May 1995.

[6] - Reneau, S. L. and D. T. Vanamin, "Fracture Characteristics in a Disposal Pit on Mesita del Buey, Los Alamos National Laboratory", Los Alamos National Laboratory informal report - unpublished - March 21,1994.

[7] - Turin, H. J., "Subsurface Transport Beneath MDA G: A Conceptual Model", Los Alamos National Laboratory Report LA-UR-94-1663, Los Alamos, NM, 1995.

[8] - K. Birdsell, W. Soll, N. Rosenberg, B. Robinson, "Numerical Modeling of Unsaturated Groundwater Flow and Radionuclide Transport at MDA G", Los Alamos National Laboratory Report LA-UR-95-2735, Los Alamos, NM, 1995.

[9] - International Technology Corporation, "Hydrologic Assessment of Technical Area 54, Areas G and L, Los Alamos National Laboratory", Final Report, Docket Number NMHWA 001007, Los Alamos National Laboratory, Los Alamos, NM, March, 1987.

[10] - Kearl, P. M., J. J. Dexter, and M. Kautsky, "Vadose zone characterization of Technical Area 54, waste disposal areas G and L, Los Alamos National Laboratory, New Mexico, Report 3: Preliminary assessment of the hydrologic system, Report GJ-44", Bendix Field Engineering Corp., March 1986a.

[11] - Kearl, P. M., J. J. Dexter, and M. Kautsky, "Vadose zone characterization of Technical Area 54, waste disposal areas G and L, Los Alamos National Laboratory, New Mexico, Report 4: Preliminary assessment of the hydrologic system through Fiscal Year 1986, Report GJ-54", UNC Technical Services, Inc., December 1986b.

[12] - Turin, H.J., Rosenberg, N.D., "Summary of TA-67 Geology, Hydrology, and Seismicity for Radiological Performance Assessment - FY93 Report", Los Alamos National Laboratory Report LA-UR-94-4399, Los Alamos, NM, 1994.

[13] - Rogers, D. B., Vold, E.L., Gallaher, B. M., "Bandelier Tuff Hydraulic Characteristics from Los Alamos National Laboratory (LANL) Borehole G-5 at MDA G, TA-54", draft, rev.1, completed July, 1995, Los Alamos National Laboratory Report, LA-UR-95-3129, Los Alamos, NM, 1995.

[14] - Koorevaar, P., Menelik,G., and Dirksen,C., Elements of Soil Physics, Elsevier Science, New York, 1983.

[15] - Loaiza, D. and Vold, E., "Moisture Profile Measurements in Subsurface Monitor Holes at the Los Alamos LLRW Disposal Site", Los Alamos National Laboratory Report LAUR-95-1922, Los Alamos, NM, submitted to the Journal, Environmental Monitoring, June, 1995.

[16] - Mualem, Y., "A new model for predicting the hydraulic conductivity of unsaturated porous media", Water Resources Research, 12, 513-522, 1976a.

[17] - Stephens, D. B., and Associates, "Laboratory analysis of soil hydraulic properties of G-5 soil samples, report no. DBSA/3854/195-1", prepared for Los Alamos National Laboratory, Los Alamos, New Mexico, January 1995.

[18] - E. Springer, "Area G Performance Assessment: Surface Water and Erosion", Los Alamos National Laboratory Report LA-UR-95-2497, Los Alamos, NM, 1995.

[19] - Conca, J., and T. J. Mockler, "Measurement of unsaturated hydraulic conductivity and recharge distribution in the Bandelier Tuff at Los Alamos", prepared for Los Alamos National Laboratory, Los Alamos, New Mexico, 24 pp., Northwest Environmental Services, March 1995.

[20] - Conca, J. L., and J. Wright, "Direct determinations of unsaturated flow and transport", Proceedings of the Twelfth Annual American Geophysical Union Hydrology Days Meeting, Fort Collins, 103-116, March 1992.

[21] - Turin, H.J., Rogers, D.B., Vold, E.L., "Determining unsaturated hydraulic conductivity of Bandelier Tuff; A comparison of characteristic curves and ultracentrifuge methods", Los Alamos National Laboratory report, LA-UR-95-1897, Los Alamos, NM, presented to the Kearney Foundation of Soil Science Conf., Davis, CA, June, 1995.

[22] - Broxton, D.E., Heiken, G.H., Chipera, S.,J., Byers, F.M., Jr., "Stratigraphy, petrography, and minerology of Bandelier Tuff and Cerro Toledo deposits", p.33 in Los Alamos National Laboratory report, LA-12934-MS, Los Alamos, NM, June, 1995.

[23] - Rogers, D. B., and B. M. Gallaher, "Moisture and Matric Suction Profiles for 1994 MDA G Wells", 7 pp. and 3 figures, Los Alamos National Laboratory Memo ESH-18/WQ&H-94-632, December 19, 1994.

[24] - Gilkeson, R., Kisiel, K., Marin, J. personnal communication, ERM/Golder Corp., unpublished moisture and matric potential data from Area G boreholes in series 1100-1125 for the LANL Environmental Restoration program (1996).

[25] - Abeele, W.V., "Hydraulic Testing of Crushed Bandelier Tuff", Los Alamos National Laboratory Report LA-10037-MS, March, 1984, and see also Abeele, W.V., Wheeler,M.L., Burton,B.W., "Geohydrology of Bandelier Tuff", Los Alamos National Laboratory report, LA-8962-MS, October, 1981.

[26] - Borduin, M., personnal communication, Los Alamos National Laboratory, CST14, plot of replicate neutron probe readings in borehole NPH-9 (ER1111), 1996.

[27] - Vold, E.L., "An Analysis of Vapor Phase Transport in the Unsaturated Zone with Application to a Mesa Top Disposal Facility, Part I", in preparation as a Los Alamos National Laboratory Report, January, 1996.

[28] - Puglisi, C., and Vold, E., "Low Impact Sampling under an Active Solid Low-level Radioactive Waste Disposal Unit Using Horizontal Drilling Technology", Los Alamos National Laboratory Report LA-UR-95-3691, in proceedings to Symposium on the Scientific Basis for Nuclerar Waste Management, Materials Research Society, Boston, MA, Nov.,1995.

[29] - Bevington, P.R., Data Reduction and Error Analysis for the Physical Sciences, McGraw Hill Book Co., New York, 1969.

[30] - Campbell, G.S., "A Simple Method for Determining Unsaturated Conductivity from Moisture Retention Data", Soil Sci., 117, 311-134 (1974).

Table I. Hydrologic Transport Properties Used in the Analysis (from Ref.2 except as noted)

Property	Unit							
	2b	2a	1b	1a	Ts-CT [1]	Otowi	crushed tuff [2]	2b (w/G5)[3]
n = # of samples (vG^4 fits)	3	9	8	9	2	12	1	7
vG^4 alpha (cm-1)	0.0061 ± 0.0002	0.0030 ± 0.0009	0.0044 ± 0.0045	0.0052 ± 0.0014	0.0152 ± 0.0030	0.006 ± 0.0009	0.143	0.0047
vG^4 N	1.898 ± 0.142	2.027 ± 0.228	1.660 ± 0.220	1.735 ± 0.118	1.506 ± 0.111	1.755 ± 0.253	1.506	2.042
vG^4 M = 1-1/N	0.473	0.506	0.397	0.423	0.335	0.430	0.335	0.510
θ-residual (>0) [5]	1.3	0.2	0.9	0.6	0.8	1.9	1.0	-
θ-saturation (%)	48.1	51.7	50.9	48	47.3	43.5	33	-
Ksat (cm/s)	4.3E-04	1.5E-04	1.7E-04	1.9E-04	8.7E-04	2.5E-04	2.9E-04	-
specific gravity-bulk-	1.37	1.26	1.2	1.14	1.12		1.2	-

1 - (Tsankawi-Cerro Toledo)
2 - from Ref.18
3 - additional unit 2b data from hole G5 as reported in Ref.17
4 - van Genuchten fitting parameters
5 - θ-residual set equal to zero in present analysis to avoid inconsistencies where field data moisture is less than the average residueal, θ < θ-residual

Table II. Flux characteristics summary by monitor hole and by 'flux region'

hole	near surface region			low flux region			v.p.[1] notch (unit 1b-1a interface)		
	depth -m-	flux[2]	source[2]	depth -m-	flux[2]	source[2]	depth -m-	flux[2]	source[2]
nph-2 (bkg p37)	0 - 4	-0.41	-0.17	4 - 14	-0.0016	-0.0009	-		
nph-3 (bkg p30)	0 - 4	-0.45	-0.27	4 - 14	-0.0010	+0.0003	-		
nph-7c	0 - 8	-2.4	-0.65	8 - 19	-0.006	-0.0009	-		
nph-6	0 - 4 4 - 10	+0.87 - 0.74	1.4 -0.24	10 - 15	-0.007	-0.002	-		
nph-4	0 - 10 10 - 17	-178. -96.	-51. -6.8	-			-		
LGM-85-06	0 - 6	-0.29	-0.17	6 - 24	-0.0016	-0.013	24 - 35	-0.43	+0.016
LGM-85-11	0 - 7	-23.	-11.	8 - 24	+0.009	-0.070	24 - 37	-0.43	+0.10
nph-8	0 -4 5 - 11	+0.49 -1.42	+0.28 -0.17	11 - 25	-0.0038	-0.0024	25 - 29	+0.04	+0.004
nph-9 (ER1111)	0 - 5 6 - 12	-0.14 -0.21	-0.008 0.0001	12 - 24	0.0001	-0.0011	24 - 29-vp 29 - 35	0.0051 0.0084	0.0011 0.0019
nph-5(G5)	0 - 16	-1.68	0.0078	16 - 25	0.029	-0.038	25 - 30	+0.38	+0.069
ER-1002	0 -7	-0.51	-0.16	8 - 29	-0.0005	-0.0006	30 - 44	-0.0046	+0.0005
summary-									
mean[3]	7.8[4,5]	-0.94[5]	-0.11-0.37[5]	21.3[4]	0.0017	-0.013	34.0[4]	-0.073	0.032
std.dev[3]	1.6[4,5]	3.9[5]	20.6-4.2[5]	5.4[4]	0.011	0.023	5.9[4]	0.311	0.042

1 - vapor phase notch.
2 - average value over the indicated interval, units - cm/yr - 'flux' (vertical flux) and 'source' are terms plotted in Figs.#.B.
3 - arithmetic statistics used in low flux and vapor phase notch regions, geometric values used in near surface region (see text).
4 - mean values for maximum of the depth range.
5 - excludes data from hole NPH4, the second value also excludes NPH-5 (G-5) and NPH-9 (ER1111) data as discussed in the text.

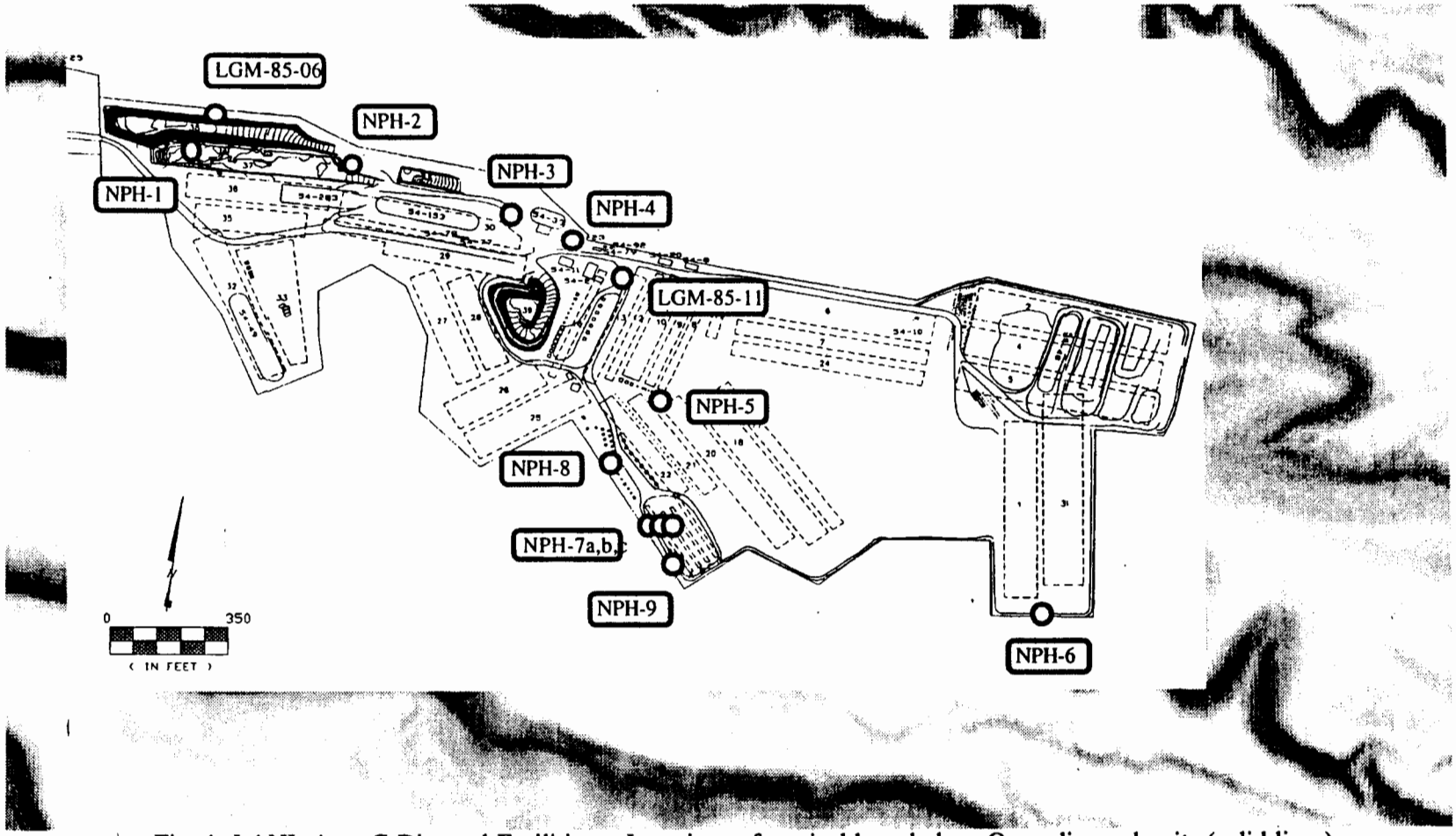

Fig. 1 LANL Area G Disposal Facilities - Locations of vertical bore holes. Open disposal units (solid lines), covered disposal units (dashed lines) and shafts (small cirles and boxes) are imposed on terrain contours of the mesa.

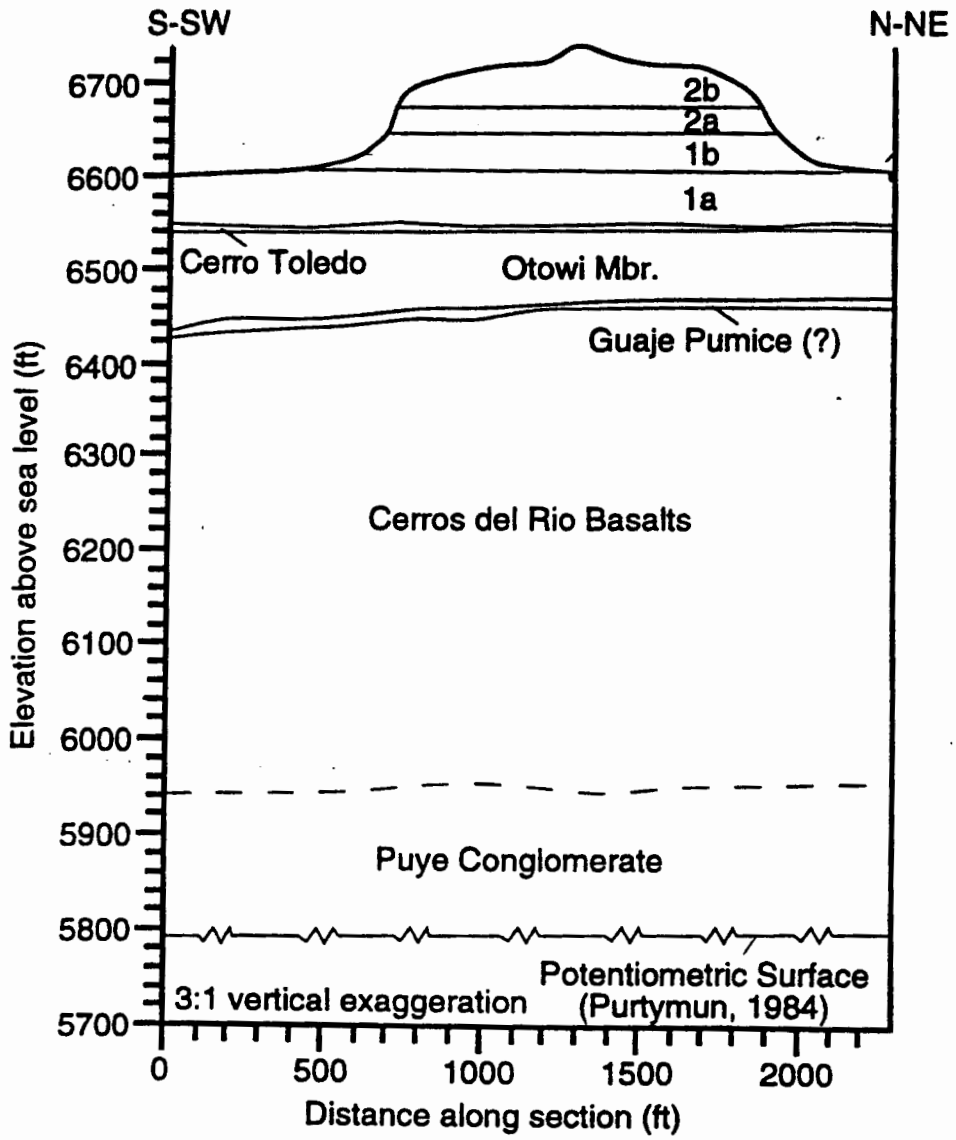

Fig.2 Stratigraphy cross-section (N-S) through the west end of the mesa-top disposal site at Area G (adapted from Krier, et.al. 1995).

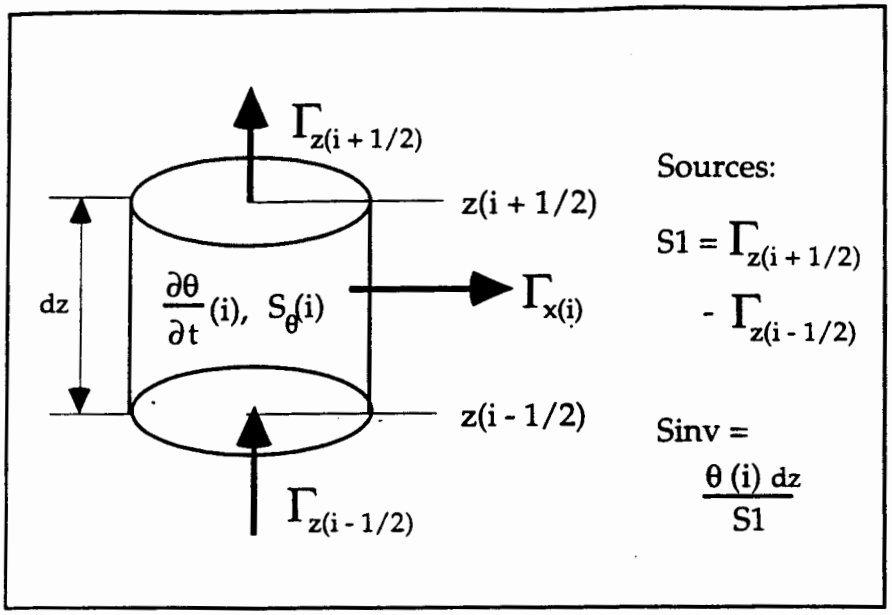

Fig.3 Schematic summary of analysis showing a control volume and flux elements through the control volume.

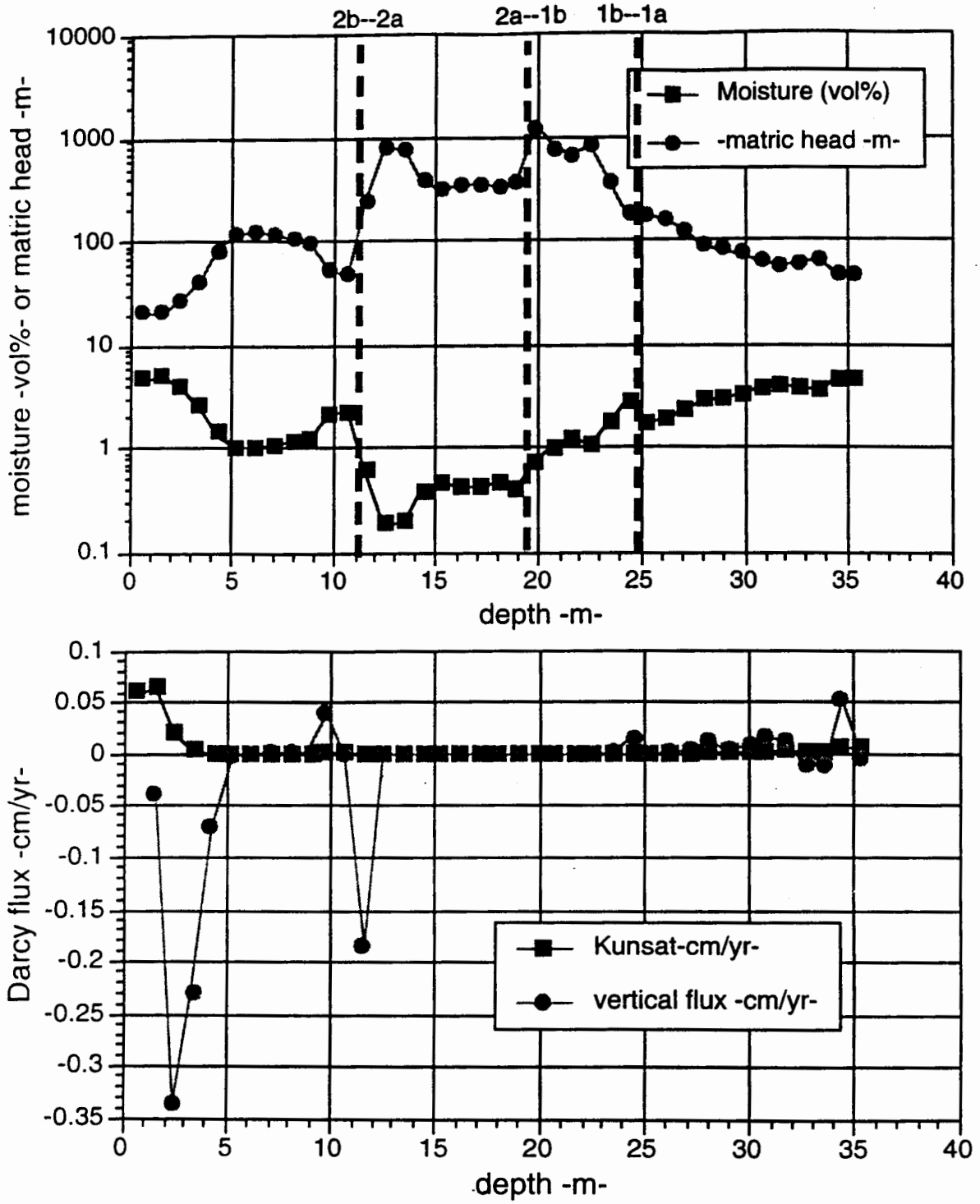

Fig. 4.A-B Vertical profiles for hole **NPH-9 (ER1111)** showing: A. volumetric moisture content (%) with the matric head (m) and stratigraphic unit interfaces indicated, and B. vertical flux and the local unsaturated hydraulic conductivity, Kunsat -cm/yr-.

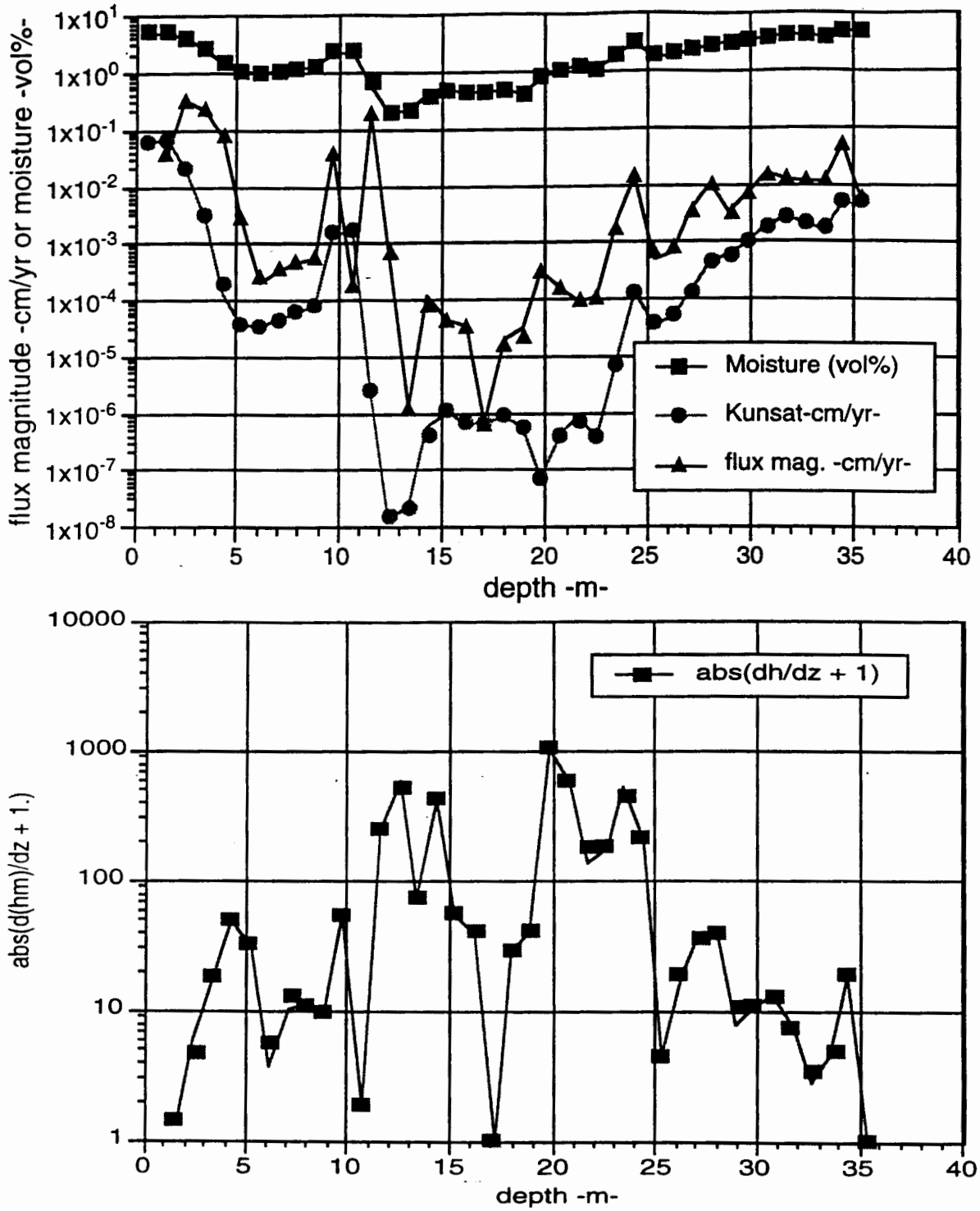

Fig. 5.A-B Vertical profiles for hole **NPH-9 (ER1111)** showing: A. volumetric moisture content (%), with the absolute magnitude of the vertical flux and the local unsaturated hydraulic conductivity, Kunsat -cm/yr-, and B. the vertical flux function, abs(d(h_m)/dz + 1).

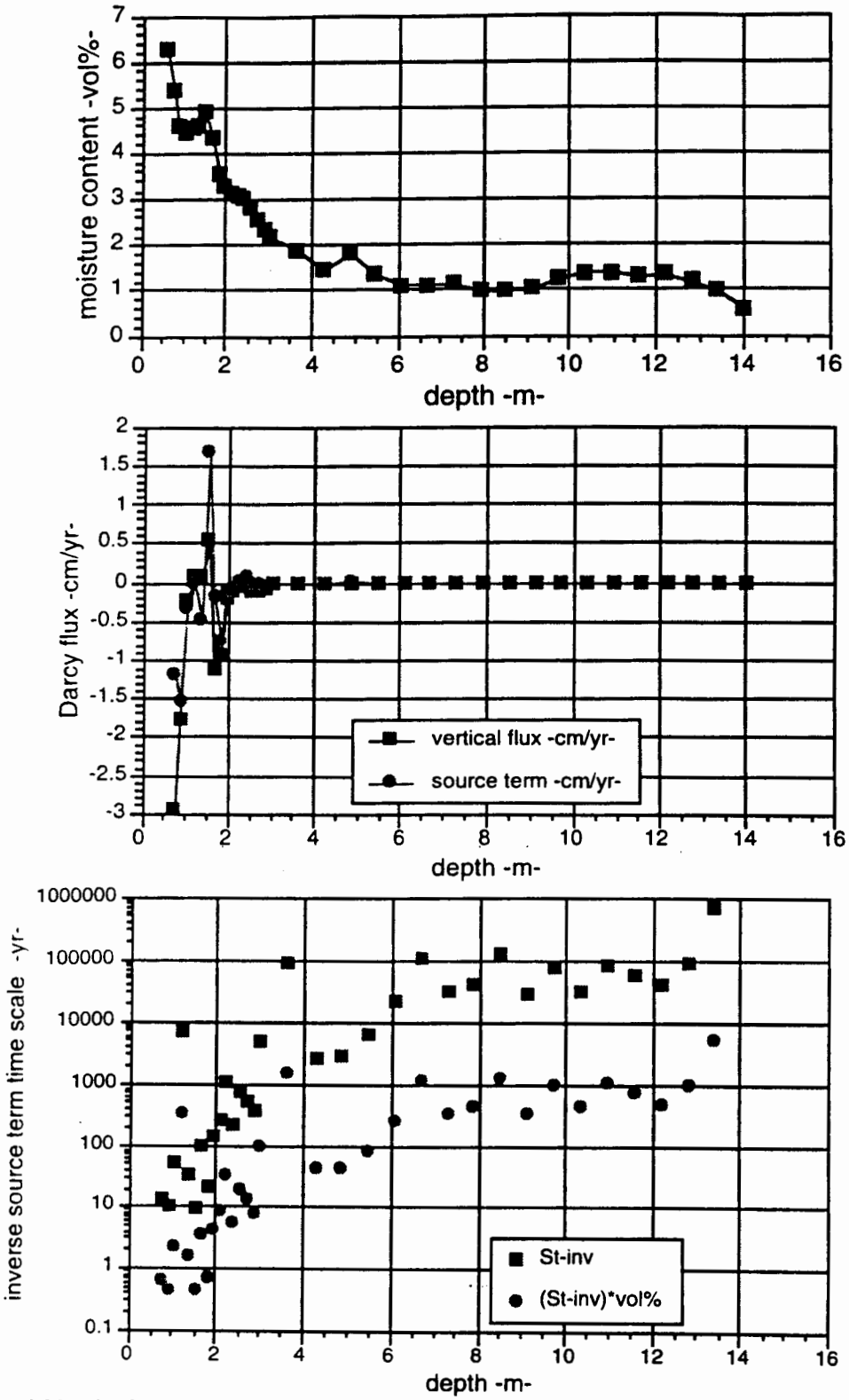

Fig. 6 Vertical profiles for hole **NPH-2 (bkg near pit 37)** showing: A. volumetric moisture content, B. vertical flux and the source term expressed as a flux, and C. source terms expressed as a characteristic response time.

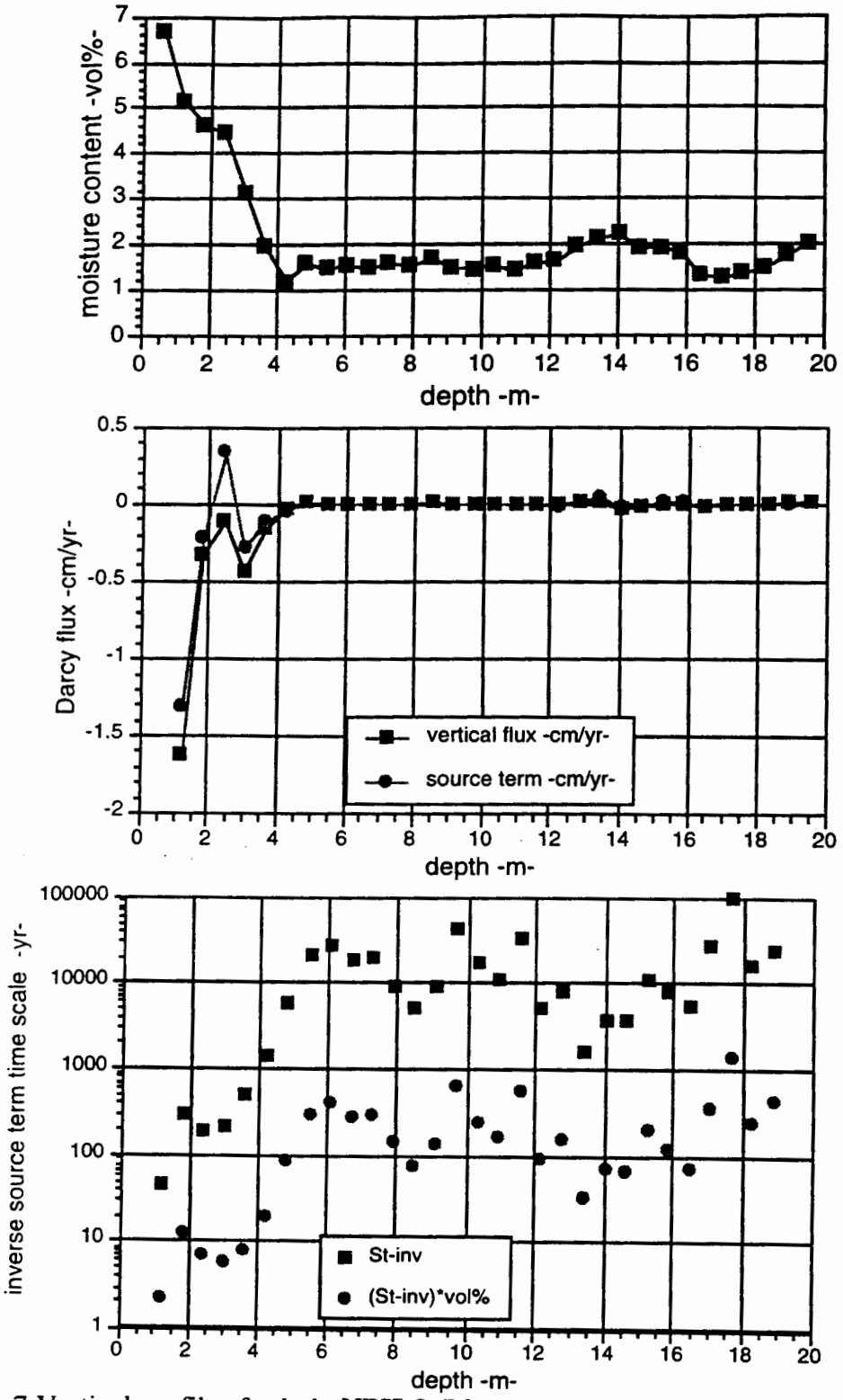

Fig. 7 Vertical profiles for hole **NPH-3 (bkg near pit 30)** showing: A. volumetric moisture content, B. vertical flux and the source term expressed as a flux, and C. source terms expressed as a characteristic

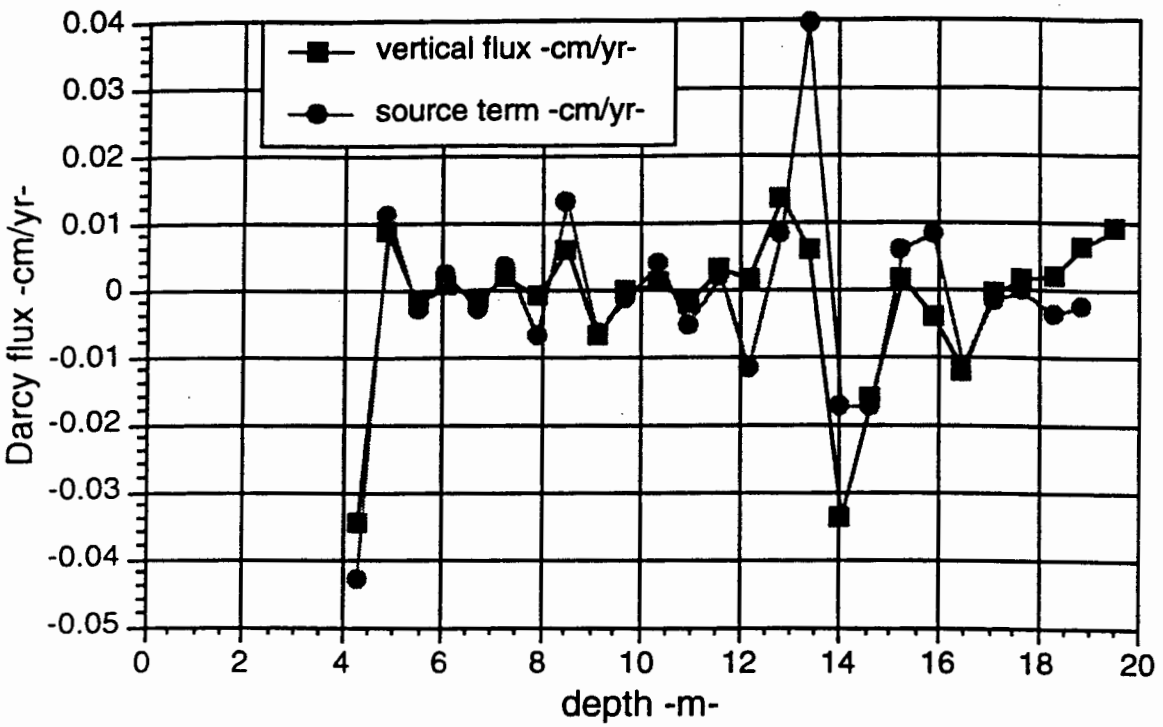

Fig. 8 Vertical profiles for hole **NPH-3 (bkg near pit 30)** showing vertical flux and the source term expressed as a flux in the limited range of depth from 4m to 20m.

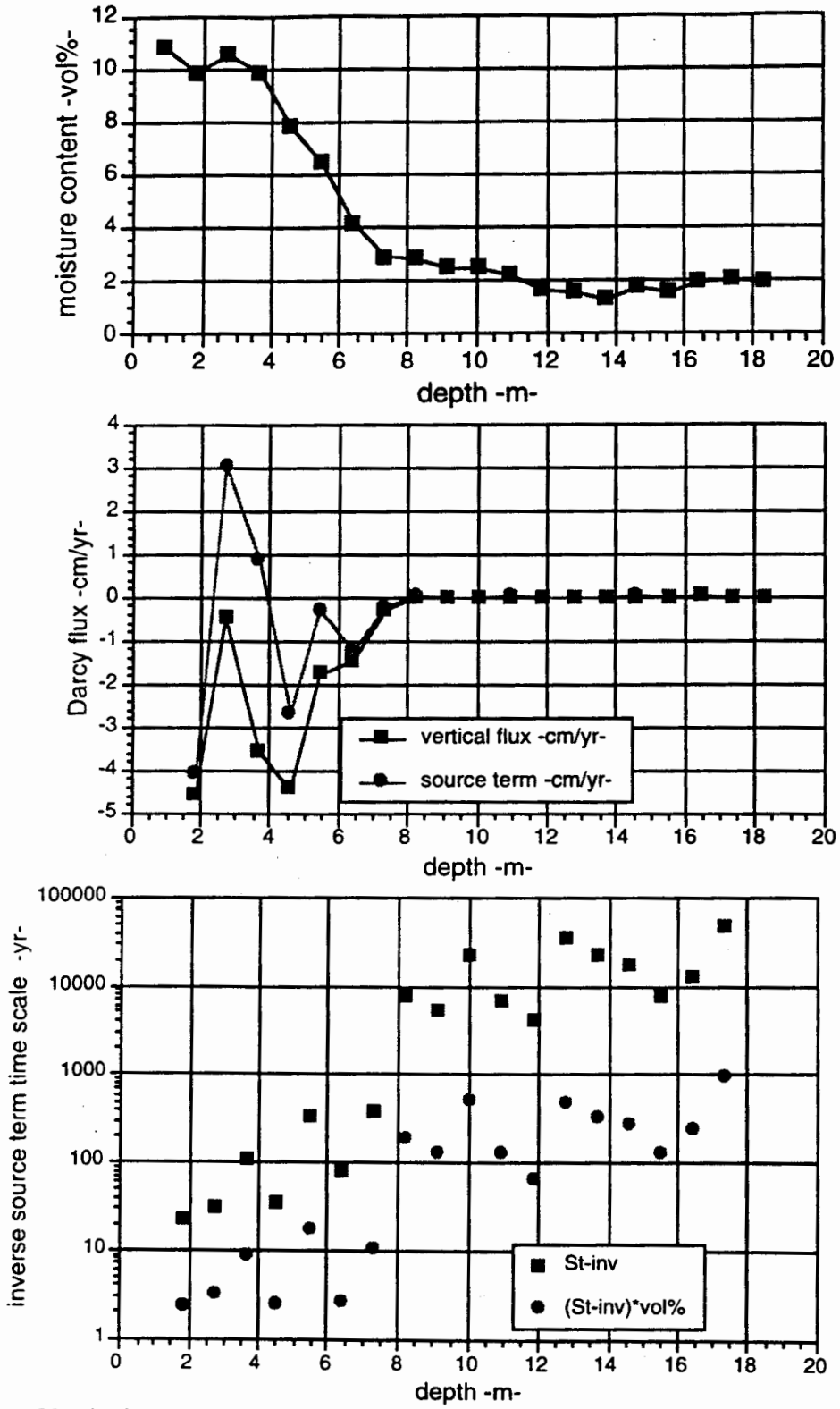

Fig. 9 Vertical profiles for hole **NPH-7c (near trenches)** showing: A. volumetric moisture content, B. vertical flux and the source term expressed as a flux, and C. source terms expressed as a characteristic response time.

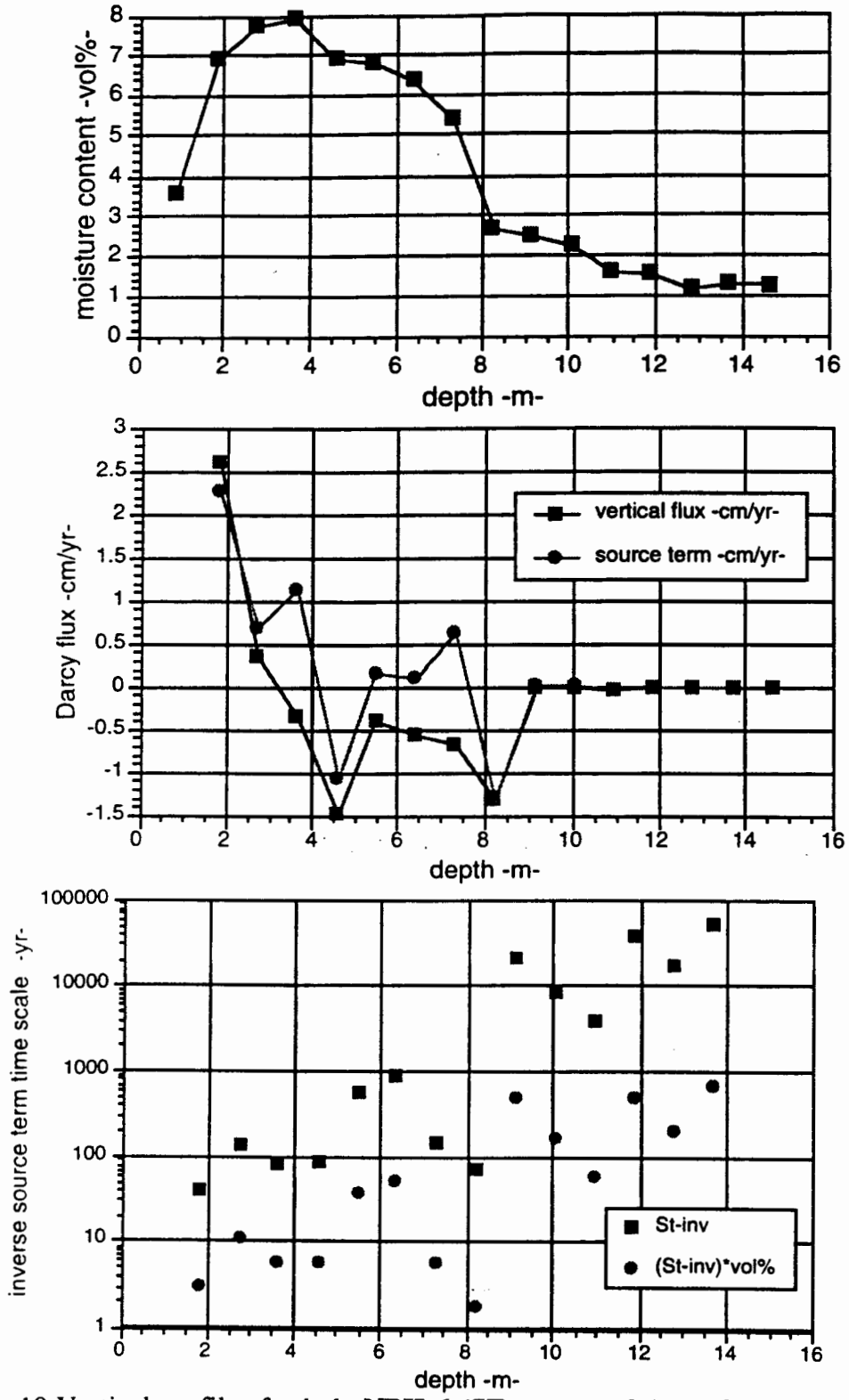

Fig. 10 Vertical profiles for hole **NPH-6 (SE corner of Area G)** showing: A. volumetric moisture content, B. vertical flux and the source term expressed as a flux, and C. source terms expressed as a characteristic response time.

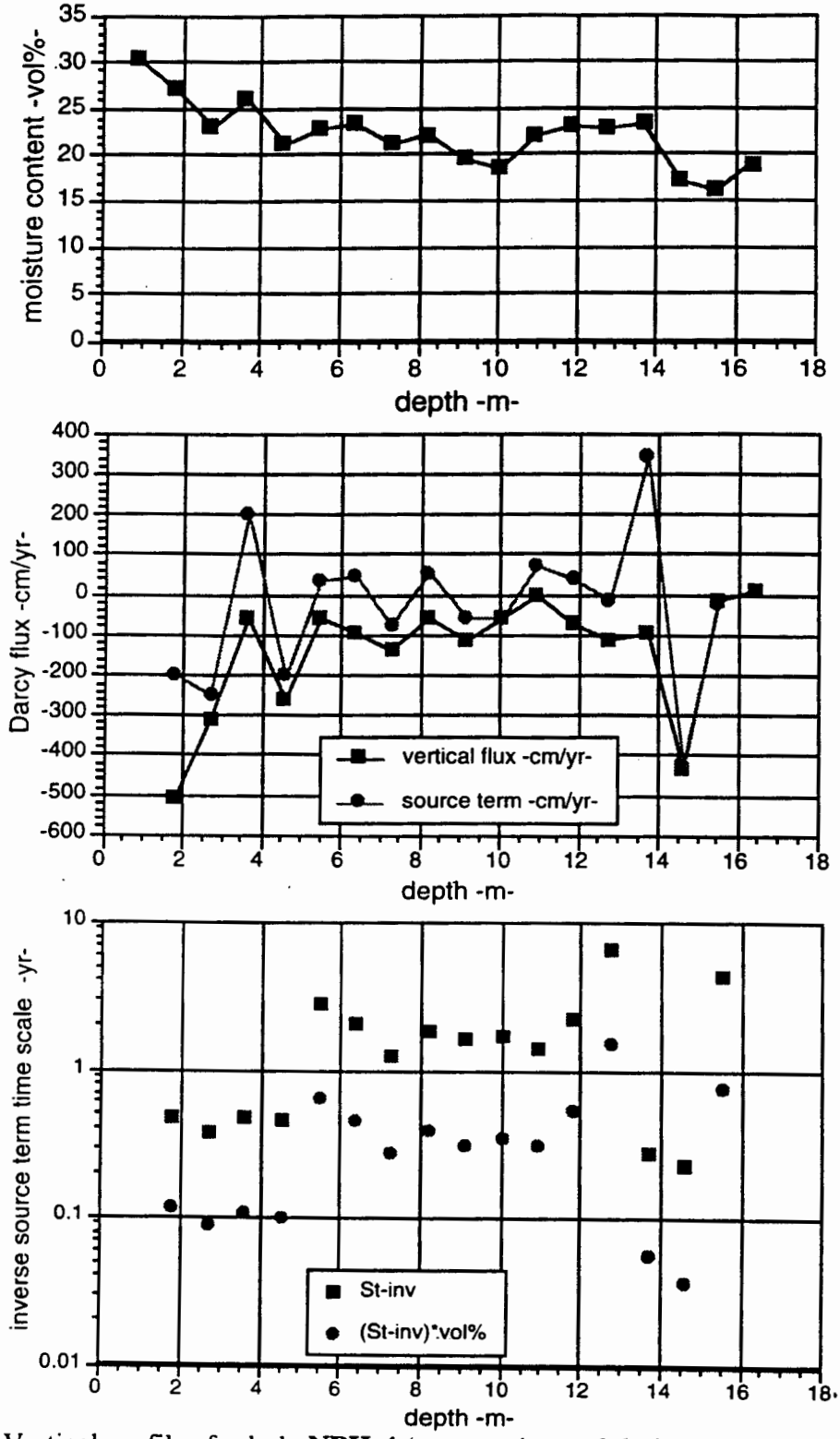

Fig. 11 Vertical profiles for hole **NPH-4** (near engineered drainage) showing: A. volumetric moisture content, B. vertical flux and the source term expressed as a flux, and C. source terms expressed as a characteristic response time.

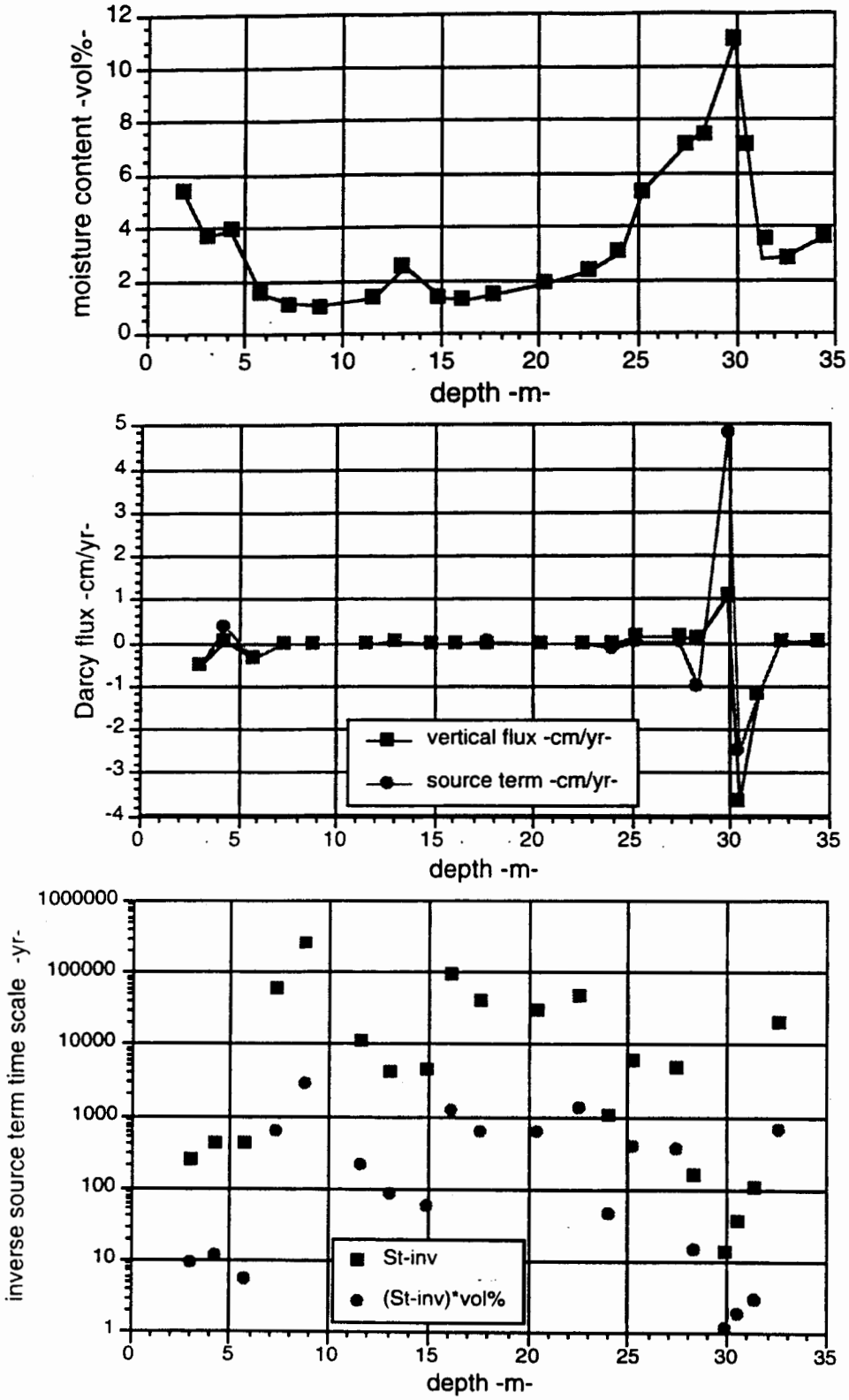

Fig. 12 Vertical profiles for hole **LGM-85-06** showing: A. volumetric moisture content, B. vertical flux and the source term expressed as a flux, and C. source terms expressed as a characteristic response time.

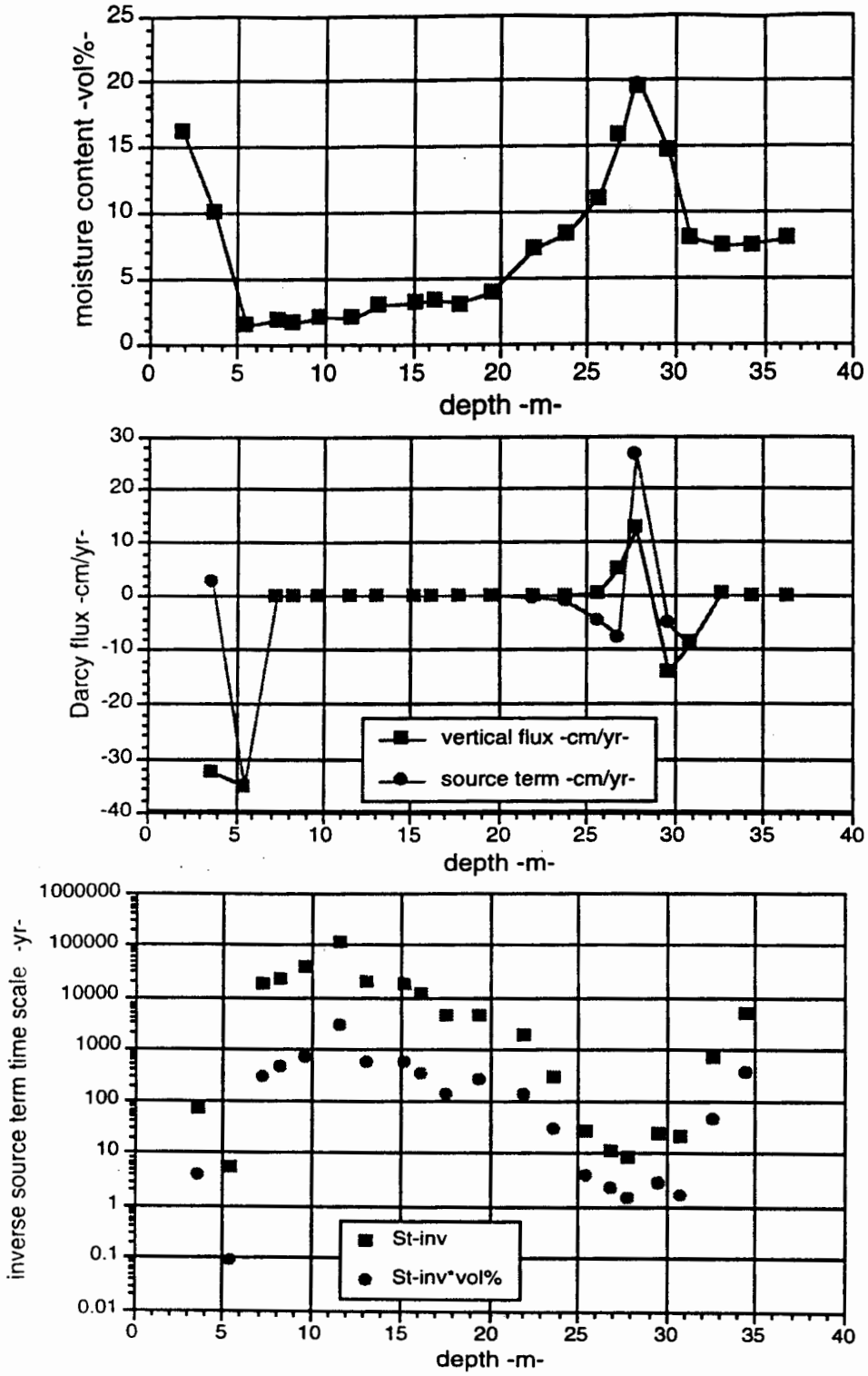

Fig. 13 Vertical profiles for hole **LGM-85-11** showing: A. volumetric moisture content, B. vertical flux and the source term expressed as a flux, and C. source terms expressed as a characteristic response time.

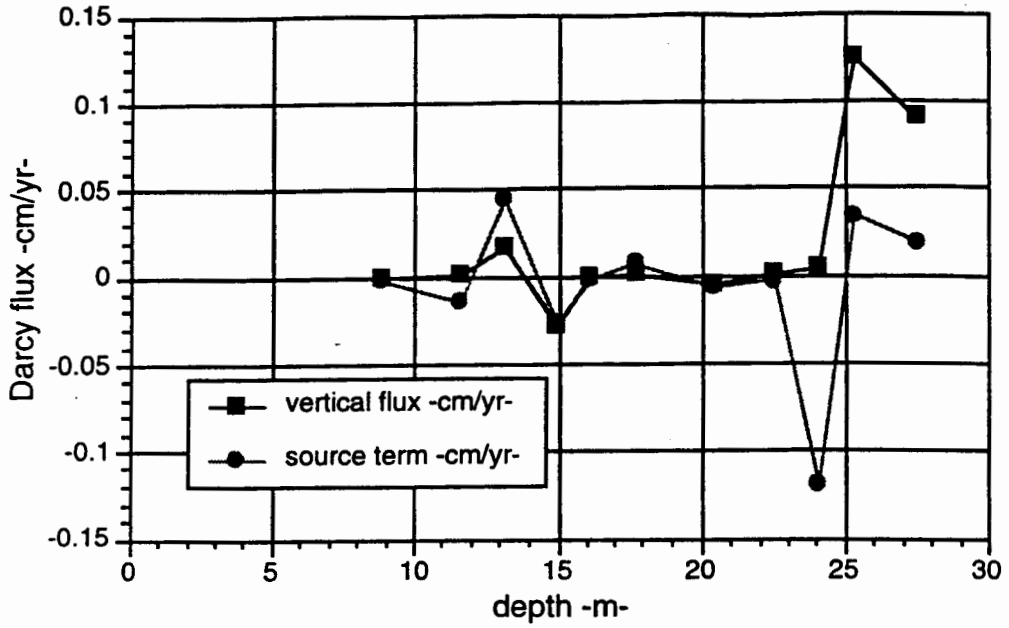

Fig. 14A Profiles for hole **LGM-85-06** showing vertical flux and the source term expressed as a flux in the 'low flux region' for the vertical range from 8m to 22m depth.

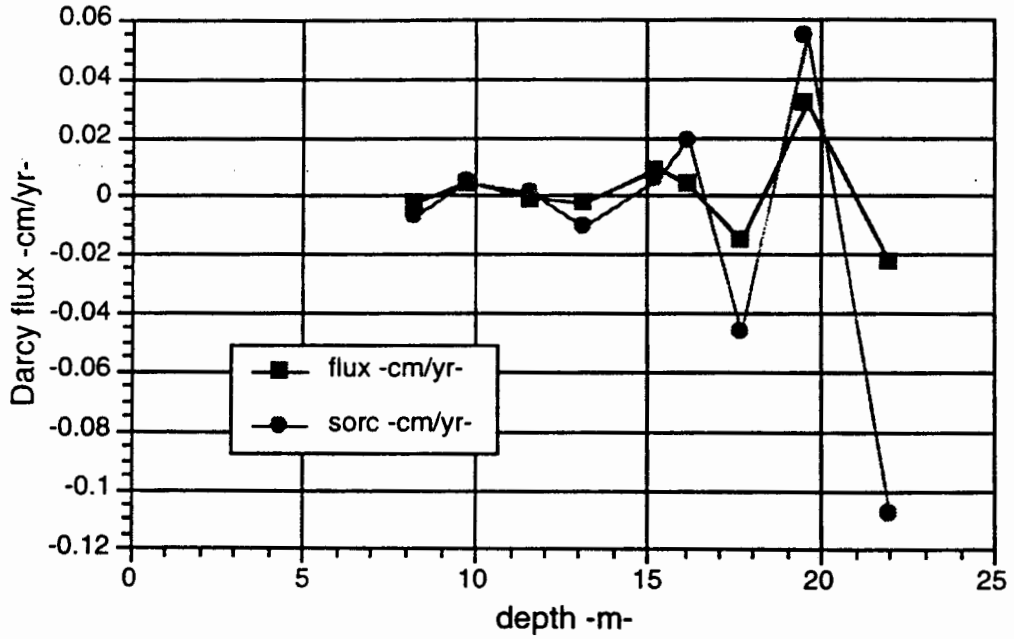

Fig. 14B Profiles for hole **LGM-85-11** showing vertical flux and the source term expressed as a flux in the 'low flux region' for the vertical range from 8m to 22m depth.

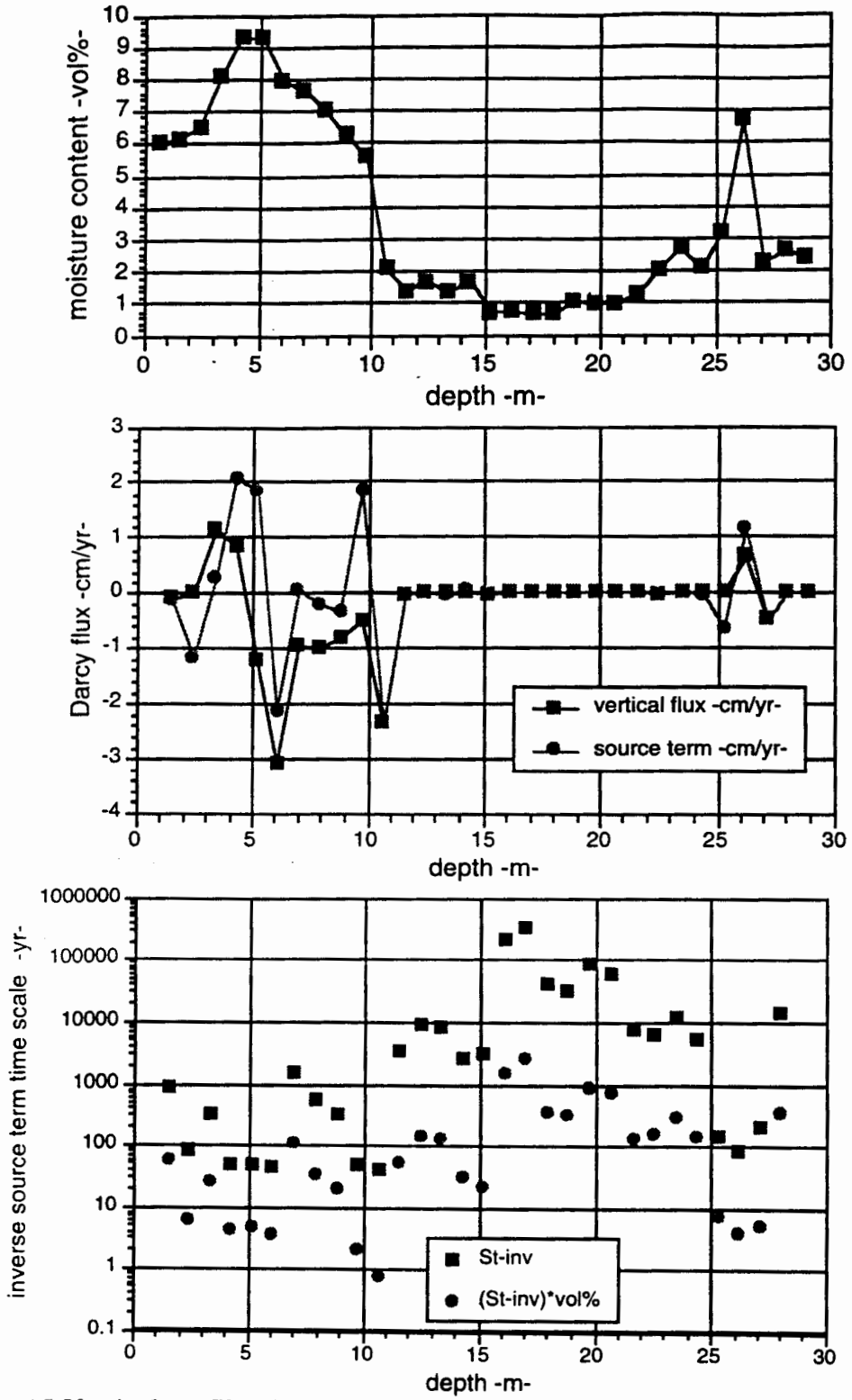

Fig. 15 Vertical profiles for hole **NPH-8 (near tritium shafts)** showing: A. volumetric moisture content, B. vertical flux and the source term expressed as a flux, and C. source terms expressed as a characteristic response time.

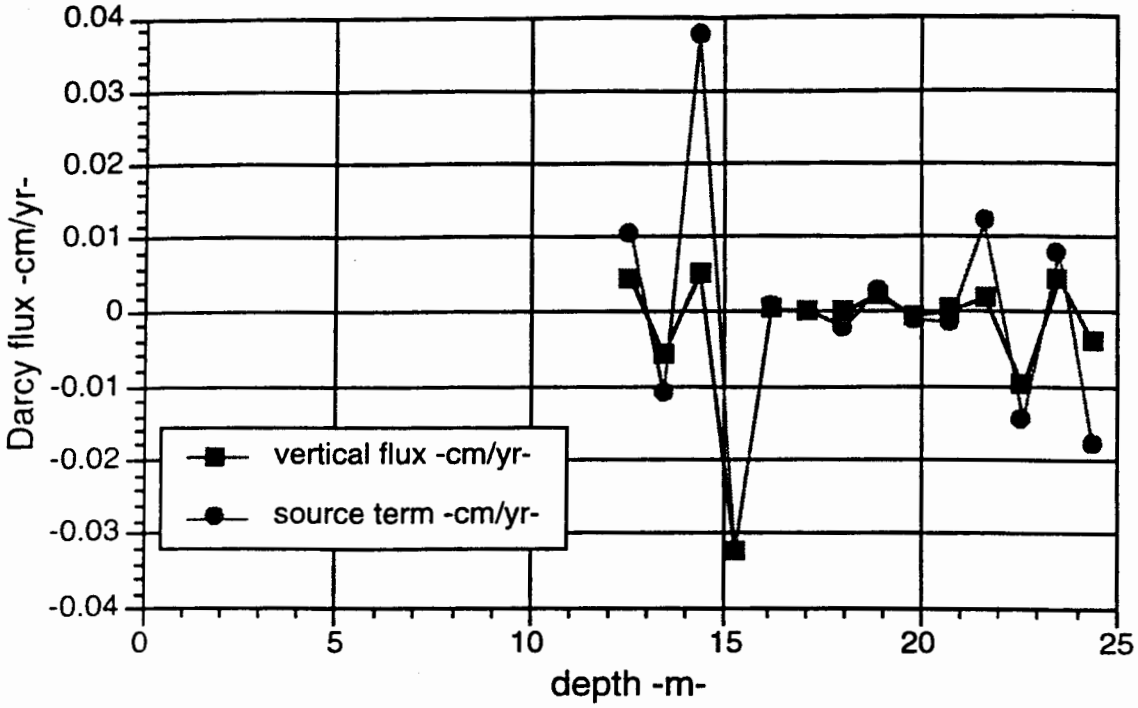

Fig. 16 Vertical profiles for hole **NPH-8 (near tritium shafts)** showing: A. volumetric moisture content, B. vertical flux and the source term expressed as a flux, and C. source terms expressed as a characteristic response time.

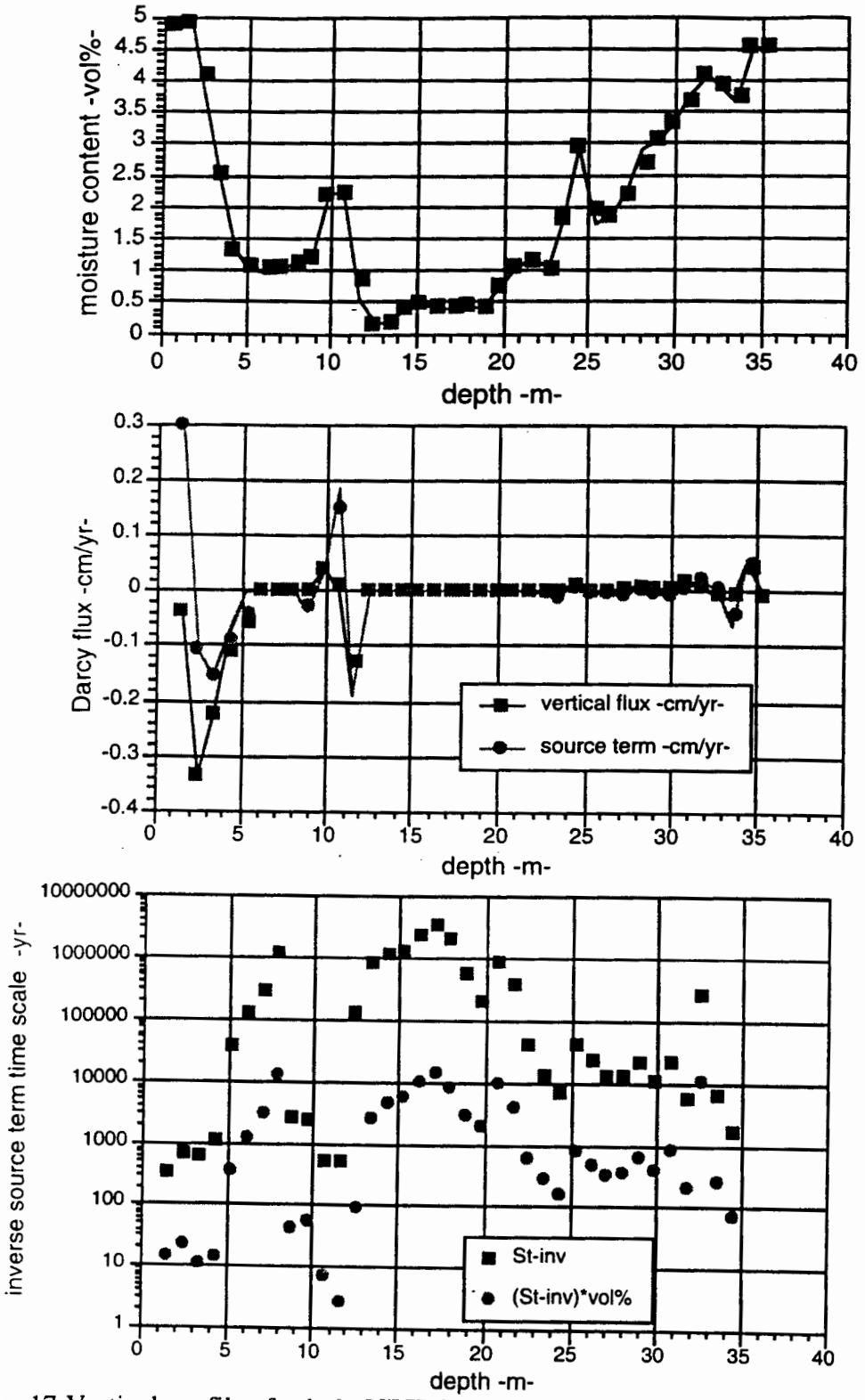

Fig. 17 Vertical profiles for hole **NPH-9 (ER 1111)** showing: A. volumetric moisture content, B. vertical flux and the source term expressed as a flux, and C. source terms expressed as a characteristic response time.

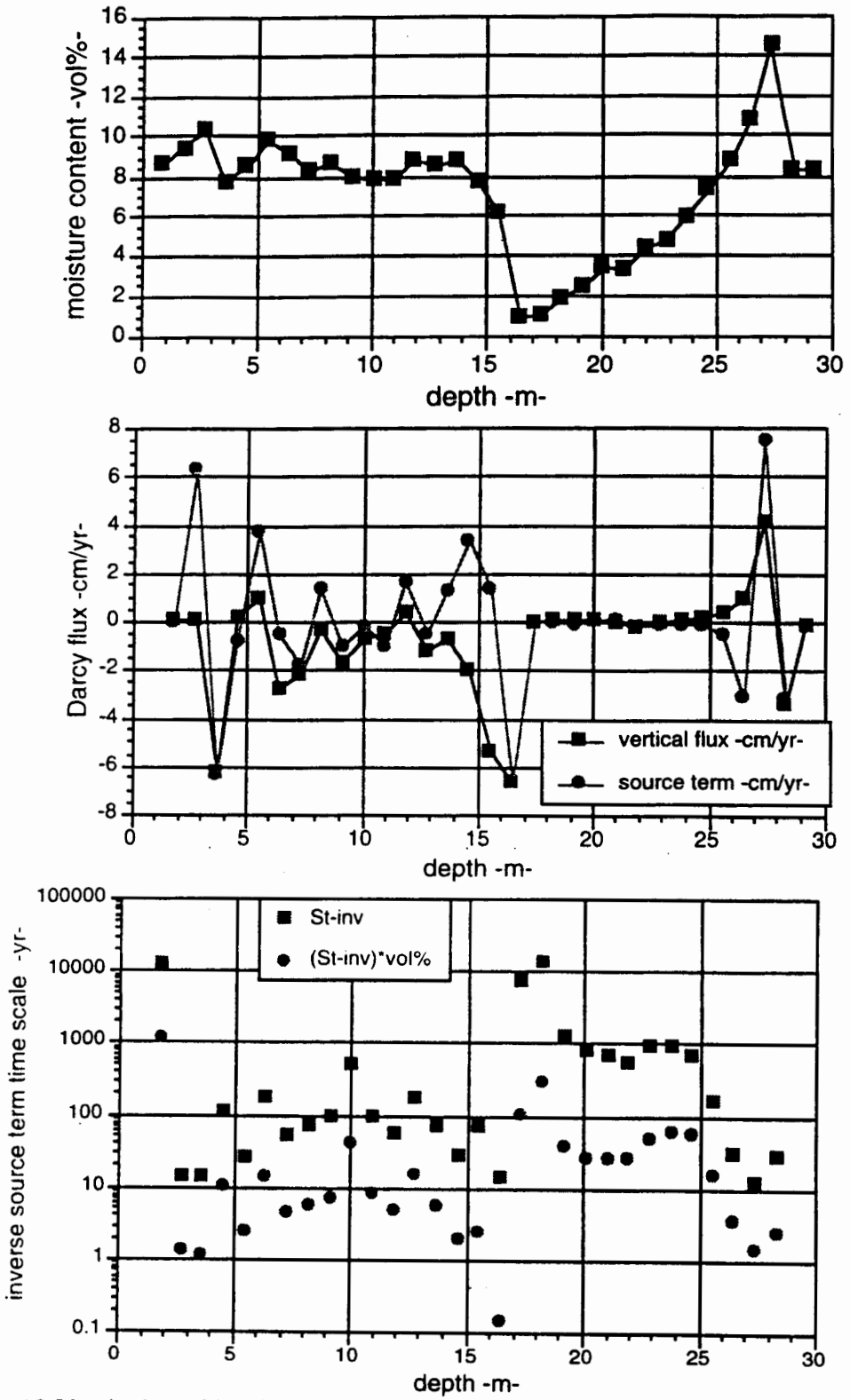

Fig. 18 Vertical profiles for hole **NPH-5 (G5)** showing: A. volumetric moisture content, B. vertical flux and the source term expressed as a flux, and C. source terms expressed as a characteristic response time.

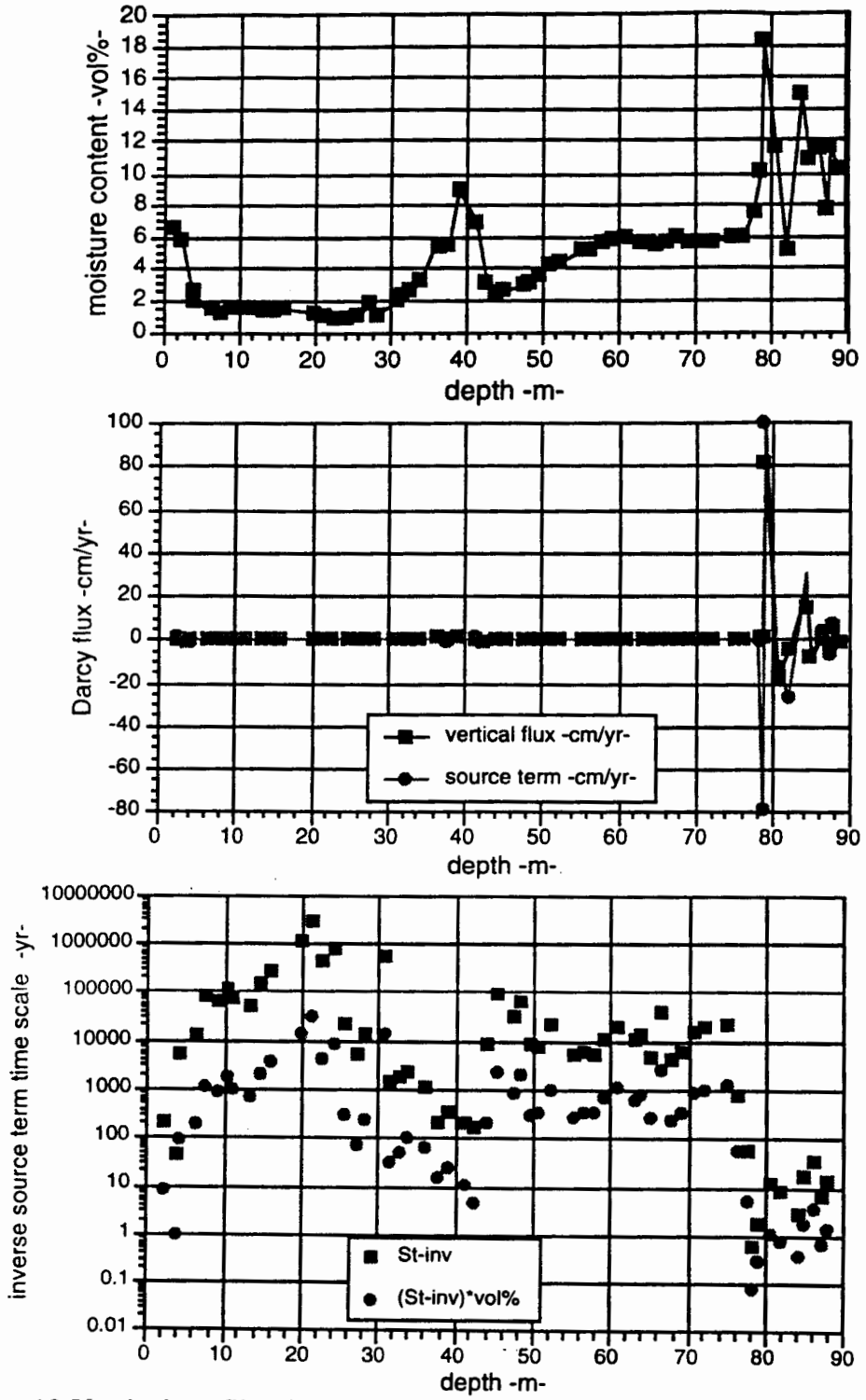

Fig. 19 Vertical profiles for hole **54-1002 (East of Area L)** showing: A. volumetric moisture content, B. vertical flux and the source term expressed as a flux, and C. source terms expressed as a characteristic response time.

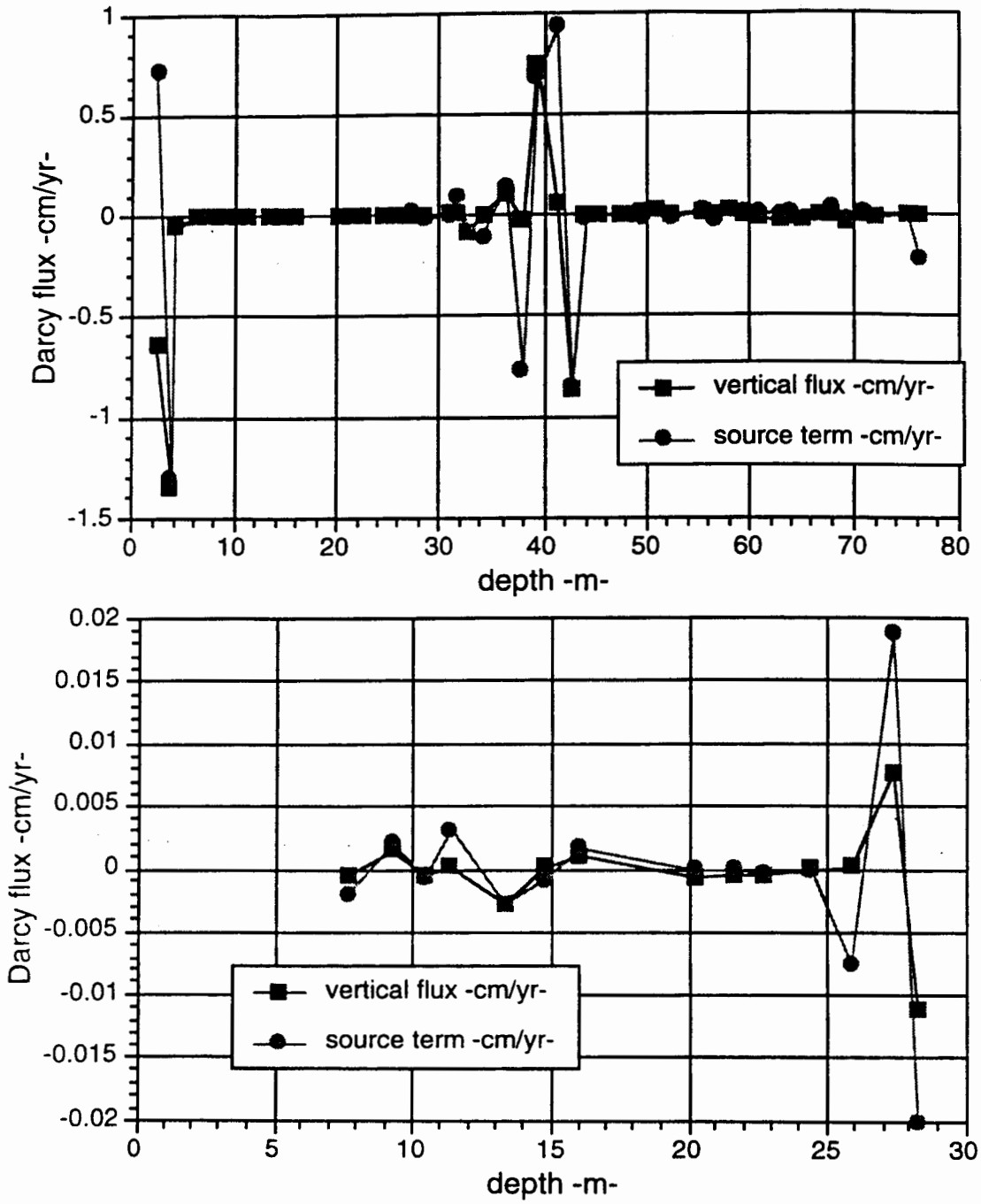

Fig. 20 Vertical profiles for hole **54-1002 (East of Area L)** showing vertical flux and the source term expressed as a flux over two restricted intervals of depth.

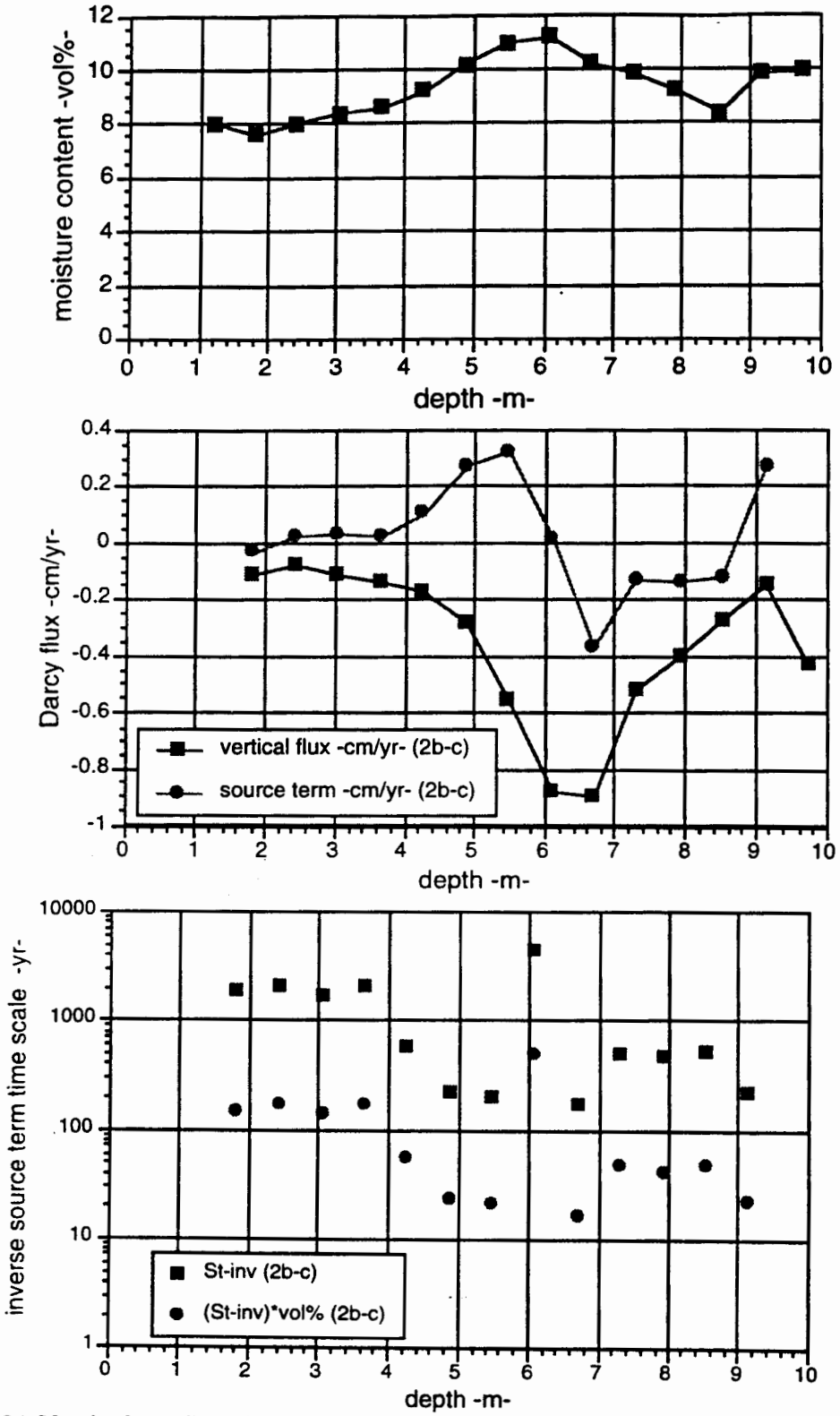

Fig. 21 Vertical profiles for hole **NPH-1 (in pit 37)** showing: A. volumetric moisture content, B. vertical flux and the source term expressed as a flux, and C. source terms expressed as a characteristic response time.

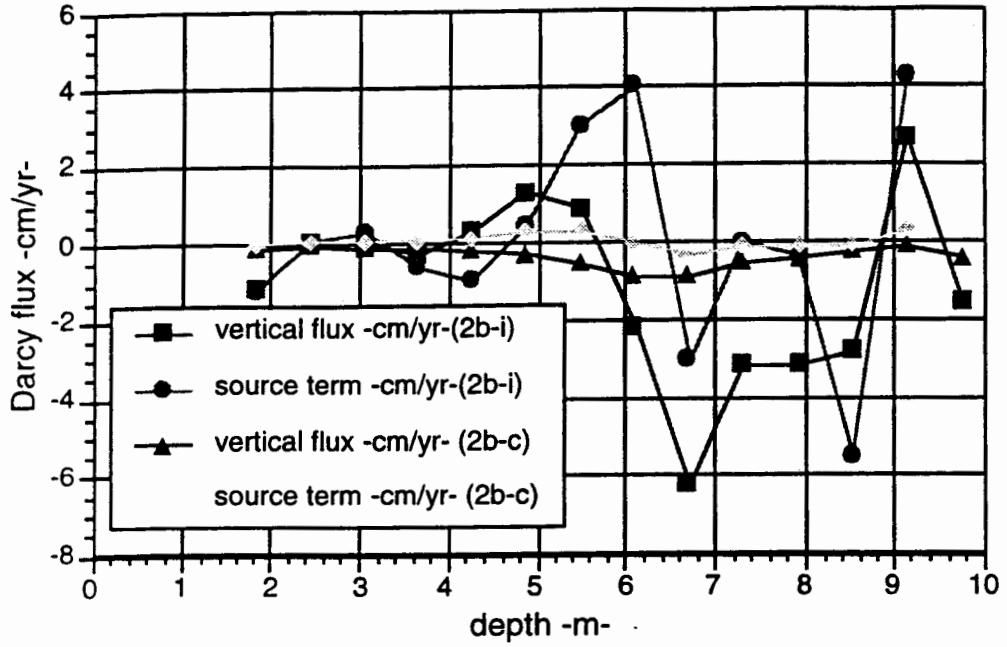

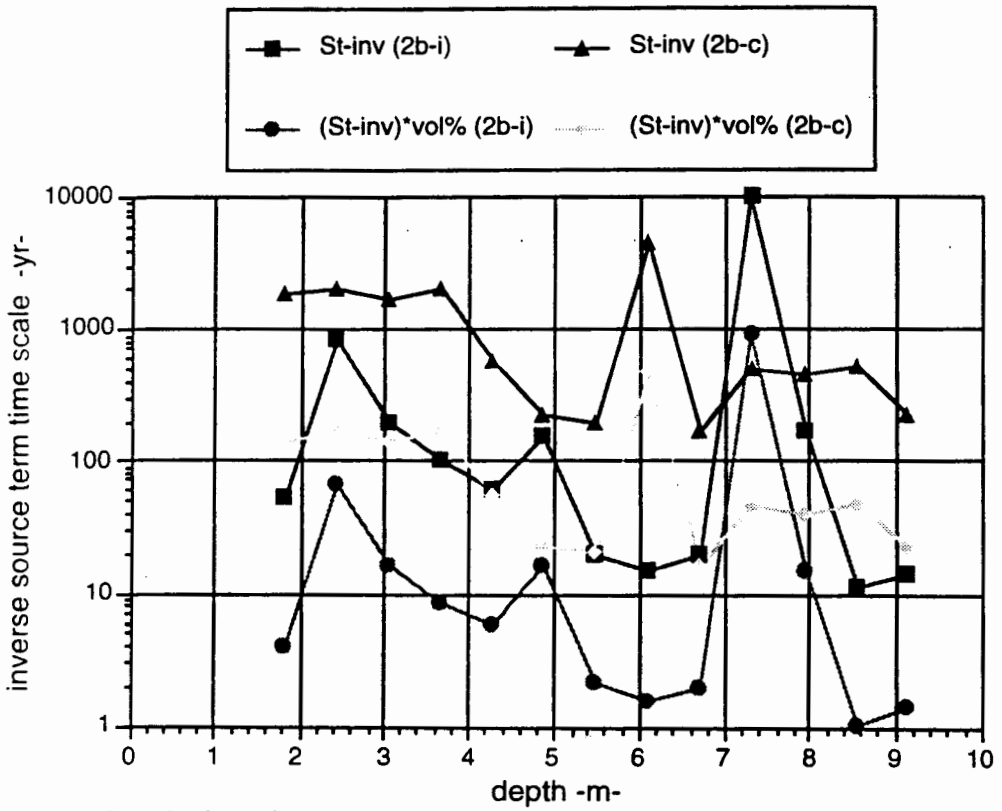

Fig. 22 Vertical profiles for hole **NPH-1 (in pit 37)** showing: A. volumetric moisture content, B. vertical flux and the source term expressed as a flux, and C. source terms expressed as a characteristic response time. (2b-i = Unit 2b intact, 2b-c = Unit 2b crushed, matric properties from Table I.)

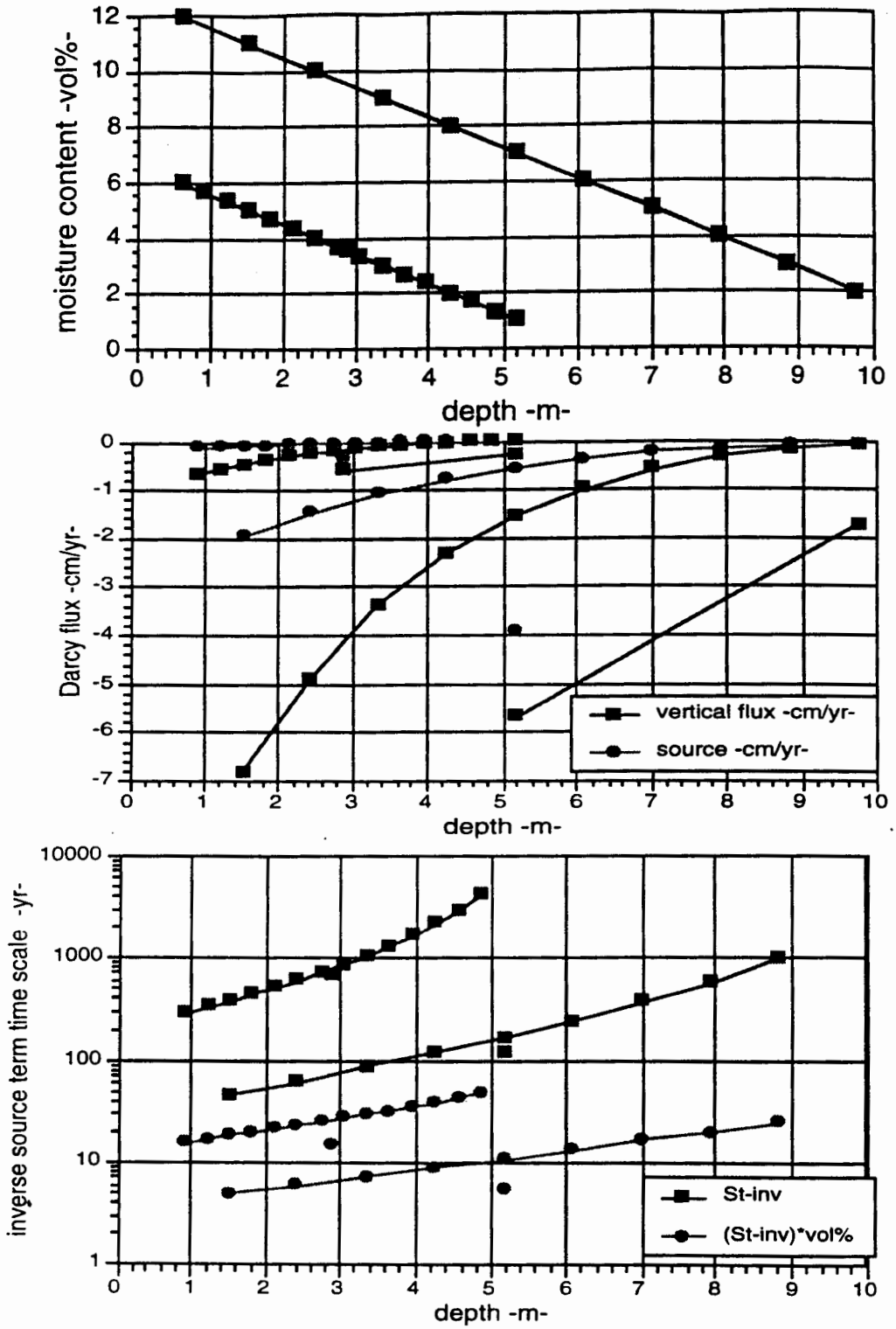

Fig. 23 Two generic linear vertical profiles for moisture content which bound the range typical for the near surface at Area G, showing: A. volumetric moisture content, B. vertical flux and the source term expressed as a flux, and C. source terms expressed as a characteristic response time.

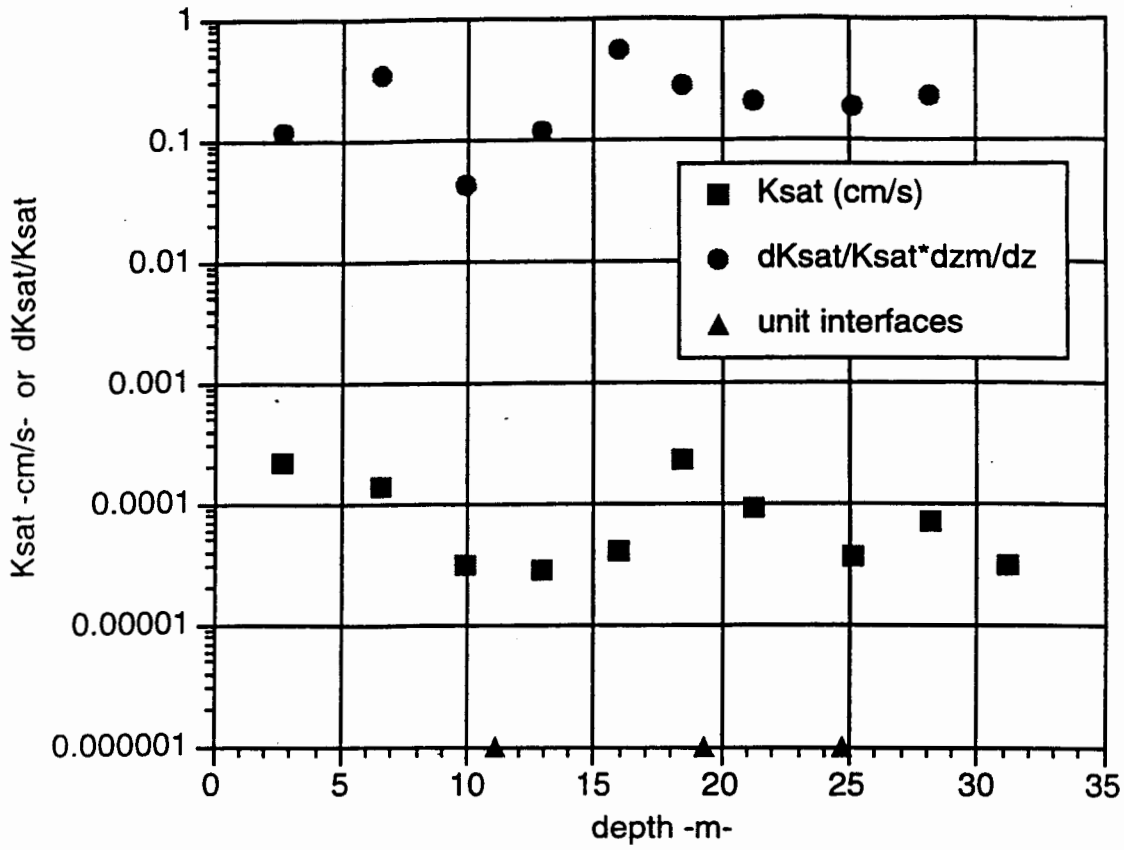

Fig.24 Variation with depth in hole NPH-5 (G-5) of the parameter, *Ksat* (data from Ref.[17]), and a measure of its error (*dKsat/Ksat*dzm/dz*) as described in the text.

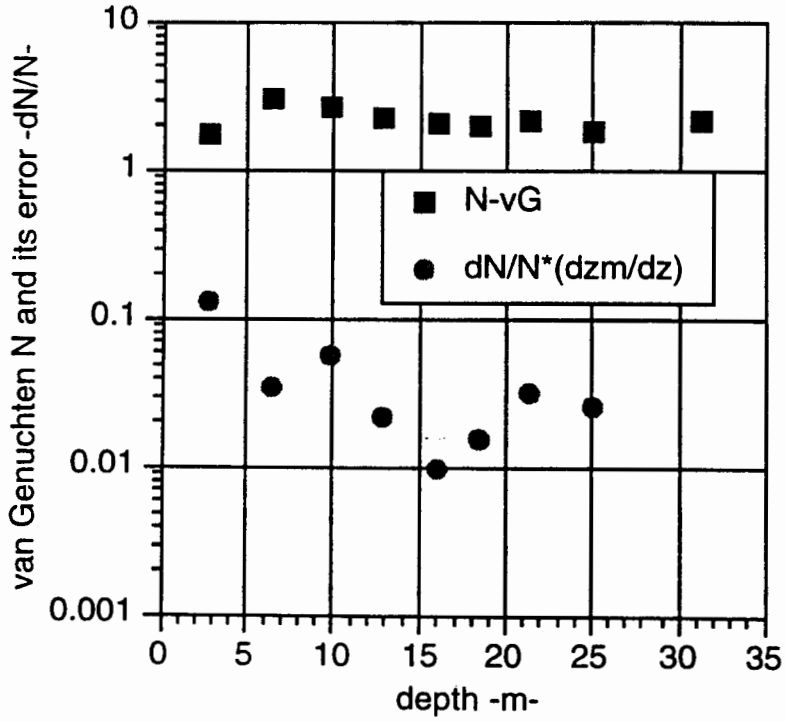

Fig.25 Variation with depth in hole NPH-5 (G-5) of the van Genuchten exponent parameter, *N* (data from Ref.[13]), and a measure of its error (*dN/N*dzm/dz*) as described in the text.

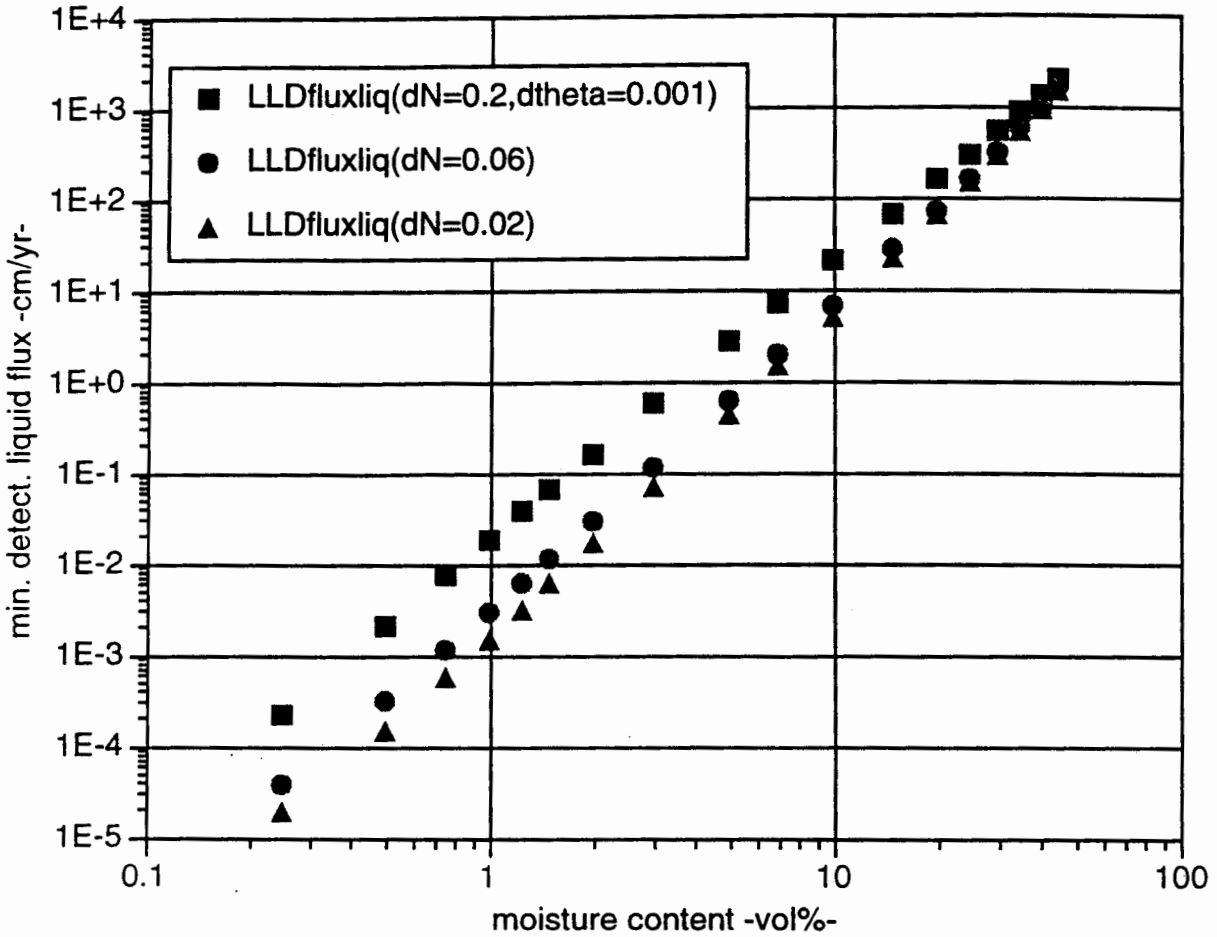

Fig.26 Flux uncertainty or minimum detectable liquid phase flux in Unit 2b from the flux analysis for three values of uncertainty in the van Genuchten exponent, dN = 0.2, 0.06, and 0.02. The best estimate for the present study conditions is dN = 0.06.

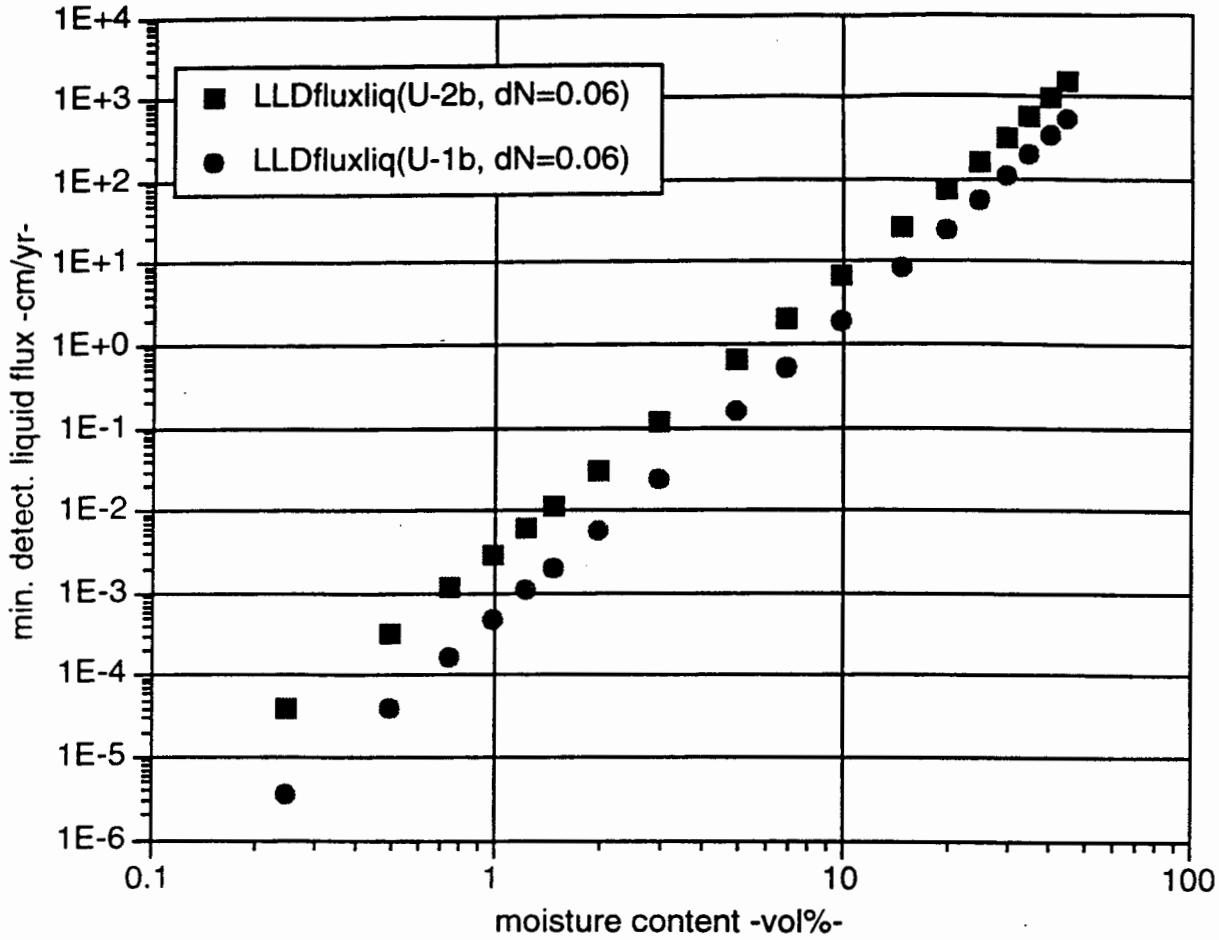

Fig.27 Flux uncertainty or minimum detectable liquid phase flux compared in Unit 2b and in Unit 1b for the best estimate of the uncertainty in the van Genuchten exponent, dN = 0.06, under the present study conditions.

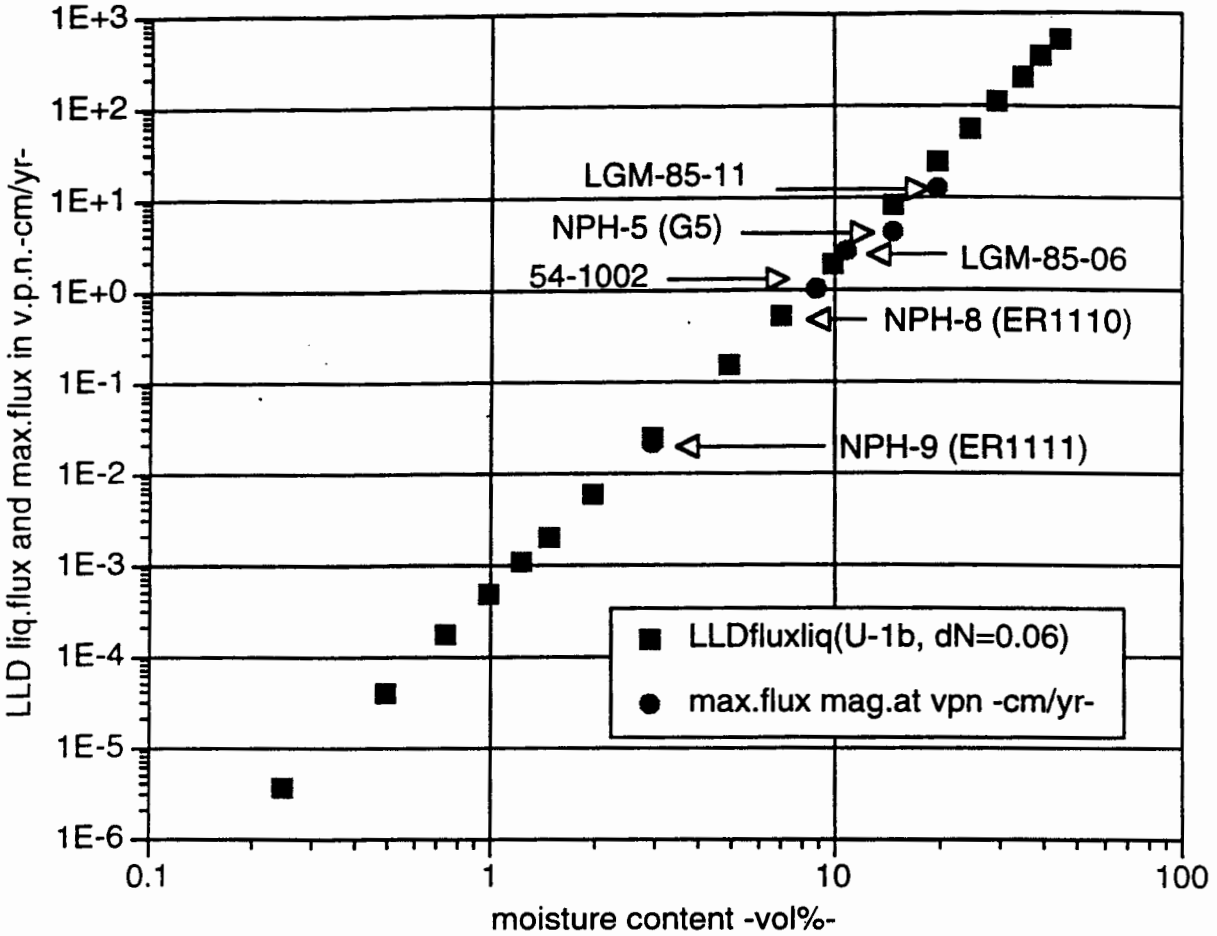

Fig.28 The maximum magnitude of the apparent flux resulting from this analysis at the vapor phase notch in 6 boreholes, compared to the minimum detectable liquid phase flux in Unit 1b for the best estimate of the uncertainty in the van Genuchten exponent, dN =0.06.

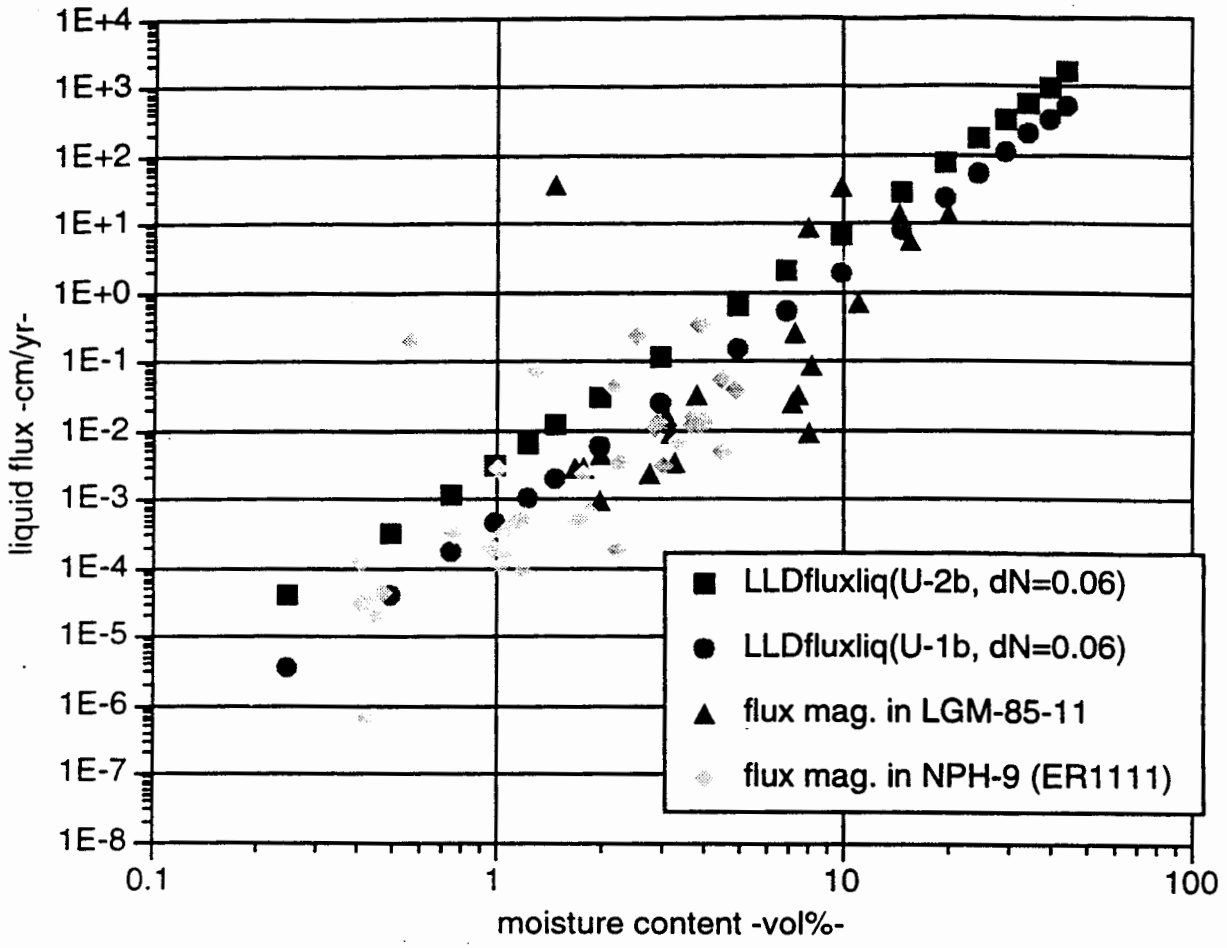

Fig.29 The magnitude of the apparent flux resulting from this analysis at all depths in 2 boreholes (where LGM-85-11 is an 'extreme moist case' and NPH-9 (ER1111) is an 'extreme dry case'), compared to the minimum detectable liquid phase flux in Unit 2b and in Unit 1b for the best estimate of the uncertainty in the van Genuchten exponent, dN =0.06.

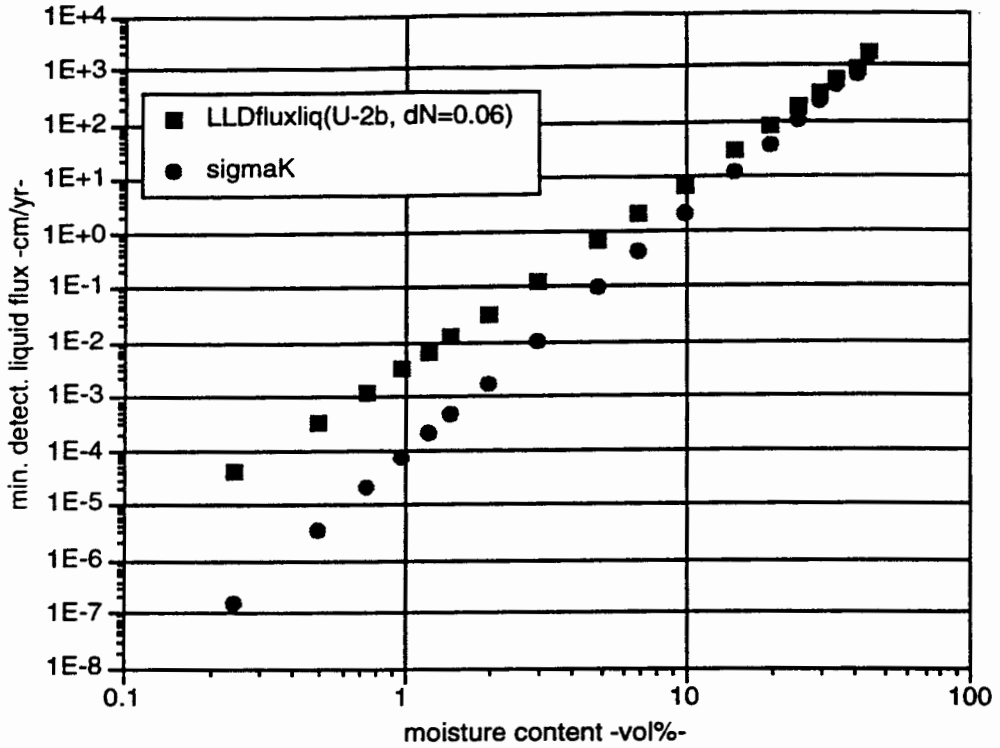

Fig. 30 Flux uncertainty or minimum detectable liquid phase flux in Unit 2b compared to the uncertainty in unsaturated hydraulic conductivity (sigmaK = σ_K) for the best estimate of the uncertainty in the van Genuchten exponent, dN = $\sigma_{nvg} = 0.06$.

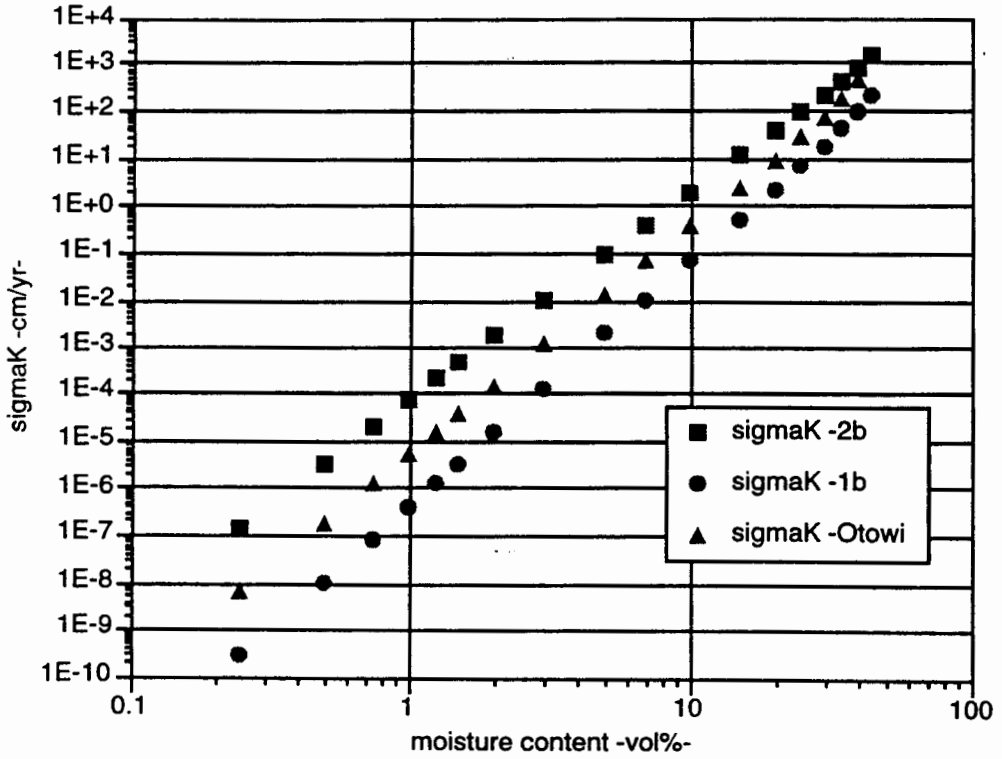

Fig. 31 Uncertainty in unsaturated hydraulic conductivity (sigmaK) in each of three stratigraphic units (2b, 1b, Otowi) for the best estimate of the uncertainty in the van Genuchten exponent, dN = 0.06.